USGS
science for a changing world

The Alaska Volcano Observatory is a consortium between the U.S. Geological Survey, the University of Alaska Fairbanks Geophysical Institute, and the Alaska Division of Geological & Geophysical Surveys

2019 Volcanic Activity in Alaska—Summary of Events and Response of the Alaska Volcano Observatory

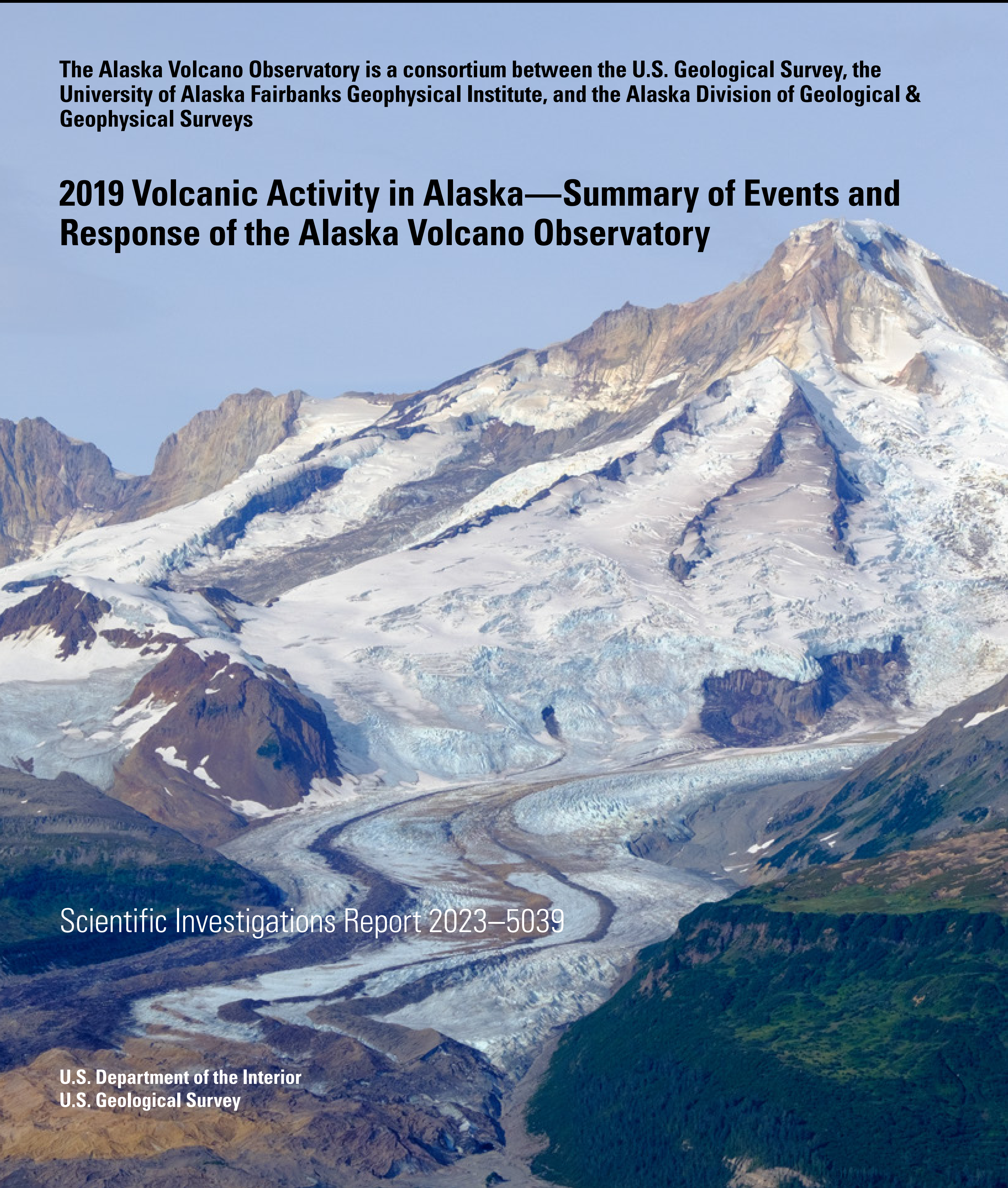

Scientific Investigations Report 2023–5039

U.S. Department of the Interior
U.S. Geological Survey

Cover: Oblique aerial photograph of the northeast face of Iliamna Volcano, with Lateral Glacier extending into the foreground, on August 14, 2019. Photograph by M. Loewen, U.S. Geological Survey

2019 Volcanic Activity in Alaska—Summary of Events and Response of the Alaska Volcano Observatory

By Tim R. Orr, Cheryl E. Cameron, Hannah R. Dietterich, James P. Dixon, Max L. Enders, Ronni Grapenthin, Alexandra M. Iezzi, Matthew W. Loewen, John A. Power, Cheryl Searcy, Gabrielle Tepp, Liam Toney, Christopher F. Waythomas, and Aaron G. Wech

The Alaska Volcano Observatory is a consortium between the U.S. Geological Survey, the University of Alaska Fairbanks Geophysical Institute, and the Alaska Division of Geological & Geophysical Surveys

Scientific Investigations Report 2023–5039

U.S. Department of the Interior
U.S. Geological Survey

U.S. Geological Survey, Reston, Virginia: 2023

For more information on the USGS—the Federal source for science about the Earth, its natural and living resources, natural hazards, and the environment—visit https://www.usgs.gov or call 1–888–392–8545.

For an overview of USGS information products, including maps, imagery, and publications, visit https://store.usgs.gov/ or contact the store at 1–888–275–8747.

Suggested citation:
Orr, T.R., Cameron, C.E., Dietterich, H.R., Dixon, J.P., Enders, M.L., Grapenthin, R., Iezzi, A.M., Loewen, M.W., Power, J.A., Searcy, C., Tepp, G., Toney, L., Waythomas, C.F., and Wech, A.G., 2023, 2019 Volcanic activity in Alaska—Summary of events and response of the Alaska Volcano Observatory: U.S. Geological Survey Scientific Investigations Report 2023–5039, 64 p., https://doi.org/10.3133/sir20235039.

ISSN 2338-0328 (online)

Acknowledgments

This report represents the work of the entire Alaska Volcano Observatory staff, colleagues from other U.S. Geological Survey volcano observatories, and cooperating State and Federal agencies. We thank those members of the public who shared observations and photographs. Technical reviews by Drew Downs, John Perrault, and Michelle Coombs improved the content and consistency of this report. The Alaska Volcano Observatory is funded by the U.S. Geological Survey Volcano Hazards Program and the State of Alaska.

Contents

Figures

Tables

Conversion Factors

U.S. customary units to International System of Units

Multiply	By	To obtain
	Length	
foot (ft)	0.3048	meter (m)
foot (ft)	0.000305	kilometer (km)
mile (mi)	1.609	kilometer (km)

International System of Units to U.S. customary units

Multiply	By	To obtain
	Length	
meter (m)	3.281	foot (ft)
kilometer (km)	3,281	foot (ft)
kilometer (km)	0.6214	mile (mi)
	Area	
square meter (m^2)	10.76	square foot (ft^2)
square kilometer (km^2)	0.3861	square mile (mi^2)
	Volume	
liter (L)	0.2642	gallon (gal)
cubic meter (m^3)	35.31	cubic foot (ft^3)
cubic kilometer (km^3)	0.2399	cubic mile (mi^3)
	Velocity	
meter per second (km/s)	3,281	foot per second (ft/s)
	Mass flow	
metric ton per day (t/d)	1.1022	ton, long [2,240 lb] per day
metric ton per day (t/d)	0.9842	ton, short [2,000 lb] per day

Temperature in degrees Celsius (°C) may be converted to degrees Fahrenheit (°F) as follows:

$$°F = (1.8 \times °C) + 32.$$

Datum

Horizontal and vertical coordinate information referenced to the World Geodetic System 1984 (WGS 84), unless otherwise noted.

Altitude, as used in this report, refers to distance above sea level of a location in the air.

Elevation, as used in this report, refers to distance above sea level of a location on the land surface.

Depth, as used in this report, refers to distance below sea level, unless otherwise noted.

Abbreviations

AKDT	Alaska daylight time; UTC–8 hours
AKST	Alaska standard time; UTC–9 hours
ASL	above sea level
AVO	Alaska Volcano Observatory
FAA	Federal Aviation Administration
GNSS	Global Navigation Satellite System
GPS	Global Positioning System
GVP	Smithsonian Institution Global Volcanism Program
HADT	Hawaii-Aleutian daylight time; UTC–9 hours
HAST	Hawaii-Aleutian standard time; UTC–10 hours
IASI	Infrared Atmospheric Sounding Interferometer
IR	infrared
LP	long-period
PIREP	pilot weather report
ppt	parts per thousand
RSAM	real-time seismic amplitude measurements
SO_2	sulfur dioxide
TROPOMI	TROPOspheric Monitoring Instrument
UNAVCO	University NAVSTAR Consortium
USGS	U.S. Geological Survey
UTC	coordinated universal time; same as Greenwich mean time
UV	ultraviolet
VT	volcano-tectonic
#	number

2019 Volcanic Activity in Alaska—Summary of Events and Response of the Alaska Volcano Observatory

By Tim R. Orr,[1] Cheryl E. Cameron,[2] Hannah R. Dietterich,[1] James P. Dixon,[1] Max L. Enders,[1] Ronni Grapenthin,[3] Alexandra M. Iezzi,[3] Matthew W. Loewen,[1] John A. Power,[1] Cheryl Searcy,[1] Gabrielle Tepp,[1] Liam Toney,[3] Christopher F. Waythomas,[1] and Aaron G. Wech[1]

Abstract

The Alaska Volcano Observatory responded to eruptions, volcanic unrest or suspected unrest, increased seismicity, and other significant activity at 17 volcanic centers in Alaska in 2019. The most notable volcanic activity was an eruption of Shishaldin Volcano, featuring eruptive activity that produced lava flows, lahars, and ash. Weak explosive activity also took place at Great Sitkin Volcano and Semisopochnoi Island. Mount Cleveland had one small ash-producing eruption followed by dome growth in early January but was quiet thereafter, and flank activity at Shrub mud volcano produced new mud deposits. Other activity documented in 2019 consists of declining unrest at Mount Veniaminof after its 2018 eruption; large ice and rock avalanches at Iliamna Volcano and Mount Spurr; anomalous seismicity and an increase in degassing at Pavlof Volcano; long-term inflation at Westdahl volcano, Akutan Volcano, and Mount Okmok; steam plumes and anomalous seismicity at Makushin Volcano; elevated seismicity at Mount Martin; and resuspended ash from the 1912 Novarupta-Katmai eruption deposits.

Introduction

The Alaska Volcano Observatory (AVO) is a joint program of the U.S. Geological Survey (USGS), the University of Alaska Fairbanks Geophysical Institute, and the State of Alaska Division of Geological & Geophysical Surveys. AVO was formed in 1988 and uses Federal, State, and university resources to monitor and study Alaska's hazardous volcanoes (fig. 1), forecast and record eruptive activity, and mitigate volcanic hazards to life and property. This report summarizes notable unrest and other kinds of activity associated with Alaskan volcanoes during 2019 (tables 1, 2) and briefly describes AVO's response. It contains information about all identified volcanic unrest, even if no formal public notification was issued at the time. Observations, images, and information that are typically not published elsewhere are included in this report. Similar summaries of volcanic unrest and AVO's response have been published annually since 1992 (appendix table 1.1).

The AVO volcano monitoring program involves daily analyses of satellite and webcam imagery, seismicity, and infrasound detections; occasional overflights and ground visits; airborne and ground-based gas measurements; and the compilation of visual observations taken from observatory personnel member, resident, mariner, and pilot weather report (PIREP) accounts. (PIREPs are reports of meteorological phenomena encountered by aircraft in flight.) AVO also receives real-time ground deformation data from permanent Global Navigation Satellite System (GNSS) stations at eight Alaskan volcanoes: Akutan Volcano, Augustine Volcano, Makushin Volcano, Mount Okmok, Redoubt Volcano, Shishaldin Volcano, Mount Spurr, and Westdahl volcano. These deformation data are supplemented with Interferometric Synthetic Aperture Radar (InSAR) imagery (for example, Lee and others, 2010). With this information, AVO assigns each monitored volcano an Aviation Color Code and Volcano Alert Level, which indicate its current activity status. No assignment is given to unmonitored volcanoes at background level. Appendix 2 defines each Aviation Color Code and Volcano Alert Level.

Duty scientists are responsible for compiling all monitoring data to provide scheduled and event-driven public notices, as appropriate. AVO scientists produce daily reports through weekly duty scientist and duty remote sensing rotations. The duty remote sensor produces a daily remote sensing report, whereas the duty scientist summarizes all observations (including remote sensing and seismicity) at volcanoes with elevated Aviation Color Codes and Volcano Alert Levels. The reports also describe any notable observations at the other volcanoes AVO monitors. All observations are archived in a relational database. A second cadre of scientists from AVO and the U.S. Geological Survey National Earthquake Information Center monitors volcano seismicity and infrasound using local and regional sensors. This team compiles three separate seismic reports daily, spaced approximately eight hours apart. Like the daily remote sensing reports, the seismic reports are also catalogued in a relational database.

Thirty-three of the historically active volcanoes and volcanic fields in Alaska were instrumented with seismometers and other instrumentation operated by AVO as of December 31, 2019. Included in this list are those

[1]U.S. Geological Survey, Alaska Volcano Observatory.

[2]Alaska Division of Geological & Geophysical Surveys.

[3]University of Alaska Fairbanks.

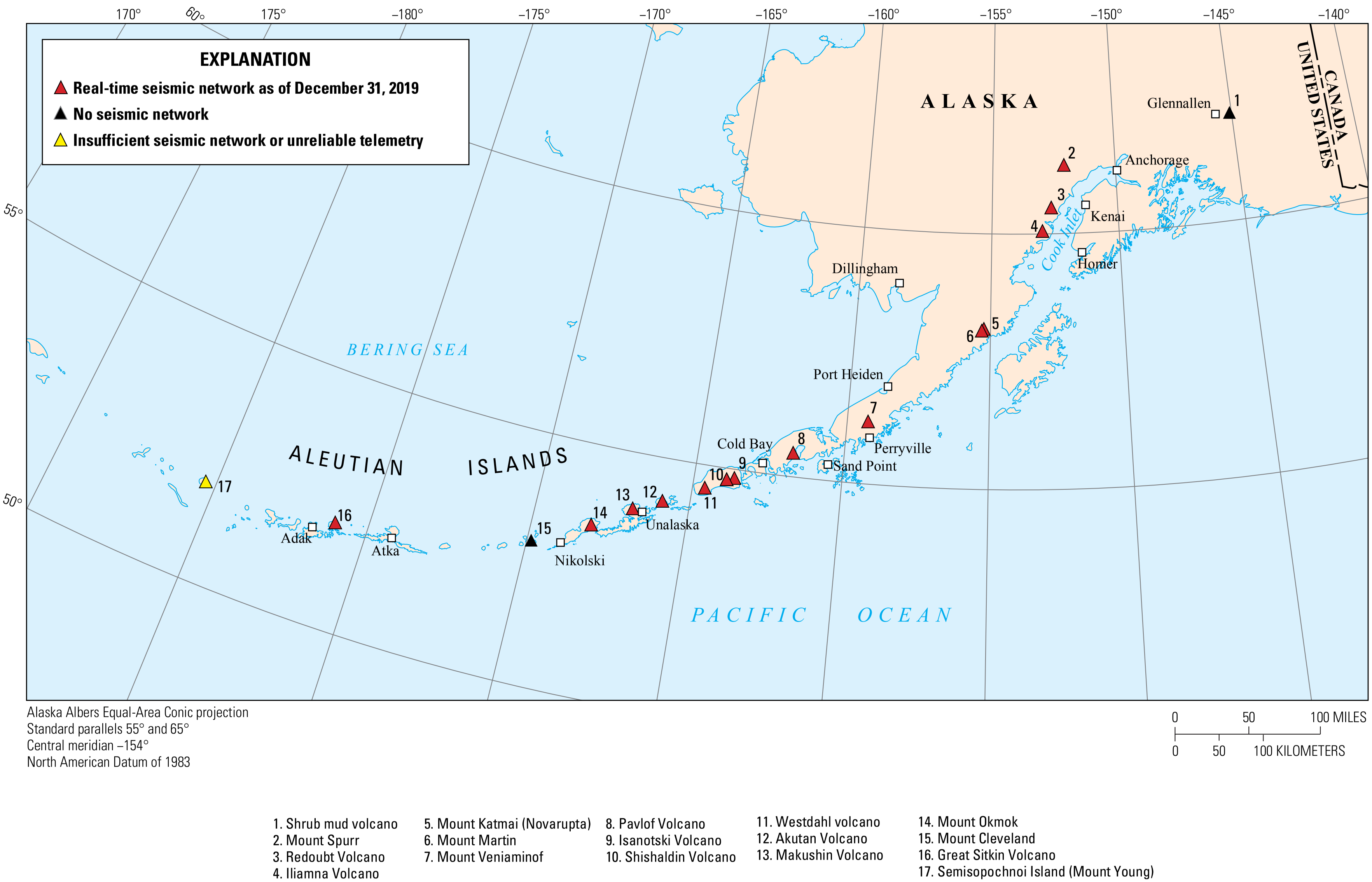

Figure 1. Map of volcanoes discussed in this report and their monitoring statuses.

Table 1. Summary of monitoring highlights at Alaskan volcanoes in 2019, including but not limited to confirmed eruptions, possible eruptions, increases in seismicity, observations of fumarolic activity, and other notable events.

[Volcano locations shown in figure 1. See appendix tables 3.1 and 3.2 for lists of volcanic activity described in past Alaska Volcano Observatory annual summaries, sorted by year and by volcano]

Volcano	Month of activity	Type of activity
Shrub mud volcano	March–End of year	Mud discharge
Mount Spurr	July	Ice and rock avalanche
Redoubt Volcano	August	Ash resuspension
Iliamna Volcano	March; June June	Ice and rock avalanches Seismic network improvements
Mount Katmai (Novarupta)	December	Resuspension of 1912 ash
Mount Martin	March September–December	Vapor plume Earthquake swarm
Mount Veniaminof	November (2018)–April; August	Waning unrest following 2018 eruption
Pavlof Volcano	May–June; October–November; December–End of year	Elevated seismicity; weak explosive activity
Isanotski Volcano	March–May	Earthquake swarm related to glacial activity
Shishaldin Volcano	July–End of year	Strombolian explosive activity; lava flows; lahars; ash emissions
Westdahl volcano	All year	Long-term inflation
Akutan Volcano	All year	No systematic deformation
Makushin Volcano	May; June	Earthquake swarms
Mount Okmok	All year September	Inflation Seismic tremor
Mount Cleveland	January	Explosive eruption and dome growth
Great Sitkin Volcano	July (2018)–February; June–July June	Elevated seismicity Small explosive eruption
Semisopochnoi Island (Mount Young)	May–End of year	Increased seismicity; sporadic, weak explosive activity

volcanoes that have insufficient seismic instrumentation to calculate reliable earthquake hypocenters and magnitudes, or whose real-time telemetry was not reliable enough to produce a complete record of earthquake activity in 2019. Specifically, Bogoslof volcano was monitored by only one seismograph station and Mount Cleveland was monitored by only two local seismograph stations, so both lacked the minimum number of stations to locate earthquakes. Little Sitkin Island and Semisopochnoi Island were also considered unmonitored because the telemetry for each of their subnetworks was unreliable. The seismic network at Mount Wrangell was reestablished in 2019, so it was moved back to the list of monitored volcanoes for the first time in several years.

The volcanoes in this report are presented in geographic order from east to west along the Aleutian Arc. Each entry has a title block containing information about that volcano: its identifier number (#) assigned by the Smithsonian Institution Global Volcanism Program (GVP); its latitude, longitude, and summit elevation; the name of its geographic region; and an abbreviated summary of its 2019 activity. The title block is followed by a description of the volcano and a summary of its past activity, then a detailed account of its activity in 2019, often with accompanying tables, images, figures, or all three. This information is derived from formal public AVO information products, internal online electronic logs compiled by AVO staff, and published material (such as Miller and others [1998] and the Smithsonian Institution Global Volcanism Network Bulletin [https://volcano.si.edu/reports_bgvn.cfm]). Beginning with the 2013 report, AVO annual summaries have also included expanded information on seismicity at Alaskan volcanoes. The volcanoes discussed in past summaries are listed in appendix 3 (by year in table 3.1 and by volcano in table 3.2).

AVO uses informal names for some volcanoes because the names approved and standardized by the U.S. Board on Geographic Names through the Geographic Names Information System may match imprecisely with their corresponding volcanoes. For example, Bogoslof volcano

Table 2. Alaska volcanoes with Aviation Color Code and Volcano Alert Level changes in 2019.

[Definitions for the Aviation Color Codes and Volcano Alert Levels located in appendix 2]

Aviation Color Code/ Volcano Alert Level	Date range
Mount Veniaminof	
ORANGE/WATCH	11/22/2018–01/04/2019
YELLOW/ADVISORY	01/04/2019–04/30/2019
GREEN/NORMAL	04/30/2019–08/01/2019
YELLOW/ADVISORY	08/01/2019–08/25/2019
GREEN/NORMAL	08/25/2019–End of year
Pavlof Volcano	
GREEN/NORMAL	08/30/2017–05/15/2019
YELLOW/ADVISORY	05/15/2019–06/12/2019
GREEN/NORMAL	05/12/2019–10/19/2019
YELLOW/ADVISORY	10/19/2019–11/06/2019
GREEN/NORMAL	11/06/2019–12/28/2019
YELLOW/ADVISORY	12/28/2019–End of year
Shishaldin Volcano	
GREEN/NORMAL	02/07/2018–07/12/2019
YELLOW/ADVISORY	07/12/2019–07/24/2019
ORANGE/WATCH	07/24/2019–09/26/2019
YELLOW/ADVISORY	09/26/2019–10/17/2019
ORANGE/WATCH	10/17/2019–End of year

Aviation Color Code/ Volcano Alert Level	Date range
Mount Cleveland	
ORANGE/WATCH	12/12/2018–01/07/2019
YELLOW/ADVISORY	01/07/2019–01/17/2019
ORANGE/WATCH	01/17/2019–02/25/2019
YELLOW/ADVISORY	02/25/2019–11/08/2019
ORANGE/WATCH	11/08/2019–11/15/2019
YELLOW/ADVISORY	11/15/2019–End of year
Great Sitkin Volcano	
YELLOW/ADVISORY	07/01/2018–02/25/2019
GREEN/NORMAL	02/25/2019–06/02/2019
YELLOW/ADVISORY	06/02/2019–07/15/2019
GREEN/NORMAL	07/15/2019–End of year
Semisopochnoi Island (Mount Young)	
UNASSIGNED	12/19/2018–07/04/2019
YELLOW/ADVISORY	07/04/2019–07/18/2019
ORANGE/WATCH	07/18/2019–09/18/2019
YELLOW/ADVISORY	09/18/2019–12/07/2019
ORANGE/WATCH	12/07/2019–End of year

comprises more islands than Bogoslof Island. Moreover, some volcanoes lack official place names, such as Takawangha volcano, requiring the use of informal names.

In this report, volcano locations (in decimal degrees latitude and longitude) and summit elevations are taken from AVO's database of Alaskan volcanoes (Cameron and others, 2022), and so might differ slightly from previously published compilations. Measurements are presented in the International System of Units, except for altitudes, which are reported in feet (ft) above sea level (ASL), in line with Federal aviation standards, followed by meters. General date references are given in local time unless specified otherwise. Most volcanoes in Alaska are in the Alaska standard time (AKST) or Alaska daylight time (AKDT) zones, but all Aleutian volcanoes west of Umnak Island (see the community of Nikolski, Alaska, on figure 1) are in the Hawaii-Aleutian standard time (HAST) or Hawaii-Aleutian daylight time (HADT) zones. During 2019, daylight saving time ran from March 10 to November 3.

What is an "eruption"?

The specific use of the term "eruption" varies from scientist to scientist and has no universally agreed-upon definition. Here, we adopt the usage of Siebert and others (2010, p. 17), who define eruptions as "* * * events that involve the explosive ejection of fragmental material, the effusion of liquid lava, or both." The critical elements of this definition are the verbs "ejection" and "effusion," which refer to dynamic surface processes that pose some level of hazard. The presence or absence of "juvenile material," or newly erupted rock, which can sometimes be ambiguous, is not relevant to this use of the term eruption, particularly when communicating a potential hazard. This definition does not, however, include passive volcanic degassing or hydrothermal fluid discharge.

What is a "historically active volcano"?

AVO defines an active volcano as a volcanic center that has had a recent eruption (see "What is an 'eruption'? ") or a period of intense deformation, seismicity, or fumarolic activity, which are inferred to reflect the presence of magma at shallow levels within the volcano. AVO considers the historical period in Alaska to be since 1741, when written records of volcanic activity began. On the basis of a rigorous reanalysis of all volcanic activity accounts in Alaska from many sources, Cameron and others (2018) concluded that 54 Alaskan volcanoes fit these criteria. In this report, we modify the number of historically active volcanoes to 52, because we consider (1) Korovin Volcano and Mount Kliuchef to be subfeatures of the Akta volcanic complex and (2) Novarupta to be a subfeature of Mount Katmai. As geologic understanding of Alaskan volcanoes improves through additional fieldwork and modern radiometric dating techniques, our list of active volcanoes will continue to evolve.

Volcanic Activity in Alaska, East to West Along the Aleutian Arc

Shrub mud volcano

Not listed in GVP database
62.149° N., 145.021° W.
897 m
Copper River Basin

MUD EXTRUSION

The Klawasi group mud volcanoes, comprising Shrub (fig. 1), Upper Klawasi, and Lower Klawasi mud volcanoes, are located in the Copper River Basin of south-central Alaska near the west slope of Mount Drum, a Pleistocene volcano in Wrangell-St. Elias National Park and Preserve. They sit on land administered by Ahtna, Incorporated, an Alaska Native regional corporation. Shrub mud volcano, the northernmost of the three, is about 25 kilometers (km) east of Glennallen, Alaska, and 280 km northeast of Anchorage, Alaska. It is 104 meters (m) tall and although classified as a mud volcano, it is shrouded in glacial debris. Note that because the name "Klawasi group" and its constituent mud volcanoes are not yet included in the U.S. Geographic Names Information System, these names are considered informal.

Shrub mud volcano was barely active for decades, with only extremely weak activity observed in the mid-1950s (Nichols and Yehle, 1961). By comparison, Upper Klawasi and Lower Klawasi mud volcanoes have historically produced minor mud discharge and weak gas emissions almost constantly. During the summer of 1996, Shrub mud volcano began to erupt CO_2-rich gas and warm, saline mud (Richter and others, 1998a), producing mud flows that traveled down the flanks of its edifice and extended out from its base. This activity waned over the following few years, eventually evolving into a bubbling mud pond approximately 40 meters (m) in diameter at the mud volcano's summit. This pond made Shrub mud volcano more like Upper and Lower Klawasi mud volcanoes, which both have similar features. The summit pond at Shrub mud volcano has remained active since it formed, with little change in behavior or appearance as of 2019.

During a field visit to the Klawasi group mud volcanoes in June 2019, AVO scientists found a new extrusion of mud at the base of Shrub mud volcano's north flank (fig. 2). The extrusion was active during the visit and had started recently, given that evergreens partly buried by the flow were just beginning to turn orange. Satellite imagery indicates this activity probably started between March 7 and March 9. The flows, which came from vents on mud deposits dating to the late 1990s and early 2000s, extended northeast and spread into the adjacent forest to the north. Satellite data showed that the extrusive activity continued until at least October 21 before stopping sometime in the subsequent winter. The vents were inactive by the time satellite views of the area resumed in early February 2020, although new vents had opened immediately south of the old ones.

Mount Spurr

GVP #313040
61.299° N., 152.254° W.
3,374 m
Cook Inlet

ICE AND ROCK AVALANCHE

Mount Spurr is a 3,374-meter-high ice- and snow-covered stratovolcano located 125 km west of Anchorage (fig. 1). Its largely ice-covered edifice might be a lava dome complex (Nye and Turner, 1990), although the last known eruption from its summit, calculated by correlating tephra deposits, took place about 5,200 years ago (Riehle, 1985). More recently, in 2004–2006, Mount Spurr experienced a period of unrest interpreted to be the result of new magma injecting to a shallow level beneath the volcano (Power, 2004; Power and others, 2004a). This unrest was marked by elevated seismicity, magmatic gas emissions, the generation of debris flows, and increased heat flux, the last of which formed a water-filled ice cauldron at the volcano's summit (Power, 2004; Neal and others, 2005; McGimsey and others, 2007; Neal and others, 2009). Although the summit of Mount Spurr has not erupted recently, a satellite vent 3.5 km south of the summit, named Crater Peak, produced explosive eruptions in 1953 and 1992 (Keith, 1995, and references therein). Both eruptions led to ashfalls that impacted populated areas in south-central Alaska.

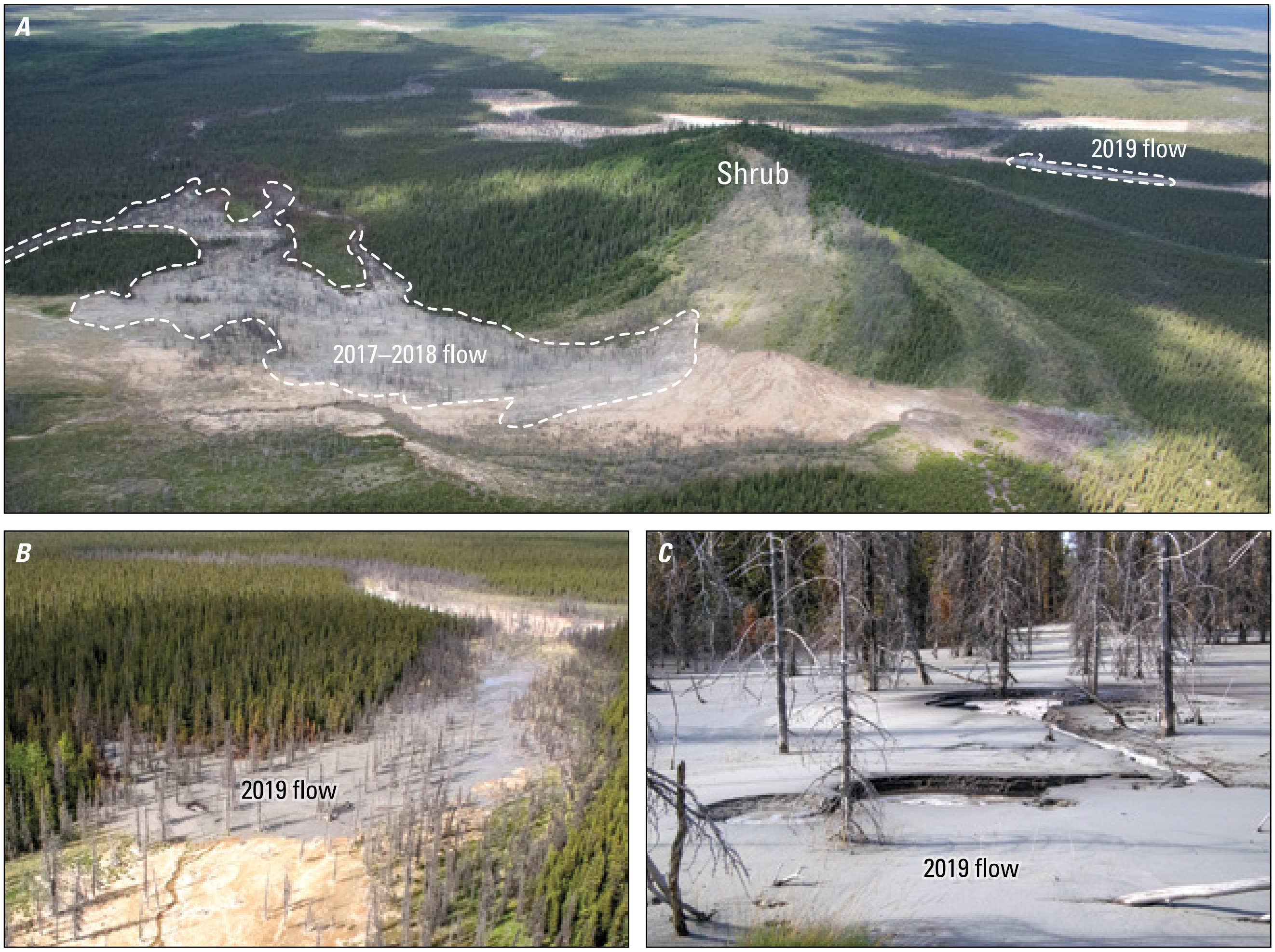

Figure 2. Photographs of recent mud flows at Shrub mud volcano, south-central Alaska. *A*, Oblique aerial photograph of Shrub mud volcano, looking west, showing the 2017–2018 mud flow and the active mud flow observed in June 2019. *B*, Oblique aerial photograph of the active mud flow observed in June 2019 at the north base of Shrub mud volcano, looking north-northeast. *C*, Ground-level photograph of the active mud flow, as seen at the vent area, looking northwest. Photographs by T. Orr, U.S. Geological Survey, June 19, 2019.

On July 15, 2019, at 16:32 UTC (08:32 AKDT), a large ice and rock avalanche took place on the southeast flank of Mount Spurr. A retrospective analysis of satellite imagery (fig. 3) indicated the starting zone of the avalanche was less than 1 km from the summit of the volcano. Clear satellite images of the flow deposit showed that it widened before splitting into two lobes that flowed around an elevated lateral moraine dividing the west and east branches of K'idazq'eni Glacier (March and others, 1997; Molnia, 2008). One lobe flowed down the west branch between the moraine and the Crater Peak cone, while the other traveled slightly farther down the east branch of the glacier (figs. 3, 4). Satellite imagery indicated the ice and rock avalanche spanned an area of approximately 2.3×10^6 square meters (m^2). Assuming an average deposit thickness of 0.5 m yields a volume of about 1.2×10^6 cubic meters (m^3).

The ice and rock avalanche generated energetic seismic and acoustic signals, recorded both locally and regionally. High-frequency signals were detected on the local seismic network (fig. 5) and long-period (LP) seismic signals were recorded more than 700 km away. Several local seismic stations also recorded approximately 10 minutes of precursory seismicity. Pre-avalanche seismicity has been previously documented at Iliamna Volcano (Caplan-Auerbach and Huggel, 2007). In addition to the recordings of seismic signals, an infrasound array in Dillingham, Alaska (fig. 1), detected acoustic waves from the event.

During an overflight on August 27, AVO staff noted the terrain of the source area consisted of exposed "slope-parallel lava, with rivulets of meltwater running on its surface." They found no evidence of increased non-meteorological heating at the summit area (a phenomenon which can trigger ice and rock avalanches) and observed nothing unusual on the other flanks of the summit cone (M. Coombs, USGS, written commun., 2019). The July 15 avalanche took place in an area known for debris flows, as documented by Coombs and others (2006), but previous flows were smaller and more water-rich than the July 15 event. Mount Spurr remained at an Aviation Color Code and Volcano Alert Level of **GREEN** and **NORMAL** throughout 2019.

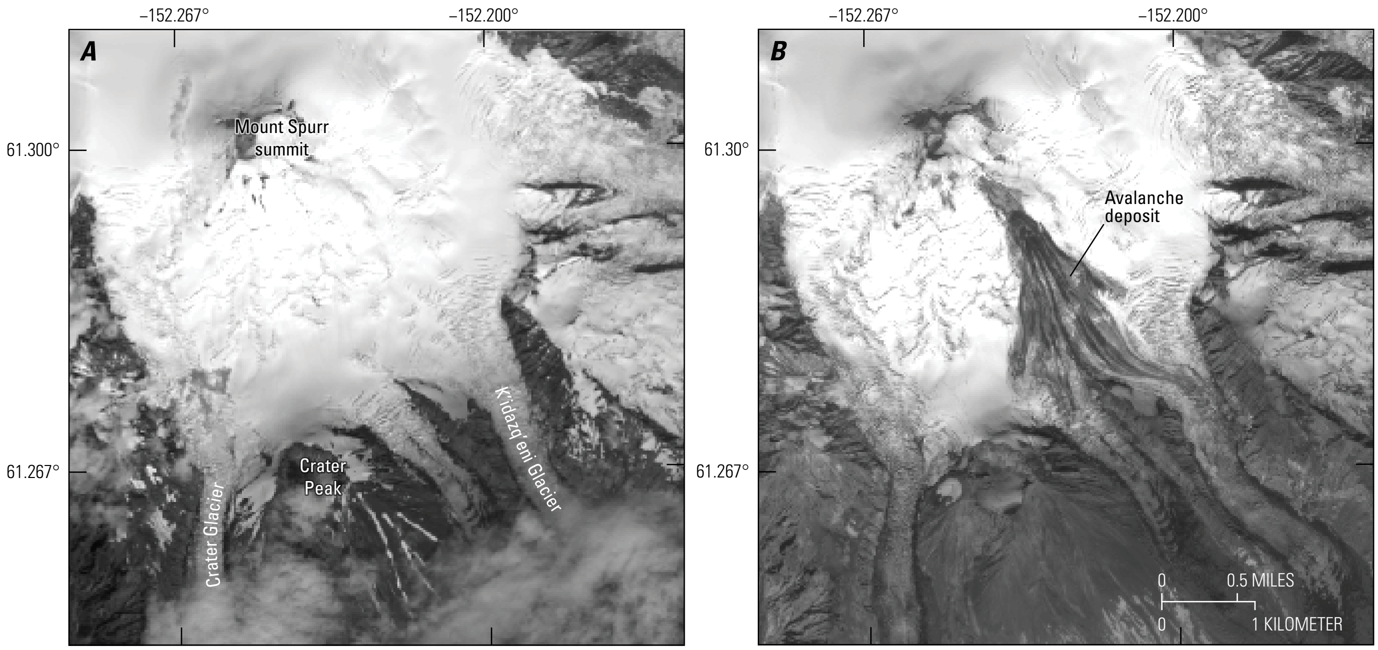

Figure 3. Satellite images taken before and after the ice and rock avalanche on July 15, 2019, at Mount Spurr, south-central Alaska. *A*, Landsat 8 band 8 (panchromatic) image, taken July 12, 2019. *B*, Sentinel-2 band 8 (near-infrared) image, taken August 16, 2019.

Figure 4. Oblique aerial photograph looking north-northwest at Mount Spurr, south-central Alaska, showing the ice and rock avalanche deposit from July 15, 2019. Photograph by C. Read, U.S. Geological Survey, July 17, 2019.

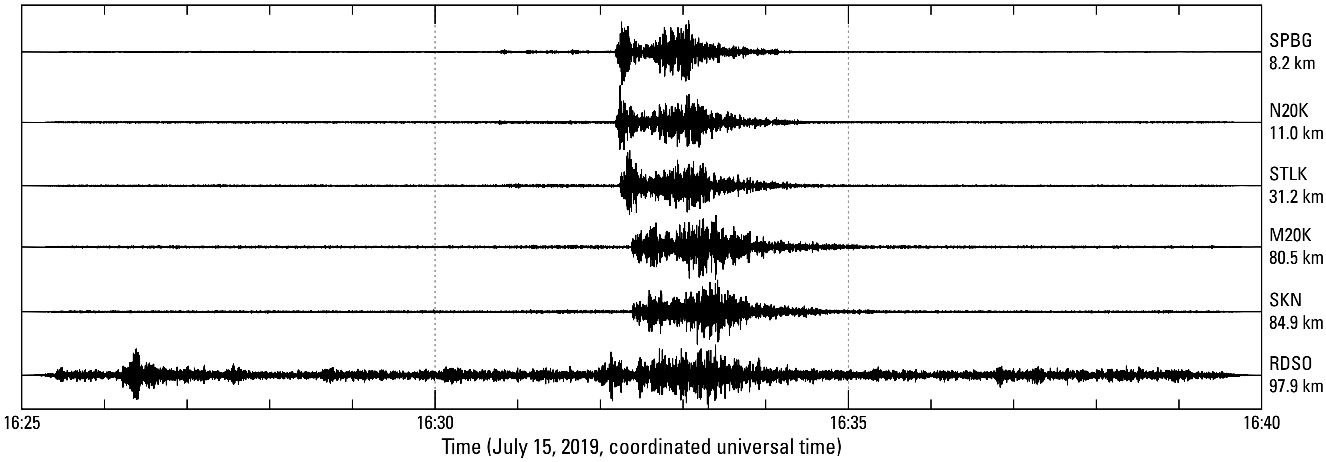

Figure 5. High-frequency vertical-component seismic signals generated by the ice avalanche of July 15, 2019, at Mount Spurr, south-central Alaska. Signals were filtered in the 1–5 hertz band and normalized to their maximum amplitudes. Station distances, listed below each station code, are measured in kilometers (km) from the crown of the avalanche, as estimated from satellite imagery.

Redoubt Volcano

GVP #313030
60.485° N., 152.744° W.
3,108 m
Cook Inlet

ASH RESUSPENSION

The heavily ice-mantled Redoubt Volcano is 170 km southwest of Anchorage and 80 km west of Kenai, Alaska, on the west side of Cook Inlet within Lake Clark National Park and Preserve (fig. 1). Recent eruptions of Redoubt Volcano took place in 1902, 1966–1968, 1989–1990, and 2009 (Waythomas and others, 1997; Schaefer, 2011; McGimsey and others, 2014). The eruptions of 1966–1968, 1989–1990, and 2009 produced lahars that traveled down the Drift River, and those of 1989–1990 and 2009 also partly flooded the Drift River Oil Terminal. Ash clouds produced by these two most recent eruptions affected air traffic and deposited minor or trace amounts of ash on communities in south-central Alaska (Miller and Chouet, 1994; Schaefer, 2011).

Although no eruptive activity was detected at Redoubt Volcano in 2019, on August 16, strong winds entrained and resuspended ash near the volcano. The resuspended ash cloud was not seen in satellite imagery but was visible in webcam views (fig. 6), and PIREPs described it as reaching an altitude as high as 10,000 ft (3,000 m) ASL. The National Weather Service Alaska Aviation Weather Unit issued a significant meteorological weather advisory for aviators, but AVO received no reports of ashfall. The Aviation Color Code and Volcano Alert Level at Redoubt Volcano remained **GREEN** and **NORMAL** throughout 2019.

Iliamna Volcano

GVP #313020
60.032° N., 153.092° W.
3,053 m
Cook Inlet

ICE AND ROCK AVALANCHES

Iliamna Volcano is a glacier-carved stratovolcano on the southwest coast of Cook Inlet, about 215 km southwest of Anchorage (fig. 1). Although Iliamna Volcano has no known historical eruptions, past geologic studies document evidence of late Holocene explosive activity and repeated, extensive mass wasting of its steep, hydrothermally altered edifice

Figure 6. Webcam image showing resuspended ash at Redoubt Volcano in south-central Alaska on August 16, 2019.

(Waythomas and Miller, 1999). Fumaroles at an elevation of about 2,740 m on the east flank of the volcano produce plumes of steam condensate and volcanic gas almost continuously (Werner and others, 2011). In the past three decades, researchers have documented two magmatic intrusions beneath Iliamna Volcano (Roman and others, 2004; Prejean and others, 2012).

Although Iliamna Volcano maintained an Aviation Color Code and Volcano Alert Level of **GREEN** and **NORMAL** throughout 2019, AVO observed seismicity episodes suggestive of ice and rock avalanches, and two large avalanches were confirmed in satellite images. Avalanches like these are common on Iliamna Volcano, where they are composed mostly of ice and snow (as much as 80 percent by volume) (Schneider and others, 2010), and they are highly mobile, traveling at mean speeds of approximately 50 meters per second (m/s) and reaching peak speeds, estimated via numerical modeling, of more than 70 m/s (Caplan-Auerbach and Huggel, 2007; Schneider and others, 2010).

The first of the two large ice and rock avalanches took place on the south flank of the volcano in late March. This first avalanche started at an elevation of 2,800 m and ran for about 3 km, reaching a final elevation of 1,450 m (fig. 7). A seismic signal inferred to be from the avalanche was detected on stations as far as approximately (~) 100 km away at 18:00 UTC (10:00 AKDT) on March 26, with a recorded duration of 3–4 minutes. This timing for the ice and rock avalanche was roughly confirmed by Landsat satellite images taken before and after the seismic signal, although the signal of the avalanche did not appear in infrasound data.

The second, much larger ice and rock avalanche took place on the east flank of Iliamna Volcano at 00:03 UTC on June 21 (June 20 at 16:03 AKDT) (Toney and others, 2021). An oblique aerial photograph taken the same day (fig. 8*A*) and satellite imagery acquired the next day (fig. 8*B*) showed the flow deposit on Iliamna Volcano's east-facing Red Glacier. Red Glacier has hosted many debris avalanches in prehistoric

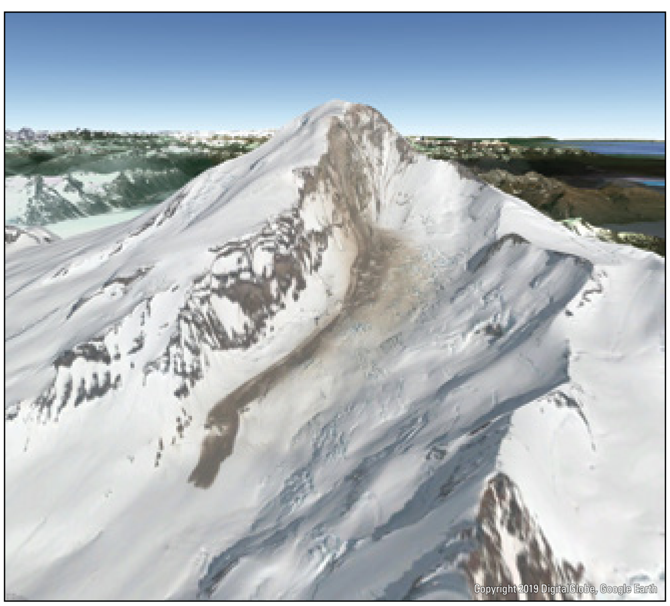

Figure 7. Satellite image acquired on April 3, 2019, draped over a three-dimensional visualization of Iliamna Volcano in south-central Alaska, showing the rock and ice avalanche deposit from March 26. Direction of view is approximately north-northeast.

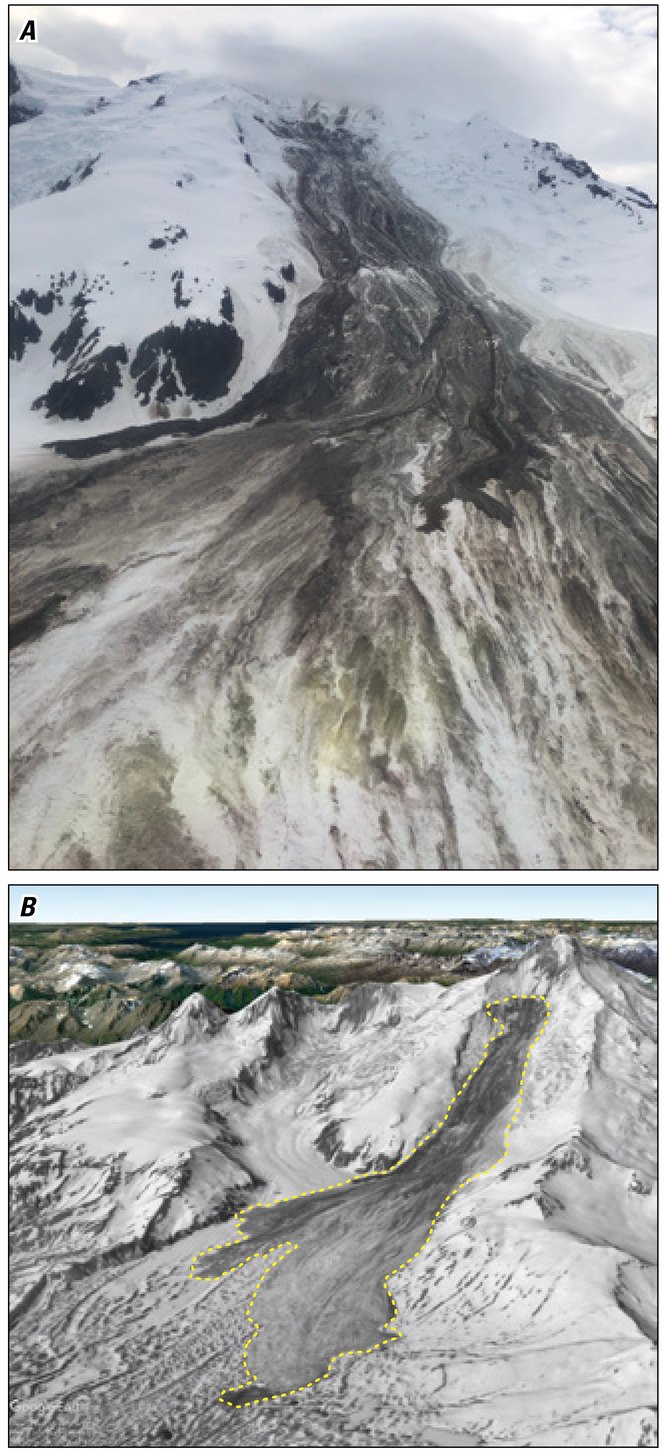

Image copyright 2019 Planet Labs PBC

Figure 8. Images of the June 21, 2019, ice and rock avalanche deposit on Iliamna Volcano, south-central Alaska. *A*, Aerial photograph taken June 21, 2019, looking west-northwest at the deposit. Photograph by L. Prosser. *B*, PlanetScope near-infrared satellite image (Planet Team, 2019) acquired on June 22, 2019, draped over a three-dimensional visualization of Iliamna Volcano's topography. The avalanche deposit is outlined. Direction of view is approximately west-southwest.

and historical time (Waythomas and others, 2000); its most recent avalanche of comparable size took place in May 2016. The June 21 rock and ice avalanche initiated less than 1 km from the volcano's summit and traveled east for about 8 km. Measurements taken from satellite imagery estimate that the deposit covered an area spanning approximately 7.1×10^6 m^2. Assuming an average deposit thickness of 0.5 m, this yields a volume of about 3.6×10^6 m^3.

The second ice and rock avalanche on Iliamna Volcano, like the July 15 ice and rock avalanche on Mount Spurr, generated energetic seismic and acoustic signals that were recorded both locally and regionally (Toney and others, 2021). One local seismic station recorded at least 100 minutes of precursory seismicity (J. Caplan-Auerbach, Western Washington University, written commun., 2019). High-frequency signals associated with the event itself were recorded on local and regional (greater than 100 km away) seismic networks (fig. 9), and LP seismic signals were recorded more than 600 km away. Pre-avalanche seismicity was also documented during Red Glacier avalanches in 1994, 1997, 2003, and 2016 (Caplan-Auerbach and Huggel, 2007; J. Caplan-Auerbach, Western Washington University, written commun., 2016). The infrasound array in Dillingham (fig. 1) detected acoustic waves from the event (fig. 10), as did the infrasound arrays in the Alaskan cities of Sand Point (fig. 1) and Fairbanks.

Mount Katmai (Novarupta)

GVP# 312170
58.279° N., 154.953° W.
2,047 m
Alaska Peninsula

RESUSPENSION OF 1912 ASH

Novarupta is a satellite vent of Mount Katmai on the Alaska Peninsula and is about 440 km southwest of Anchorage (fig. 1). Its eruption, the 1912 Novarupta-Katmai eruption, was the largest eruption of the 20th century, producing approximately 17 cubic kilometers (km^3) of fall deposits and 11 km^3 of pyroclastic material that filled nearby valleys, creating what is today known as the Valley of Ten Thousand Smokes (Hildreth and Fierstein, 2012). The pyroclastic deposit in this valley is as much as 200 m thick, and the valley remains almost entirely devoid of vegetation more than a century after the eruption. When the landscape is snow-free, and particularly when the ground has little moisture content, strong winds can pick up this ash and create large ash clouds. The wind can then transport the resuspended ash southeast across Shelikof Strait, Kodiak Island, and the Gulf of Alaska. These ash clouds are often seen by individuals downwind and are recorded in satellite imagery in which they commonly appear to originate from a broad area rather than a specific volcanic source. Although they look identical to dispersing volcanic ash clouds in satellite imagery, they are not the result of volcanic activity. This resuspension phenomenon has been observed and documented many times over the last several decades (Hadley and others, 2004; Wallace and Schwaiger, 2019), including once in 2019.

On December 26, 2019, strong northeast winds entrained and resuspended ash from the Mount Katmai (Novarupta) region, carrying it as far as 90 km to the southeast (fig. 11). Satellite imagery showed the resuspended ash cloud extending over Shelikof Strait to Kodiak Island at an altitude of about 6,000 ft (1,800 m) ASL, although AVO received no reports of ashfall on Kodiak Island. The National Weather Service Alaska Aviation Weather Unit issued a significant meteorological weather advisory for aviators and AVO issued an Information Statement. The Aviation Color Code and Volcano Alert Level remained **GREEN** and **NORMAL** for Mount Katmai (Novarupta) during 2019.

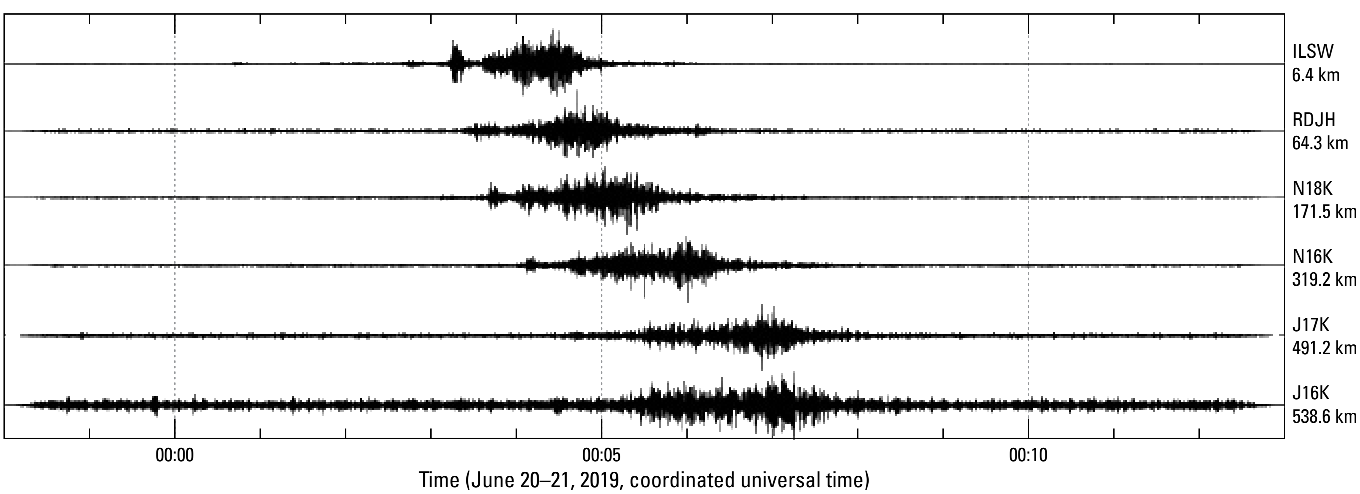

Figure 9. High-frequency vertical-component seismic signals generated by the ice and rock avalanche of June 21, 2019, at Iliamna Volcano, south-central Alaska. Signals were filtered in the 1–5 hertz band and normalized to their maximum amplitudes. Station distances, listed below each station code, are measured in kilometers (km) from the crown of the avalanche, as estimated from satellite imagery.

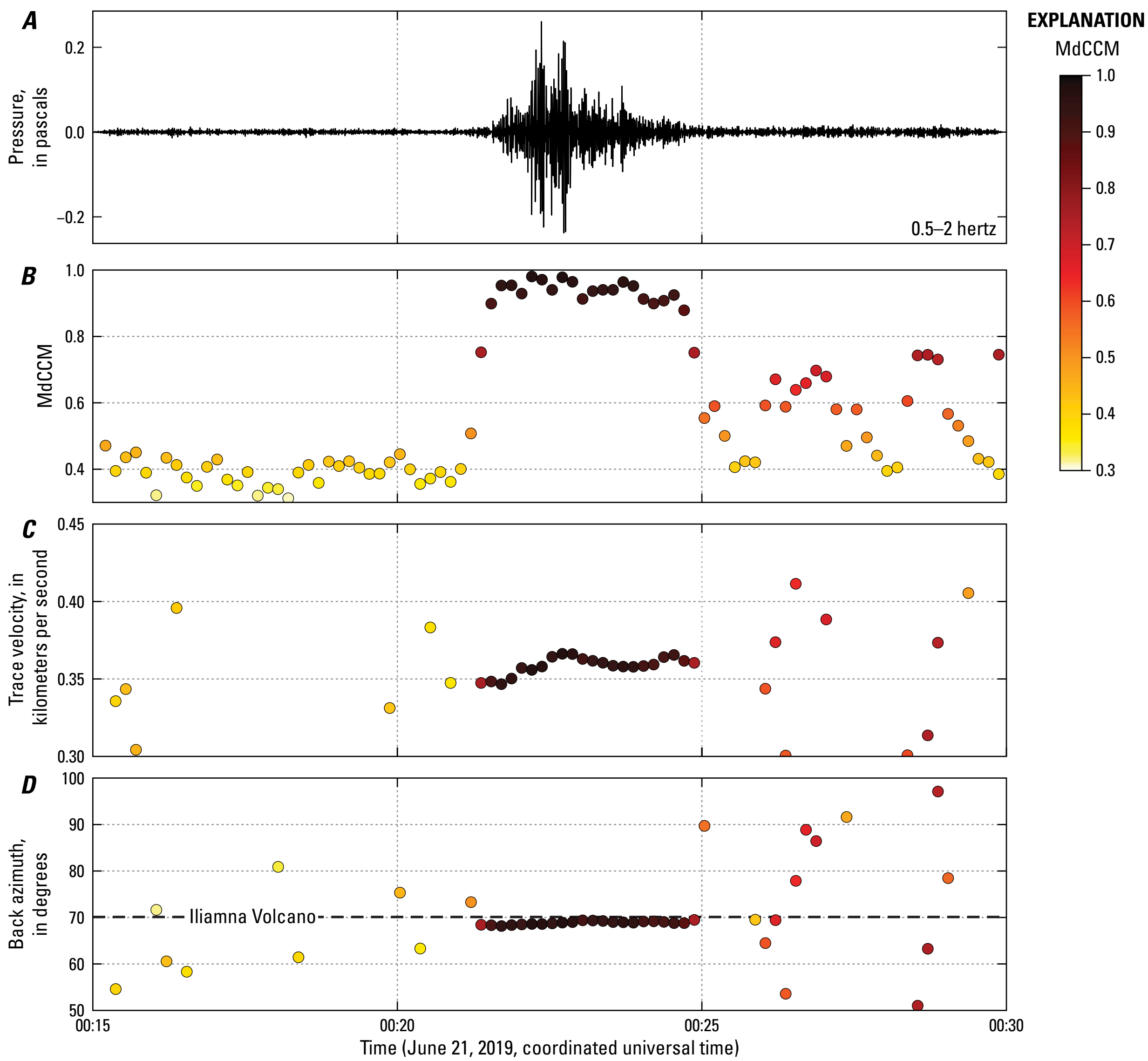

Figure 10. Array processing results for infrasound generated by the ice and rock avalanche at Iliamna Volcano (south-central Alaska) on June 21, 2019, as recorded at the infrasound array in Dillingham, Alaska. The graphs show variations in pressure (*A*), median cross-correlation maxima (MdCCM) (*B*), trace velocity (*C*), and back azimuth (*D*). MdCCM measure the coherency of acoustic waves traversing the array. Note the consistent back azimuth toward Iliamna Volcano during the period of high MdCCM.

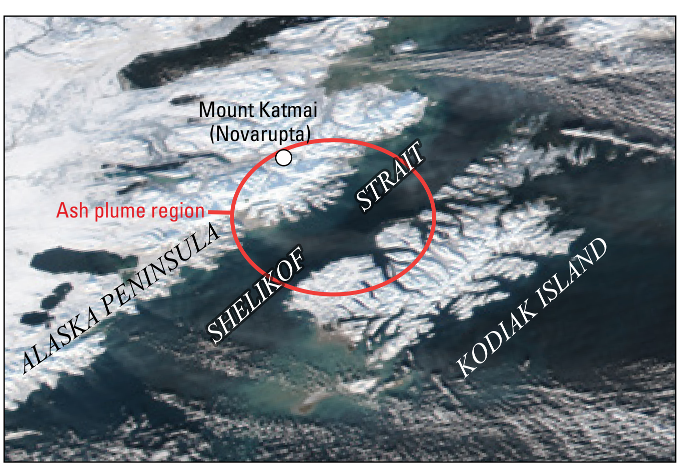

Figure 11. Oblique satellite image showing the resuspended ash plume extending from the Novarupta region across Shelikof Strait to Kodiak Island, southwest Alaska, on December 26, 2019. Image acquired by a Visible Infrared Imaging Radiometer Suite instrument on the Suomi-NPP satellite, looking north.

Mount Martin

GVP #312140
58.169° N., 155.357° W.
1,860 m
Alaska Peninsula

VAPOR PLUME; EARTHQUAKE SWARM

Mount Martin is a stratovolcano in Katmai National Park and Preserve on the Alaska Peninsula, about 475 km southwest of Anchorage (fig. 1). Mount Martin's summit cone, which reaches an elevation of about 1,850 m, features a crater about 300 m in diameter. This crater contains an ephemeral, shallow lake and vigorous fumaroles that emit jets of sulfur-rich volcanic gases. A series of thick lava flows, the oldest of which were emplaced more than 6,000 years ago, extend north and northwest from the summit (Fierstein and Hildreth, 2000).

Although no historical eruptions of Mount Martin are known, its fumarolic field frequently produces towering vapor plumes that can reach as high as 1,000 m above the summit when environmental conditions are right. Such a plume was observed on March 14, as described in two PIREPs released by the Federal Aviation Administration (FAA). The reports, which described steaming to 10,000 ft (3,000 m) from "a mountain," were linked to Mount Martin and quickly verified as typical activity for this volcano.

Mount Martin showed an increase in seismicity during 2019, although the cause was undetermined. Earthquakes at the volcano are common—AVO typically locates as many as one dozen weekly—but approximately 400 located earthquakes took place in September 2019 (fig. 12), a swarm that was the largest at Mount Martin since 2006 (O'Brien and others, 2012). The activity declined to about 100 earthquakes per month in October and November, then returned to background levels in December. Background-level earthquakes at Mount Martin typically cluster at a shallow depth in a diffuse pattern north of the summit. In contrast, the 2019 swarm was located predominantly in the west half of this background cluster zone and at a slightly greater depth. AVO closely monitored Mount Martin's temporary increase in seismicity but kept the Aviation Color Code and Volcano Alert Level at **GREEN** and **NORMAL** throughout the year.

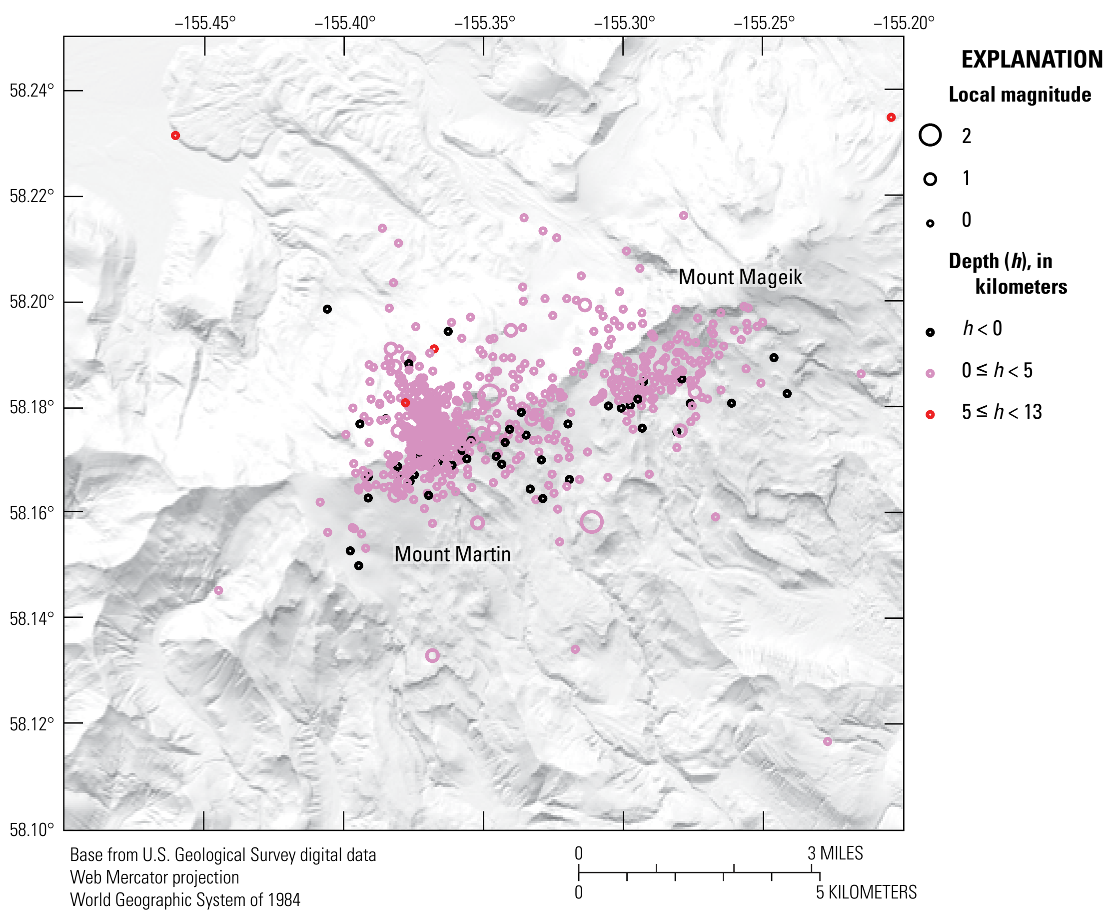

Figure 12. Map of earthquakes at Mount Martin, southwest Alaska, during September–November 2019. The finalized dataset spanning this timeframe and geographic region contains 741 located earthquakes. The increased seismicity during late 2019 was similar in depth to Mount Martin's background seismicity, which is typically shallower than 4 kilometers. Depths calculated relative to sea level; negative depths reflect elevation above sea level.

Mount Veniaminof

GVP #312070
56.198° N., 159.393° W.
2,507 m
Alaska Peninsula

WANING UNREST AFTER 2018 ERUPTION

Mount Veniaminof is an ice-clad andesite and dacite stratovolcano on the Alaska Peninsula, 775 km southwest of Anchorage and 35 km north of Perryville, Alaska (fig. 1). Featuring an ice-filled caldera 10 km in diameter and with a total volume of about 350 km^3, it is one of the largest and most active volcanoes of the Aleutian Arc (Miller and others, 1998; Bacon and others, 2009). Extensive pyroclastic flow deposits around the volcano indicate two Holocene caldera-forming eruptions have taken place (Miller and Smith, 1987). Mount Veniaminof has also erupted at least 19 times in the past 200 years alone, all from its ~300-meter-high intracaldera cone. The activity at Mount Veniaminof during 2019 was mostly associated with a prior eruptive period that took place from early September to late December 2018 (Cameron and others, 2020). Unrest at the volcano declined gradually after this period until it seemed likely that the eruption had paused or ended. On January 4, 2019, AVO lowered the Aviation Color Code and Volcano Alert Level from **ORANGE** and **WATCH** to **YELLOW** and **ADVISORY**.

Satellite imagery showed slightly elevated surface temperatures on Mount Veniaminof throughout 2019, although cloud cover frequently impeded observations. The elevated surface temperatures were probably associated with the cooling of lava flows emplaced on the intracaldera cone in 2018 (fig. 13) (Cameron and others, 2023). Minor steam emissions were occasionally visible in webcam views from nearby Perryville (fig. 14). Seismicity indicative of minor unrest—primarily low-amplitude tremor and discrete events—continued into April 2019 before finally declining to background levels. AVO lowered the Aviation Color Code and Volcano Alert Level to **GREEN** and **NORMAL** on April 30, 2019, after about four months with no significant unrest.

On August 1, 2019, AVO received a PIREP of steaming at Mount Veniaminof's intracaldera cone, which coincided with a weak tremor signal. These observations marked a small but distinct departure from the background level of unrest at the volcano, and as a result, AVO raised the Aviation Color Code and Volcano Alert Level to **YELLOW** and **ADVISORY**. Weak seismicity and occasional long-period earthquakes

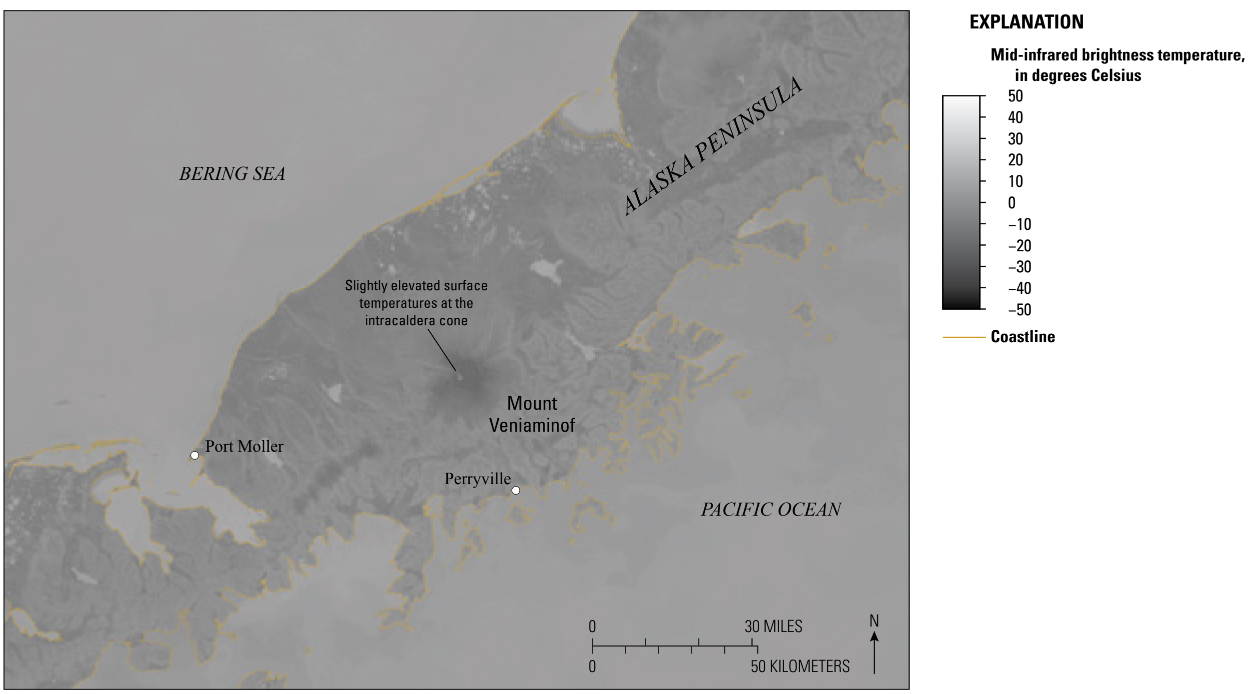

Figure 13. Mid-infrared satellite image of Mount Veniaminof, southwest Alaska, on August 19, 2019. The image shows slightly elevated surface temperatures (about 10 degrees Celsius above background) at the intracaldera cone associated with cooling lava flows that were emplaced in September–December 2018. Slightly elevated surface temperatures were detected at the intracaldera cone throughout 2019 when viewing conditions were cloud-free. Image acquired by a Visible Infrared Imaging Radiometer Suite instrument on the Suomi-NPP satellite.

Figure 14. Photograph of Mount Veniaminof in southwest Alaska, taken January 29, 2019, at 3:00 coordinated universal time (January 28, 2019, at 18:00 Alaska standard time). The image shows steam emissions from the intracaldera cone that were typical of activity in January 2019. As the year progressed, the robustness and persistence of the emissions declined. Image from the Federal Aviation Administration Perryville NorthWest [sic] webcam in Perryville, Alaska. Direction of view is northwest.

continued intermittently throughout most of August, but by the end of the month, the volcano returned to its background activity level. AVO subsequently lowered the Aviation Color Code and Volcano Alert Level to **GREEN** and **NORMAL** on August 25, 2019. No additional unrest took place at Mount Veniaminof for the remainder of 2019.

Pavlof Volcano

GVP #312030
55.417° N., 161.894° W.
2,518 m
Alaska Peninsula

ELEVATED SEISMICITY

Pavlof Volcano is a conical stratovolcano composed of basaltic andesite lava flows and pyroclastic rocks. It is located on the Alaska Peninsula about 60 km northeast of the City of Cold Bay, Alaska, and 950 km southwest of Anchorage (fig. 1). Eruptions at Pavlof Volcano range in style from Strombolian to Vulcanian (Waythomas and others, 2006) and with at least 37 eruptions since 1790, it is considered one of the most active volcanoes in North America (Miller and others, 1998). The volcano is dominantly an open vent system, and many of its eruptions have little precursory seismicity or ground deformation visible in InSAR (Lu and Dzurisin, 2014; Pesicek and others, 2018). The last significant eruption at Pavlof Volcano was in March 2016 and was characterized by continuous seismic tremor, infrasound detections, and lightning accompanying an ash cloud that rose to a maximum altitude of about 30,000 ft (9,100 m) ASL (Fee and others, 2017; Cameron and others, 2020).

In 2019, Pavlof Volcano showed signs of weak activity that caused AVO to raise the Aviation Color Code and Volcano Alert Level to **YELLOW** and **ADVISORY** three times (table 2). The first change was made on May 15, 2019, in response to an increase in seismic tremor and webcam images of robust summit degassing. The Aviation Color Code and Volcano Alert Level were lowered back to **GREEN** and **NORMAL** on June 12, after activity declined. They were raised again to **YELLOW** and **ADVISORY** on October 19 when small explosion signals were detected by the infrasound array in Sand Point (fig. 1) and on the local seismic network, then were lowered back to **GREEN** and **NORMAL** on November 6. AVO raised the Aviation Color Code and Volcano Alert Level to **YELLOW** and **ADVISORY** for the last time on December 28, again on the basis of an increase in seismic tremor levels. Ash emissions from the volcano were not observed during any unrest periods in 2019.

A total of 90 earthquakes were located within 20 km of Pavlof Volcano during 2019 (fig. 15). Of these events, 44 were classified as volcano-tectonic (VT) earthquakes, with a collective depth range of −2.85 to 31.5 km and a local magnitude (M_L) range of −0.41 to 1.65. The other 46 were classified as LP earthquakes, with a depth range of 8 to 34 km and a M_L range of −0.36 to 1.65. Of the 46 LP events, 21 were located ~5 km northeast of Pavlof Volcano beneath Pavlof Sister, a pattern also seen in the seismicity of previous years (Power and others, 2004b).

AVO recorded several tremor episodes at Pavlof Volcano in 2019. There is no obvious temporal relationship between the tremor and the earthquake activity. Figure 16 summarizes the timing and nature of Pavlof Volcano's seismic activity, comprising tremor episodes, VT events, and LP events, recorded throughout the year. The activity in 2019 started with weak, intermittent tremor on May 15–19. Two brief tremor signals (~3 minutes each) were then observed on May 29, followed by several brief tremor bursts on May 31. AVO again recorded weak tremor bursts on July 24–25 and low-amplitude tremor on July 29. A deep LP earthquake took place on August 1, followed by more weak tremor bursts on August 6–8. On August 15, seismometers recorded LP events with strong frequency banding accompanied by continuous, weak tremor. The activity of 2019 ended with additional tremor pulses that took place on October 18 and December 14.

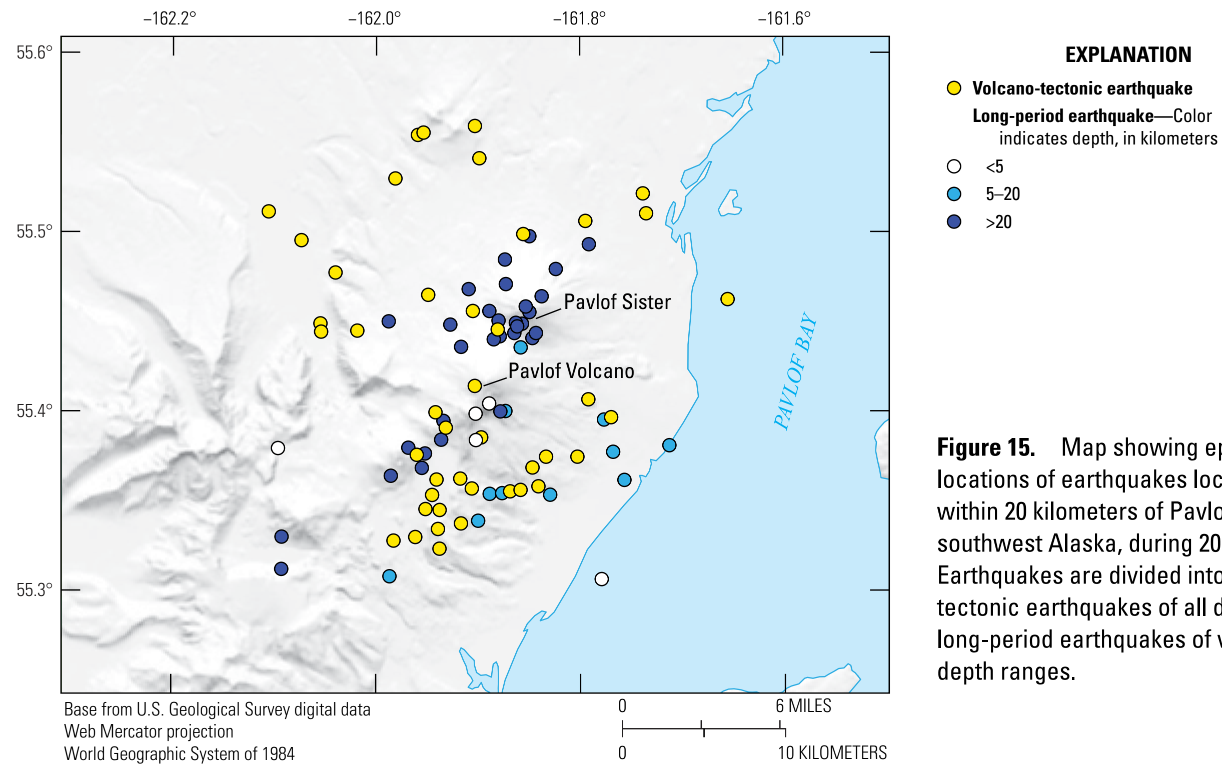

Figure 15. Map showing epicentral locations of earthquakes located within 20 kilometers of Pavlof Volcano, southwest Alaska, during 2019. Earthquakes are divided into volcano-tectonic earthquakes of all depths and long-period earthquakes of various depth ranges.

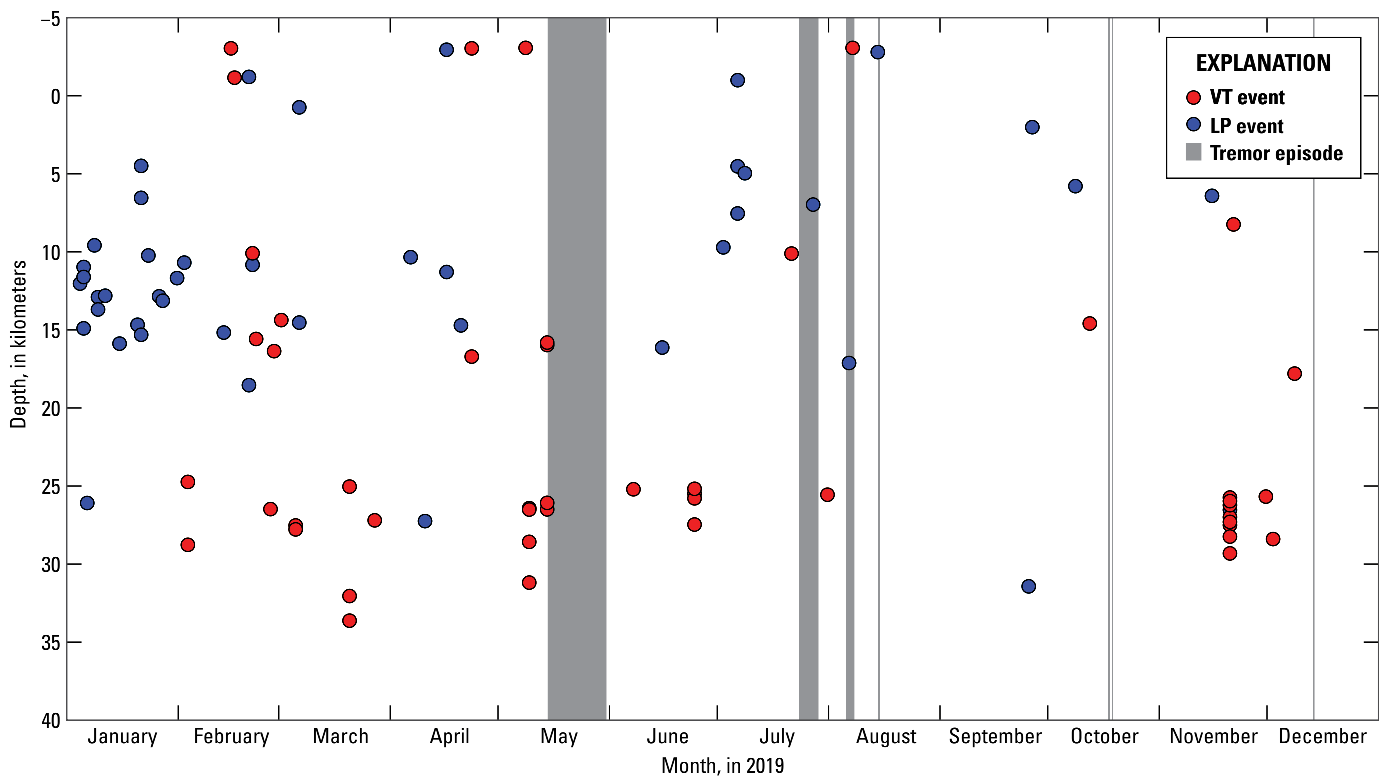

Figure 16. Graph showing hypocentral depths in kilometers (km) and occurrence dates of volcano-tectonic (VT) and long-period (LP) earthquakes and tremor episodes that took place in 2019 at Pavlof Volcano, southwest Alaska. Event depths were calculated relative to sea level; negative depths reflect elevation above sea level.

The annual number of earthquakes located at Pavlof Volcano increased between 2017 and 2019 (fig. 17). This trend is probably influenced by improvements made to Pavlof Volcano's seismic network in the summer of 2017, but the fact that AVO located significantly fewer events in 2019 than 2018 suggests a change in activity level unrelated to the network improvements.

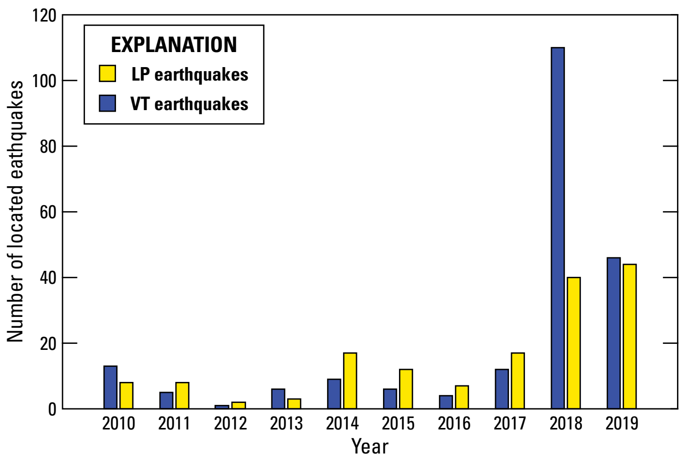

Figure 17. Bar graph showing the number of long-period (LP) and volcano-tectonic (VT) earthquakes located at Pavlof Volcano, southwest Alaska, each year from 2010 to 2019. The sharp increase in 2018 is partly due to network improvements made in 2017.

Isanotski Volcano

GVP #311370
54.768° N., 163.729° W.
2,470 m
Unimak Island, Fox Islands, Aleutian Islands

EARTHQUAKE SWARM RELATED TO GLACIAL ACTIVITY

Isanotski Volcano is a glacially dissected, snow- and ice-covered stratovolcano with a basal diameter of about 10 km. It lies on the east side of Unimak Island, about 80 km southwest of the City of Cold Bay and 1,080 km southwest of Anchorage (fig. 1). Isanotski Volcano is between Shishaldin Volcano and Roundtop Mountain, together arranged in a roughly east-west alignment, but it is much more deeply eroded than its neighbors (Miller and others, 1998). Isanotski Volcano has not erupted during the Holocene.

A series of small earthquakes thought to be associated with glacial activity took place near the summit of Isanotski Volcano in the spring of 2019. Around 13,000 earthquakes were detected from March 12 to May 11, forming several swarms that each lasted hours to days (fig. 18). Tremor bursts were also recorded within a few days after some of the swarms (fig. 19). Sporadic seismicity continued into the summer, although this seismicity was less significant than that of the spring. Most earthquakes recorded near Isanotski Volcano in

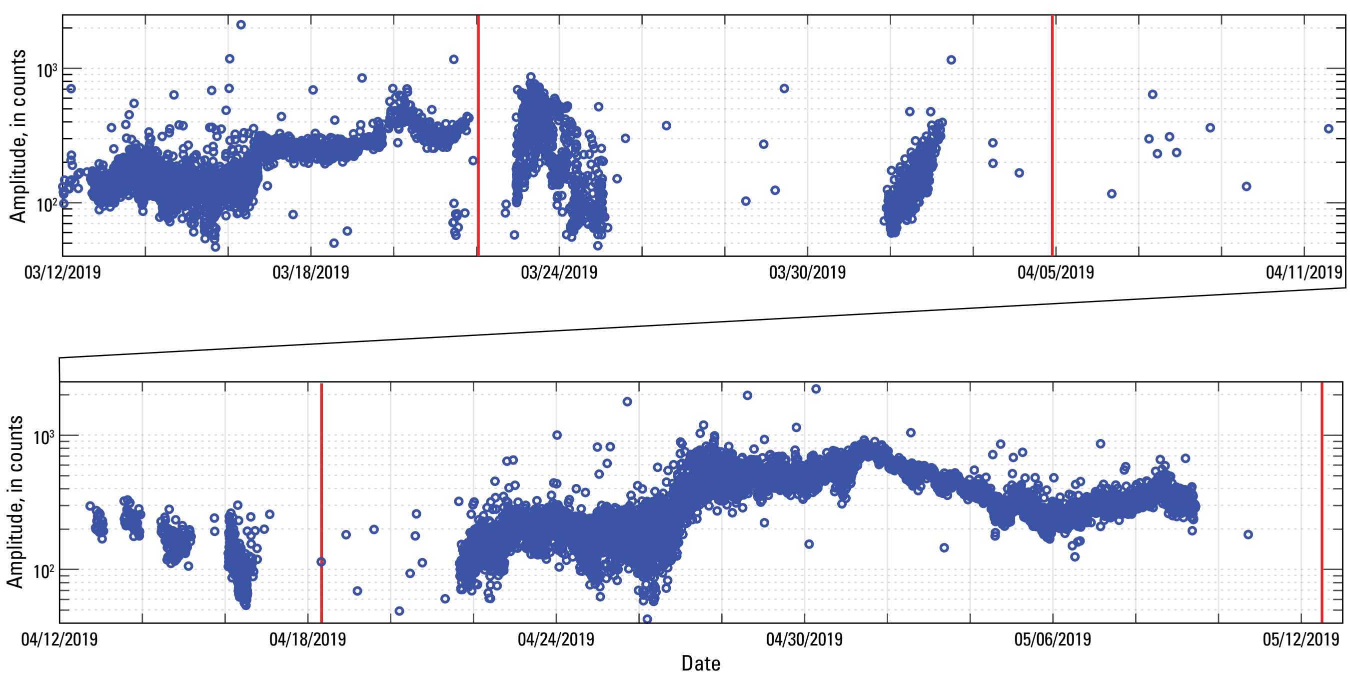

Figure 18. Timeline of earthquakes during the spring 2019 seismic sequence at Isanotski Volcano in the eastern Aleutian Islands, Alaska, from March 12 to May 13. The earthquakes plotted here were cataloged using a matched filter detector with six templates. Not all earthquakes that took place during this period are included in the catalog owing to detector limitations. Dates shown as month/day/year.

2019 were too small to be located, so their local magnitudes could not be determined. However, a larger event on May 1 was located close to the surface near the summit of Isanotski Volcano and had an M_L of −0.3. These traits are consistent with a glacial seismicity source. Photographs taken in August 2019 (fig. 20) show crevasses in the ice on the north side of Isanotski Volcano that may be related to the spring seismicity.

The 2019 seismic sequence began on March 12 at 05:20 UTC (March 11 at 21:20 AKDT) (fig. 18). For the first four days, the earthquakes in the sequence had low amplitudes, but on March 16, events suddenly increased in amplitude and decreased in rate. These events continued until late on March 21. After a 3-hour pause, in the early morning of March 22, a 4-minute-long tremor burst followed the earthquakes (fig. 19*A*). A second swarm began several hours later and ended on March 25. The seismicity resumed on March 31 with a third earthquake swarm that continued for about a day and a half. This was followed by a series of short tremor bursts and LP earthquakes on April 4 (fig. 19*B*).

Another series of earthquake swarms, each lasting less than a day, took place on April 12–16. These were followed by a 1.5-minute-long tremor burst on April 18 (fig. 19*C*). The last large swarm of the sequence started on April 21 and continued until May 9. Like the opening swarm in March, the earthquakes of this final swarm sharply increased in amplitude after about 5 days. The swarm was also followed by a 6-minute-long tremor burst on May 12 (fig. 19*D*). Although the tremor burst concluded the main sequence, tremor was also noted on May 30 and June 1. Occasional earthquakes occurred during the pauses between the March–May swarms, and more occurred afterward until at least July. These sporadic events are difficult to describe thoroughly because they typically had very low amplitudes (which could easily be masked by noise) and because local monitoring is limited.

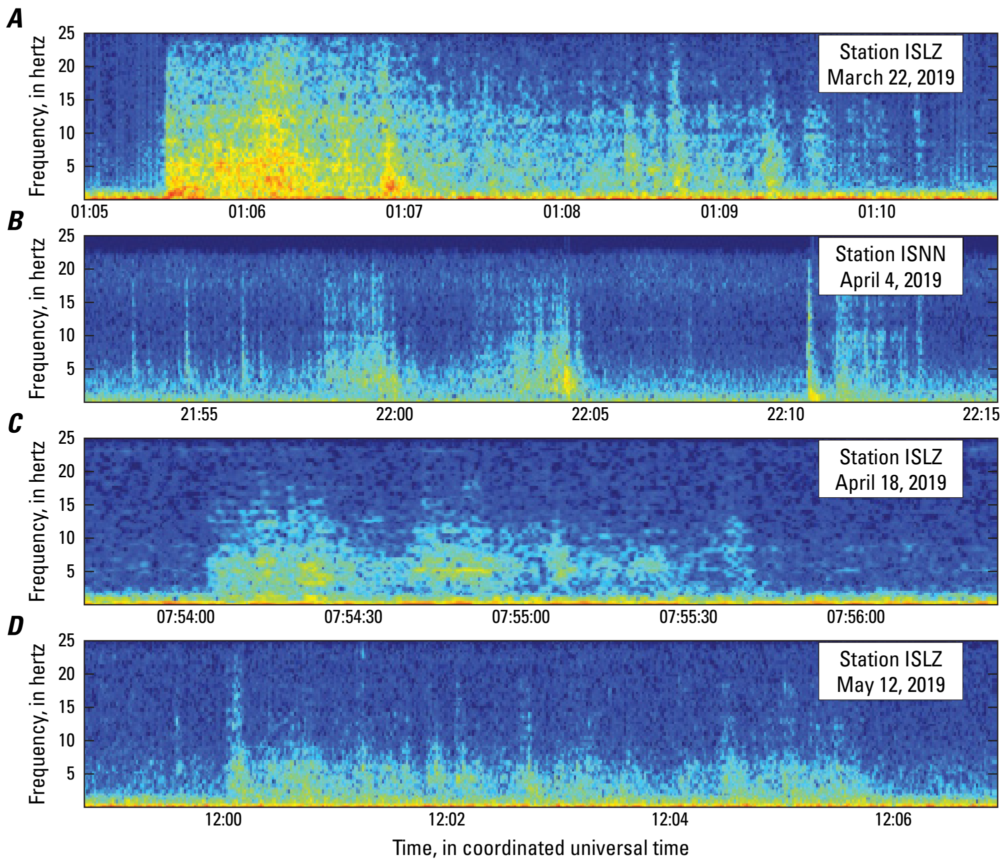

Figure 19. Spectrograms showing timing, frequencies in hertz (Hz), and amplitudes of tremor bursts that took place at Isanotski Volcano in the eastern Aleutian Islands, Alaska. Spectrograms show tremor from March 22 (*A*), April 4 (*B*), April 18 (*C*), and May 12 (*D*), 2019. Durations of these tremor bursts are approximately 4 minutes (min), 8 min (comprising tremor lasting 2 min, 3 min, and 3 min), 1.5 min, and 6 min, respectively. The colors in the spectrum range represent high spectral energy (red) to low spectral energy (blue) at the time and frequency shown.

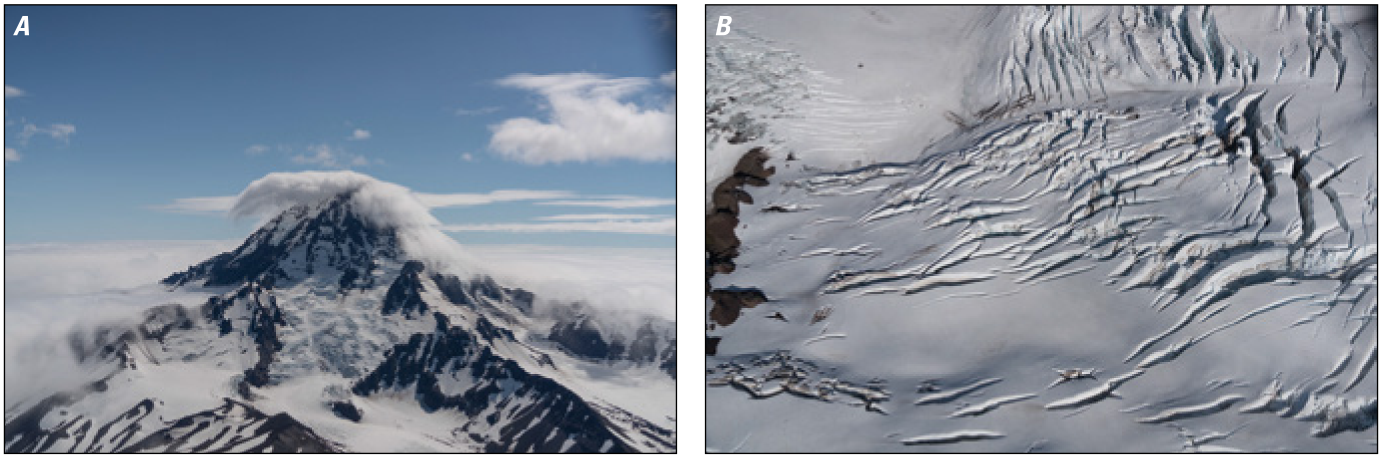

Figure 20. Oblique aerial photographs showing crevasses on the north flank of Isanotski Volcano in the eastern Aleutian Islands, Alaska, taken at a distance, looking south (*A*) and up close, looking northeast (*B*). Photographs by C. Waythomas, U.S. Geological Survey, taken August 2, 2019.

Shishaldin Volcano

GVP #311360
54.755° N., 163.971° W.
2,857 m
Unimak Island, Fox Islands, Aleutian Islands

STROMBOLIAN ERUPTION, LAVA FLOWS, LAHARS, AND ASH CLOUDS

Shishaldin Volcano is a spectacular symmetrical cone with a basal diameter of approximately 16 km. It lies near the center of Unimak Island in the eastern Aleutian Islands, 95 km southwest of the City of Cold Bay and 1,095 km southwest of Anchorage (fig. 1). A steam plume, sometimes with a minor amount of entrained ash, often emanates from the volcano's small summit crater. Shishaldin Volcano is one of the most active volcanoes in the Aleutian Arc (Miller and others, 1998); most of its historical eruptions comprised small ash and steam plumes, although an eruption in April–May 1999 produced a subplinian ash cloud (Nye and others, 2002).

Shishaldin Volcano erupted from July 2019 through the end of the year, with Strombolian explosions, lava flows and lahars on the volcano's flanks, and sporadic ash clouds. The eruption was the most significant at Shishaldin Volcano since 1999, when an eruption produced Strombolian explosions, lahars, and a subplinian ash cloud that reached 45,000 ft (13,700 m) ASL (Nye and others, 2002; Stelling and others, 2002; McGimsey and others, 2004). Prior to 2019, the most recent eruption to send lava flows down the volcano's flanks took place in 1955 (Anchorage Daily News, 1955). A questionable news report from 1976 (Andersen, 1976) described lava flows at Shishaldin Volcano that should probably be attributed instead to Pavlof Volcano, which was erupting at that time. Although Shishaldin Volcano erupted from September through October 1975, no lava flows were reported. Thus, the 2019 flows were likely the first on the flanks of Shishaldin Volcano in 64 years and represent a departure from the typical style of its historically observed eruptions. Eruptions at Shishaldin Volcano more commonly consist of Strombolian explosions and lava fountaining within the summit crater.

The initial 2019 eruptive activity of Shishaldin Volcano began in July, continued into September, and featured the growth of a small spatter cone in the summit crater. The lava column then withdrew in mid-September, causing the crater floor to collapse and pausing the eruption for approximately one month. Activity resumed in mid-October with a new, rapidly growing spatter cone within the summit crater, while small lava flows spilled out of the crater and ran ~2 km down the volcano's north flank. These flows melted into the snow and ice, producing small lahars that followed drainages north to the Bering Sea. Several collapse events from the summit spatter cone in November and December left lobate flowage deposits on Shishaldin Volcano's north flank and produced small ash plumes that drifted downwind. Finally, a collapse event on December 12 produced a larger ash plume, which reached an altitude as high as 23,000 ft (7,000 m) ASL, generated three detected lightning strokes, and deposited ash on the southeast flank of the volcano.

The following paragraphs describe each phase of the 2019 eruption in greater detail. See figure 21 for a summarized timeline of the eruption.

Eruption Buildup (July 1–July 23)

Satellite imagery indicated elevated surface temperatures at Shishaldin Volcano starting July 1, and the brightness temperatures continued increasing for the next two weeks (fig. 21). Tremor and LP earthquakes were also detected during the same period and may have started occurring as early as mid-June. On July 10, field crews noted that the summit plume was unusually vigorous, although no sulfur dioxide (SO_2) was detected in satellite data that day.

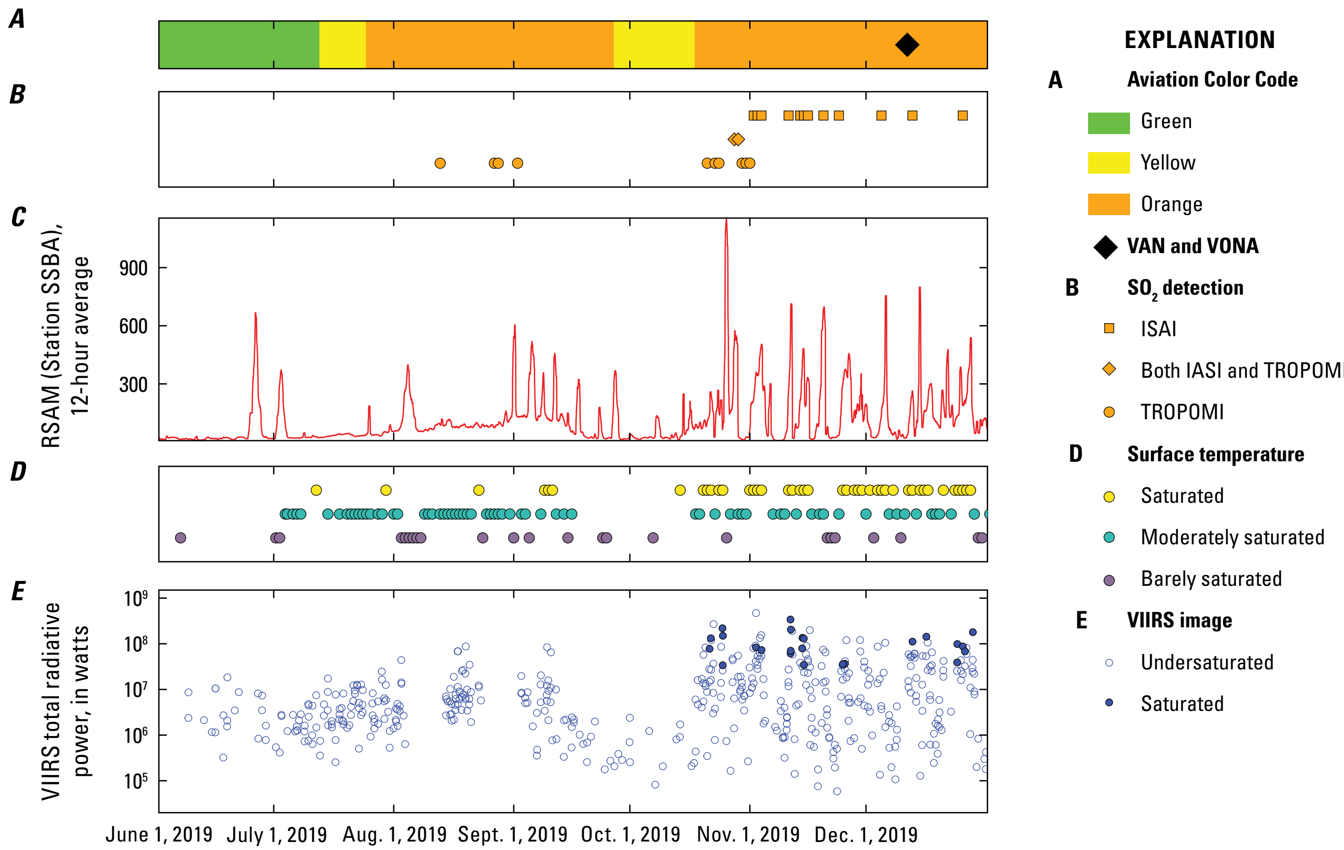

Figure 21. Summary of eruptive activity during June–December 2019 at Shishaldin Volcano, eastern Aleutian Islands, Alaska. *A*, Timeline showing changes in Aviation Color Code and an ash-related Volcanic Activity Notice (VAN) and Volcano Observatory Notice for Aviation (VONA) announcement. *B*, Timeline of sulfur dioxide (SO_2) detections made by Infrared Atmospheric Sounding Interferometer (IASI) instruments onboard the Meteorological Operational satellite series and by the TROPOspheric Monitoring Instrument (TROPOMI) onboard the Copernicus Sentinel-5 Precursor satellite. *C*, Graph of seismic tremor as real-time seismic amplitude measurements (RSAM) (Endo and Murray, 1991). RSAM data were collected at station SSBA, located about 10 kilometers northwest of the volcano's summit. *D*, Timeline of qualitative surface temperature anomalies based on daily satellite observations. *E*, Graph of quantitative radiative power, calculated from Visible Infrared Imagine Radiometer Suite (VIIRS) imagery following the method described in Loewen and others (2021).

On July 12, an overflight by a crew associated with the Plate Boundary Observatory recorded visible incandescence within the summit crater (K. Austin, University NAVSTAR Consortium [UNAVCO], written commun., 2019). This report, along with increasing surface temperatures detected in satellite data and increased seismic activity, prompted AVO to raise the Aviation Color Code and Volcano Alert Level to **YELLOW** and **ADVISORY** on July 13. Elevated surface temperatures and an increasing amplitude of seismic tremor continued from July 12 to 23.

Cone Eruption (July 24–September 19)

On July 23, AVO field crews photographed several new volcanic features at the summit of Shishaldin Volcano: a small cone within the summit crater, active lava flowing around the base of this cone, and minor tephra deposits on the inside walls of the crater (fig. 22). The confirmation of active lava at the surface triggered AVO to raise the Aviation Color Code and Volcano Alert Level to **ORANGE** and **WATCH** on July 24.

Clear, high-resolution satellite images documented the spatter cone as it continued to grow and showed signs of activity through mid-September (fig. 23). These images also showed occasional light ash deposits on the upper flanks of the volcano, but no lava or significant amounts of ash appeared outside the summit crater.

Bursts of seismic tremor, thought to be caused by Strombolian explosions, were first detected on July 25 and occurred intermittently through August. This eruptive style was confirmed on August 16 by a passing observation plane operated by the National Oceanic and Atmospheric Administration Alaska Fisheries Science Center, which recorded visible and infrared video of the volcano (fig. 24). Seismic tremor, recorded as real-time seismic amplitude measurements (RSAM) (fig. 21), also steadily increased through August, peaked around September 6, and then decreased markedly after September 14. Minor SO_2 emissions were detected on August 27–28 and September 2 in sensitive ultraviolet (UV) satellite images (from the TROPOspheric Monitoring Instrument [TROPOMI] on the Copernicus Sentinel-5 Precursor satellite), but not by less-sensitive

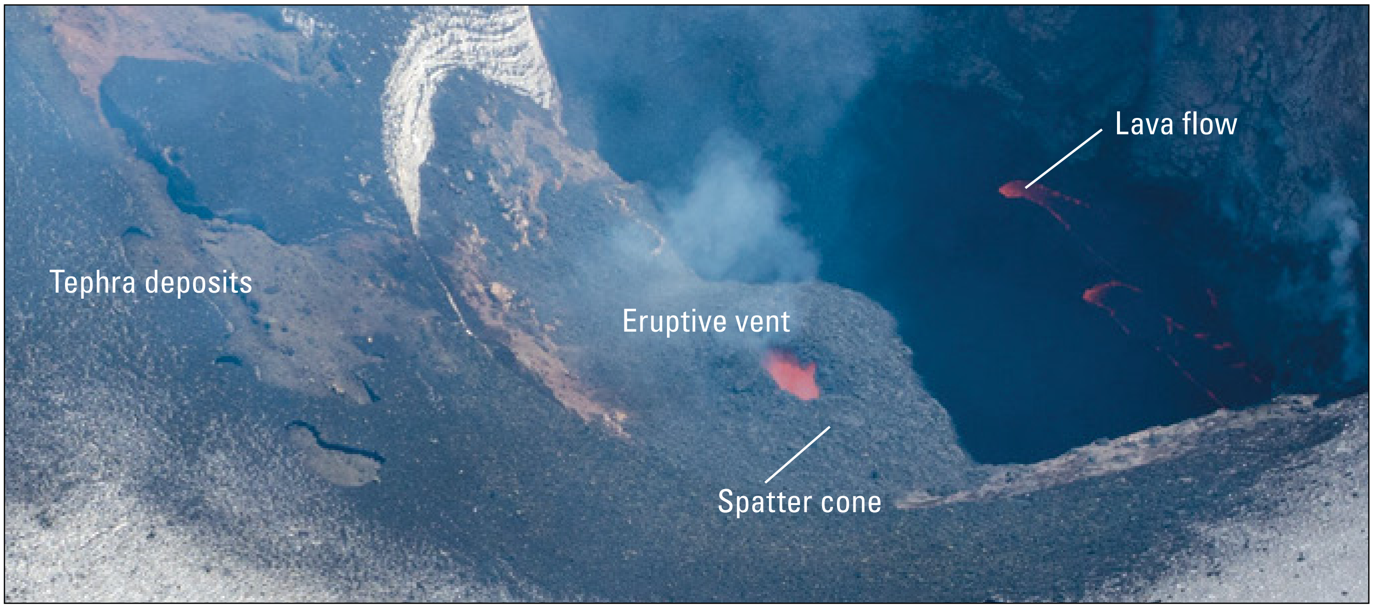

Figure 22. Aerial photograph taken July 23, 2019, showing the eruptive vent, a small spatter cone, a lava flow, and tephra deposits within the summit crater of Shishaldin Volcano, located in the eastern Aleutian Islands, Alaska. Photograph by D. Ketner, U.S. Geological Survey.

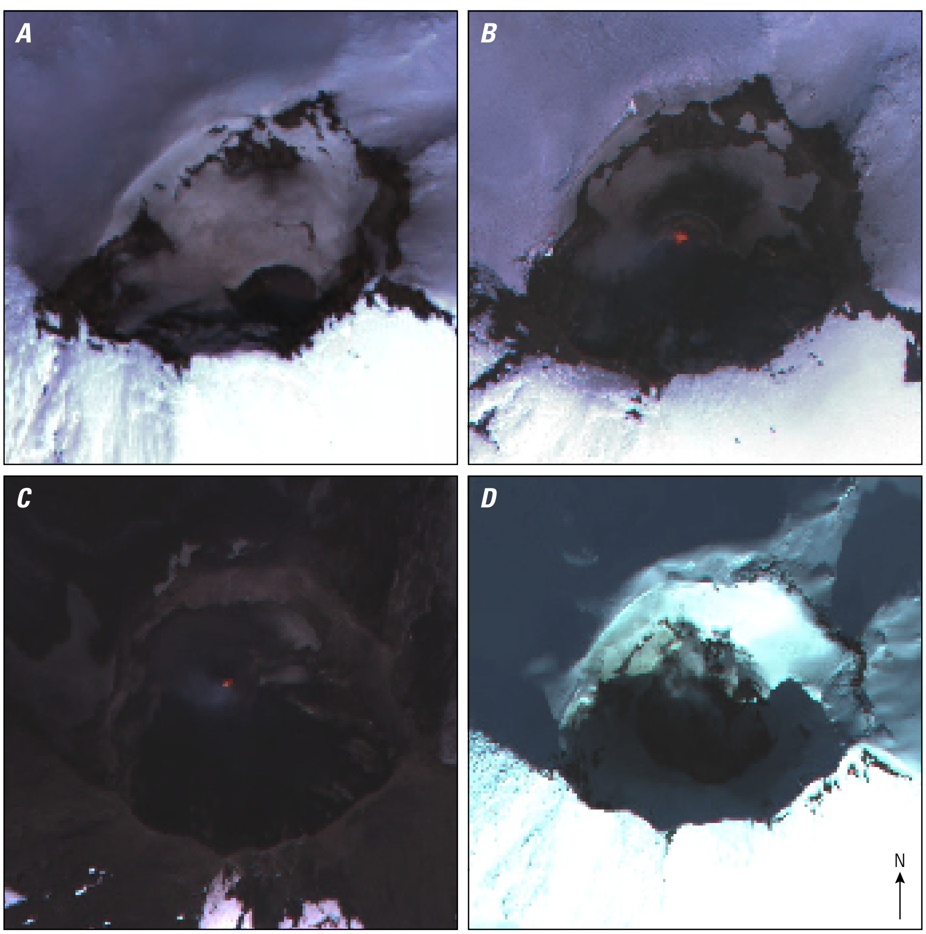

Figure 23. Near-infrared satellite images of eruptive activity at Shishaldin Volcano (eastern Aleutian Islands, Alaska) from July to October 2019. *A*, WorldView-2 image acquired on July 3 at 21:59 coordinated universal time (UTC), showing a snow-free area at the bottom of the summit crater but no recent ash deposits or high-temperature spectral signatures. *B*, WorldView-3 image acquired on July 20 at 22:23 UTC, showing recent ash deposits within the summit crater and a high-temperature spectral signature at the top of a growing spatter cone. *C*, WorldView-3 image acquired on August 15 at 22:43 UTC, showing continued cone activity and growth. *D*, WorldView-3 image acquired on October 3 at 02:23 UTC during a period of quiescence, showing the collapsed cone area and light steaming but no active lava. The crater is 230 meters in diameter across its longest axis; all images are at the same scale but are not orthorectified, resulting in different apparent crater dimensions due to the satellite viewing angles.

Figure 24. Still image from an aerial video taken August 16, 2019, during an overflight of Shishaldin Volcano in the eastern Aleutian Islands, Alaska. Video recorded by S. Dahle, National Oceanic and Atmospheric Administration Alaska Fisheries Science Center.

infrared (IR) satellite sensors (Infrared Atmospheric Sounding Interferometer [IASI] instruments onboard the Meteorological Operational satellite series). The last visual confirmation of eruptive activity at the summit during this period was a Landsat 8 satellite image taken on September 9.

Clear, high-resolution satellite images showed that the spatter cone continued growing with signs of activity through mid-September, although it remained confined within the summit crater (fig. 23). Besides the occasional dusting of light ash on the upper flanks of the volcano, no lava or significant amounts of ash were deposited outside the crater.

Pause (September 19–October 13)

On September 19, the spatter cone, which had grown since July, collapsed into the crater. The event was recognized during a retrospective analysis of borehole tiltmeter data from stations installed on the flanks of Shishaldin Volcano by the UNAVCO Plate Boundary Observatory (fig. 25). This collapse was the largest-amplitude tilt signal recorded during the eruption and is interpreted to reflect the drainage of magma from the conduit.

Although cloudy conditions blocked satellite views at the time of the collapse event, clear satellite images taken on September 23 showed reduced mid-IR signatures, indicating lower surface temperatures and a lack of significant eruptive activity. More satellite images taken on September 26 confirmed the crater floor had collapsed and that no evidence of ongoing eruptive activity remained. As a result, on September 26, AVO downgraded the Aviation Color Code and Volcano Alert Level to **YELLOW** and **ADIVSORY**. The lack of eruptive activity and the collapse of the cone were again confirmed in a clear, high-resolution satellite image taken on October 3 (fig. 23*D*).

Renewed Eruption; North Flank Lava Flows and Lahars; Cone Collapses (October 13–End of Year)

On October 13, satellite imagery showed an increase in surface temperatures at Shishaldin Volcano, signaling renewed eruptive activity. More satellite observations from October 17 confirmed the growth of a new spatter cone within the summit crater. In response, AVO changed the Aviation Color Code and Volcano Alert Level to **ORANGE** and **WATCH** later that day. Activity at the volcano escalated rapidly, as indicated by the detection of Strombolian explosions in infrasound data, observations of incandescence in webcam images, the detection of SO_2 emissions in satellite data, and an increase in seismic tremor. Infrasound signals were first recorded on October 18 and took place at 15–30-second intervals by October 21. The first observation of incandescence at Shishaldin Volcano during this period was made from a webcam on the southwest flank of Isanotski Volcano during the night of October 19–20. On October 21, satellite TROPOMI sensors detected SO_2 emissions, and AVO recorded a spike of seismic tremor at the volcano. This first tremor spike, as well as subsequent ones, was characterized by RSAM values that increased slowly over several days and sharply decreased over several hours, resulting in a “shark fin” pattern.

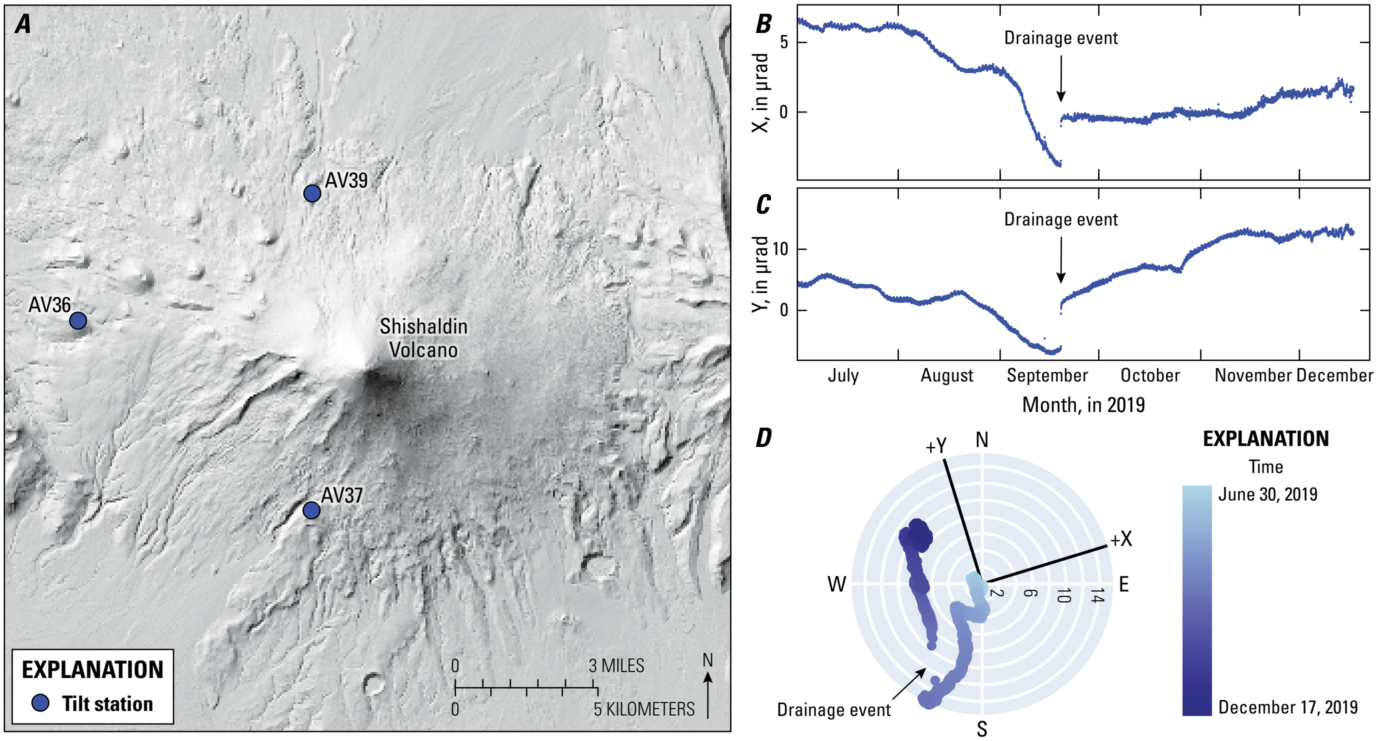

Base map modified from Esri and its licensors, copyright 2022
Web Mercator projection
World Geographic System of 1984

Figure 25. Tilt station network map and tiltmeter data from the latter half of 2019 at Shishaldin Volcano in the eastern Aleutian Islands, Alaska. *A*, Shaded relief map of Shishaldin Volcano showing the tilt station network. *B*, Time series graph showing variation of horizontal-axis (X) tilt in microradians (µrad) at station AV37 from July 1 to December 21, 2019 (after which frost-related deformation dominated). *C*, Time series graph showing variation of vertical-axis (Y) tilt in µrad at AV37 over the same period. *D*, Rose plot of X and Y tilts, rotated into north-south and east-west coordinates, with tilt in µrad. The most notable tilt signal, recorded September 19, 2019, is interpreted to reflect the drainage of the magma column from the conduit system. During this event, AV37 moved rapidly toward the edifice, likely because of depressurization.

On October 24, during another seismic tremor peak, a clear satellite image captured an active, 800-meter-long lava flow traveling down the northwest flank of Shishaldin Volcano (fig. 26). The flow melted snow and ice, generating a lahar that had traveled ~3 km down drainages to the north. In addition, minor ash deposits were seen on snow 8 km southeast of the summit in the image. The same day, an anonymous pilot of a passing airplane reported to AVO the presence of clouds over the volcano that looked like “smoke rings.” The regional infrasound array at Sand Point, Alaska, detected clear explosions associated with this activity.

Cyclic increases in seismic tremor, presumably from Strombolian-type explosions, were accompanied by ash and gas emissions and continued to take place through the end of 2019. Observers on a passing U.S. Fish and Wildlife Service flight and AVO field crews on Unimak Island confirmed this Strombolian-type explosive behavior on November 11 and December 20, respectively. At times of increasing tremor amplitude and when viewing conditions permitted, active lava flows on the north flank of the volcano (fig. 26) were seen in satellite and webcam views and by observers in the City of Cold Bay (fig. 27). Infrared satellite sensors also detected an increase in radiative power at the volcano, reflecting the increased effusive activity (fig. 21).

In partnership with UNAVCO, AVO scientists experimented with recording high-rate tilt data (1 sample per second) using the tiltmeter at station AV36, located on the western margin of Shishaldin Volcano (fig. 25). The

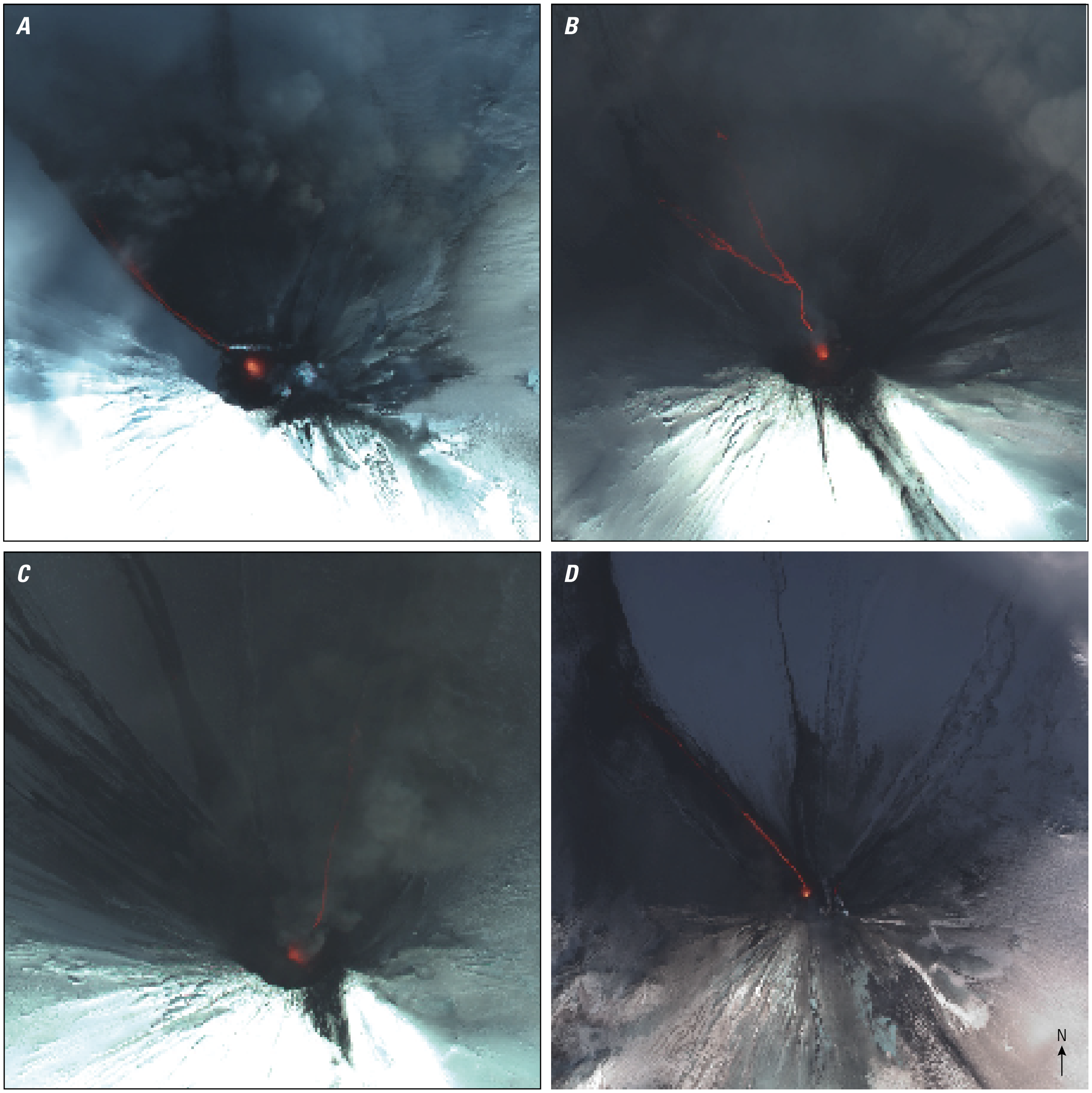

Figure 26. Near-infrared satellite images of lava flow activity at Shishaldin Volcano (eastern Aleutian Islands, Alaska) in October–December 2019. Images taken October 24 by WorldView-2 (*A*), November 3 by WorldView-3 (*B*), November 11 by WorldView-3 (*C*), and December 26 by WorldView-2 (*D*). Lahars extend farther down-drainage from this lava flow, beyond the image extent. The crater is 230 meters in diameter across its longest axis; images are not orthorectified, resulting in distance offset due to satellite viewing angle and terrain. Part *D* shown at a smaller scale than parts *A*–*C*.

Figure 27. View of Shishaldin Volcano erupting on the evening of December 12, 2019, as seen from the City of Cold Bay in the eastern Aleutian Islands, Alaska. Photograph by A. Merculief.

instrument detected several episodes of explosive activity at the summit while recording at this sampling rate; during each episode, the data showed an hours-long increase in amplitude culminating in several hours of high-amplitude activity bursts (for example, see figure 28). Ground motions during these events were generally tangential to the edifice. These data show that open-system volcanoes like Shishaldin Volcano generate appreciable ground deformation over timescales and at amplitudes that can be recorded by borehole tiltmeters.

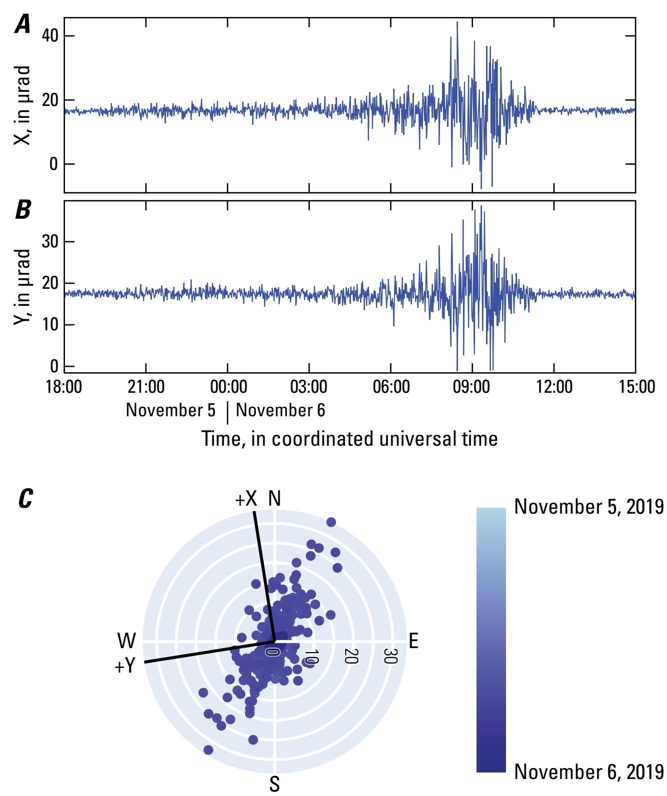

Figure 28. Tiltmeter data graphs from Shishaldin Volcano (eastern Aleutian Islands, Alaska) containing 21 hours of high-rate (1 sample per second) tilt data from station AV36, spanning November 5, 2019, at 18:00 coordinated universal time (UTC) (09:00 Alaska standard time [AKST]) to November 6, 2019, at 15:00 UTC (06:00 AKST). *A*, Time series graph showing variation of horizontal-axis (X) tilt in microradians (µrad). *B*, Time series graph showing variation of vertical-axis (Y) tilt in µrad. Graphs *A* and *B* illustrate high-frequency ground motions due to explosive activity at the summit; note the gradual increase of noise beginning at about 20:00 UTC (09:00 AKST) on November 5. *C*, Rose plot of X and Y tilts, rotated into north-south and east-west coordinates, with tilt in µrad.

During the summer and early fall of 2019, only UV satellite instruments, such as TROPOMI, detected SO_2 at Shishaldin Volcano as a result of their higher sensitivity than IR sensors. Detections from these instruments stopped in November, however, as the available UV light decreased. In contrast, IR SO_2 sensors, such as IASI sensors, although less sensitive, do not lose effectiveness in the winter. IASI sensors began detecting SO_2 from Shishaldin Volcano on October 28, and these detections continued in November and December (fig. 21). Considering the lower sensitivity of satellite IR to SO_2, the IASI detections indicate that gas emissions were higher at the end of the year than earlier in the eruption.

After each tremor and emission spike, activity quickly decreased and clear satellite images showed a pause in lava effusion. Synthetic Aperture Radar (SAR) images from the TerraSAR-X and TanDEM-X satellites, provided during the eruption by S. Plank (German Aerospace Center), indicated that the summit spatter cone experienced partial collapses during many of these episodes. Collapse events were specifically noted on November 11, November 23, December 5, and December 12. Lobate flowage deposits appeared downslope from the cone after each event.

The largest of these collapse events, which took place on December 12 at 16:10 UTC, was detected in seismic and infrasound data, webcam photos, and satellite imagery. Photographs of the volcano after the event showed an ash cloud reaching an altitude of about 25,000 ft (7,600 m) ASL. Three lightning strokes were also detected from this cloud. Unlike other collapse events, the December 12 event was followed by elevated tremor and continued lava effusion, the latter of which was visible in satellite images and in photographs taken from the City of Cold Bay (fig. 27). This event was associated with the largest ashfall of 2019, although only a minor amount of ash was deposited on the southeast flank of Shishaldin Volcano.

A field crew visited Shishaldin Volcano on December 20, 2019 (fig. 29), and although the lava flows were inactive during the visit, the vent itself was producing regular

Figure 29. Photograph taken December 20, 2019, of an Alaska Volcano Observatory geologist collecting tephra (mixed with wind-scoured snow) from the December 12 cone collapse event at Shishaldin Volcano, in the eastern Aleutian Islands, Alaska. Ash emissions from Strombolian activity at the summit are visible in the background. Photograph by W. Mayo, Alaska Division of Geological & Geophysical Surveys.

Strombolian explosions. The crews sampled the December 12 ash deposit, later analysis of which determined the tephra to be a mix of lithic, tachylite, and sideromelane grains (figs. 30, 31). The sideromelane grains were basaltic, with glass composed of ~52 weight percent SiO_2 and minerology consisting of plagioclase, olivine, and magnetite, although only plagioclase and olivine existed as larger (greater than 0.1 millimeter) phenocryst phases. The high proportion of tachylite and lithic grains in the tephra supports a cone-collapse origin for the deposit—the composition indicates a high proportion of the material was mobilized from previously deposited and cooled grains.

The next active lava effusion periods were noted on December 21 and December 26 (after the December field visit). Cloudy conditions generally obscured activity at Shishaldin Volcano during the last few days of the year, but eruptive activity continued into January 2020.

Although the 2019 eruption deposited only minor amounts of ash on the flanks of Shishaldin Volcano, the lava flows from the event extended 1–2 km down its north flank. Associated lahar deposits traveled even farther, reaching as far north as the Bering Sea (fig. 32). The lava flows of 2019 were the first historically well-documented ones at Shishaldin Volcano and likely represented the first lava flow activity outside its summit crater in more than 60 years.

Westdahl volcano

GVP #311340
54.571° N., 164.648° W.
1,560 m
Unimak Island, Fox Islands, Aleutian Islands

LONG-TERM INFLATION

Westdahl volcano is a broad, gently-sloping, ice-capped volcano on the west end of Unimak Island, 140 km northeast of the City of Unalaska, Alaska, and 1,145 km southwest of Anchorage (fig. 1). The volcano comprises Westdahl Peak, Westdahl caldera, Pogromni Volcano, and several other related intracaldera and flank features. Its summit ice cap is inferred

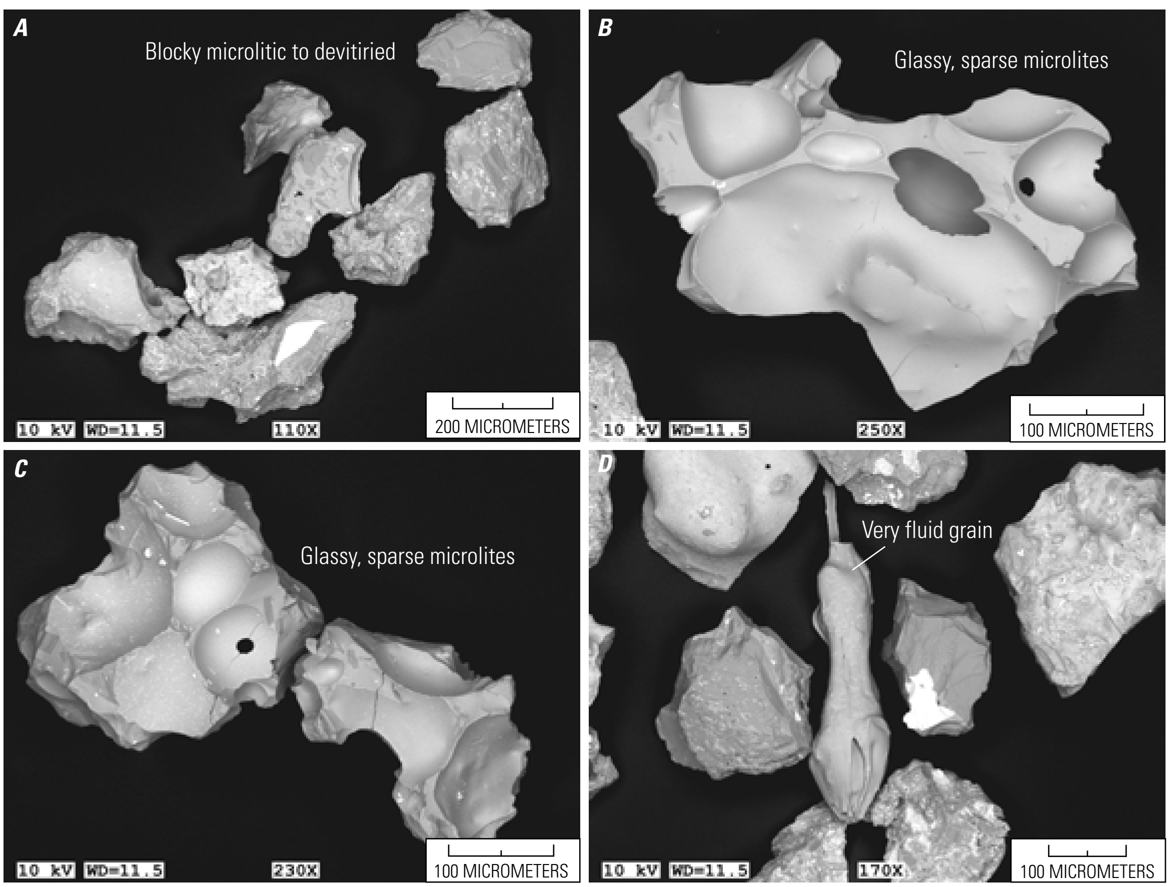

Figure 30. Scanning electron microscope (SEM) images of tephra that erupted from Shishaldin Volcano (eastern Aleutian Islands, Alaska) on December 12, 2019, and was collected by crews on the southeast flank of the volcano on December 20. Morphology types include glassy grains with blocky microlites to devitrified grains (*A*), glassy grains with sparse microlites (*B, C*), and grains with very fluid shapes (*D*). Images captured using a JEOL brand 6510LV SEM in low vacuum mode, with accelerating voltage shown in kilovolts (kV) and working distance (WD) shown in millimeters (mm).

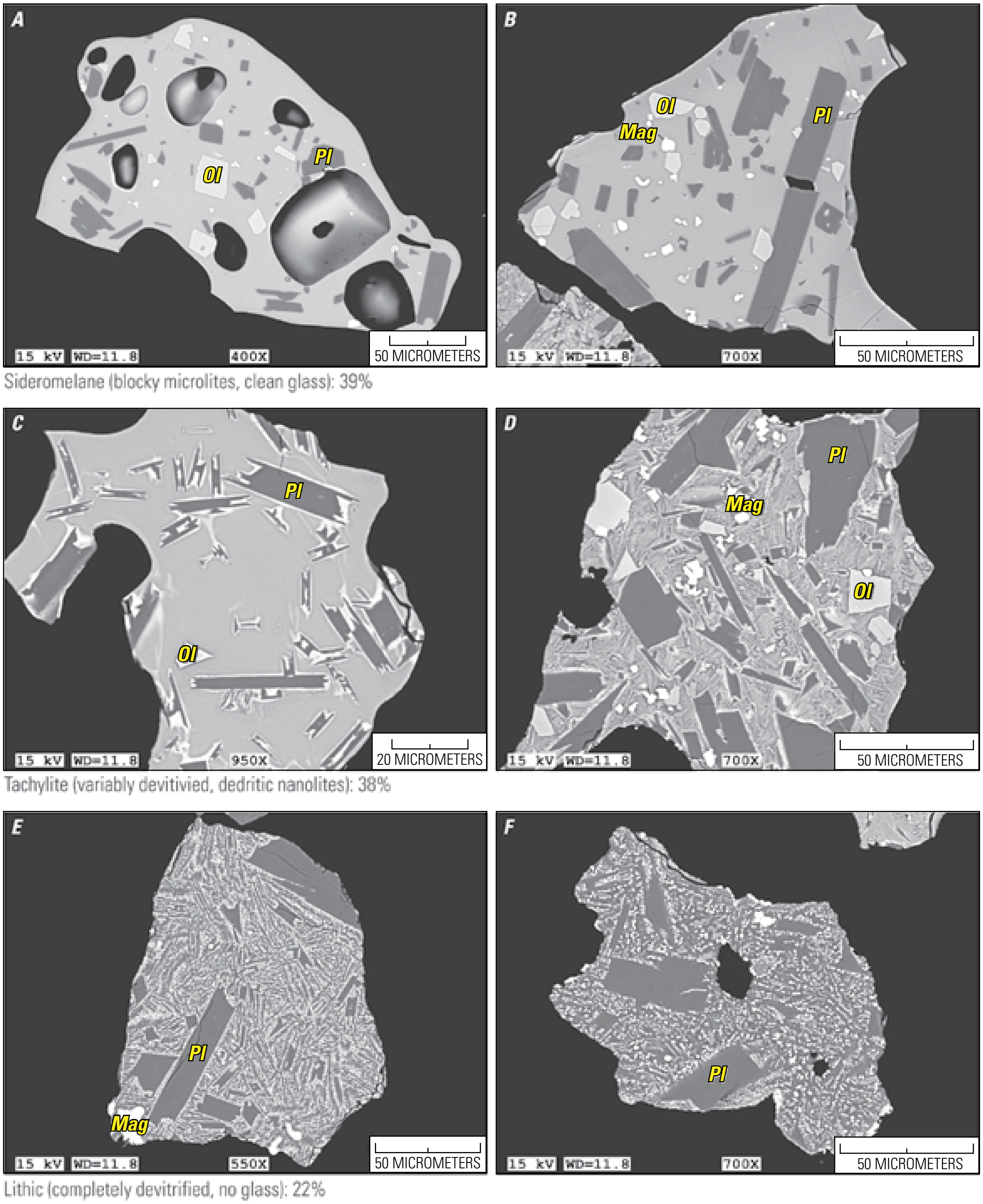

Figure 31. Backscattered electron images of tephra components erupted from Shishaldin Volcano in the eastern Aleutian Islands, Alaska, on December 12, 2019 (collected December 20), showing three compositional groups. *A*, *B*, Sideromelane grains with a glassy matrix, rounded vesicles, and blocky microlites, which includes 39 percent (%) of tephra grains. *C*, *D*, Tachylite grains with partially devitrified matrix glass and dendritic nanolites, which includes 38 percent of tephra grains. *E*, *F*, Lithic grains with no remaining glass and few or no vesicles, which includes 22 percent of tephra grains. Dark gray crystals are plagioclase (Pl), light gray are olivine (Ol), and white are magnetite (Mag). Componentry classification made following Loewen and others (2021). Images captured using a JEOL 6510LV Scanning Electron Microscope, with accelerating voltage shown in kilovolts (kV) and working distance (WD) shown in millimeters (mm).

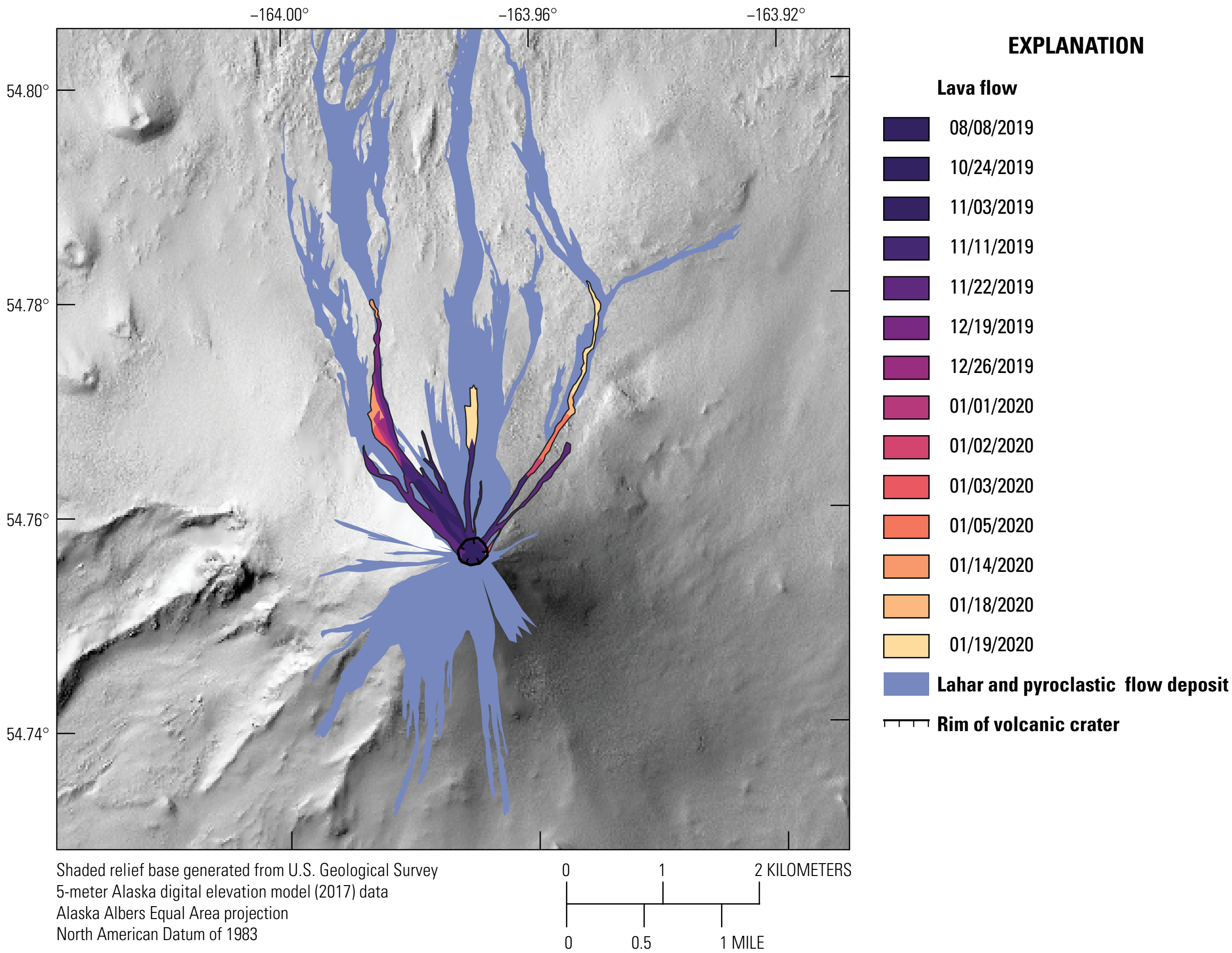

Figure 32. Map of Shishaldin Volcano, located in the eastern Aleutian Islands, Alaska, showing lava flows, lahar deposits, and pyroclastic density current deposits emplaced in 2019. Deposit outlines are approximate and based on orthorectified WorldView-1, WorldView-2, and WorldView-3 satellite images.

to fill an older caldera (Calvert and others, 2005). Continued volcanism after this caldera's collapse produced several vents, the youngest of which are Faris and Westdahl Peaks. In contrast, the satellite volcano Pogromni Volcano, located northwest of Westdahl volcano's summit, probably predates the formation of the caldera (Calvert and others, 2005). Most known historical eruptions at Westdahl volcano have included an explosive phase involving the interaction of lava and ice, followed or accompanied by the production of blocky lava flows and lahars (McGimsey and others, 1995; Miller and others, 1998; Dean and others, 2002). The last notable unrest at Westdahl volcano was a period of increased seismicity in 2010 (Neal and others, 2014).

In 2019, Westdahl volcano continued its long-term trend of steady inflation, which has persisted since the trend was first observed after the installation of a GNSS network on Unimak Island in 2008 (figs. 33, 34). An analysis of Westdahl volcano InSAR data by Lu and others (2003) indicated a magma reservoir exists beneath the volcano at a depth of about 6 km below sea level. Continued inflation of Westdahl volcano is consistent with an ongoing accumulation of melt at relatively shallow depths. The volcano remained at **GREEN** and **NORMAL** throughout 2019.

Akutan Volcano

GVP #311320
54.133° N., 165.986° W.
1,303 m
Akutan Island, Fox Islands, Aleutian Islands

NO SYSTEMATIC DEFORMATION

Akutan Volcano (comprising Akutan Peak and other related intracaldera and flank volcanic features) is a symmetrical stratocone that composes the west half of Akutan Island (fig. 1). It is one of the most active volcanoes of the Aleutian Arc and has

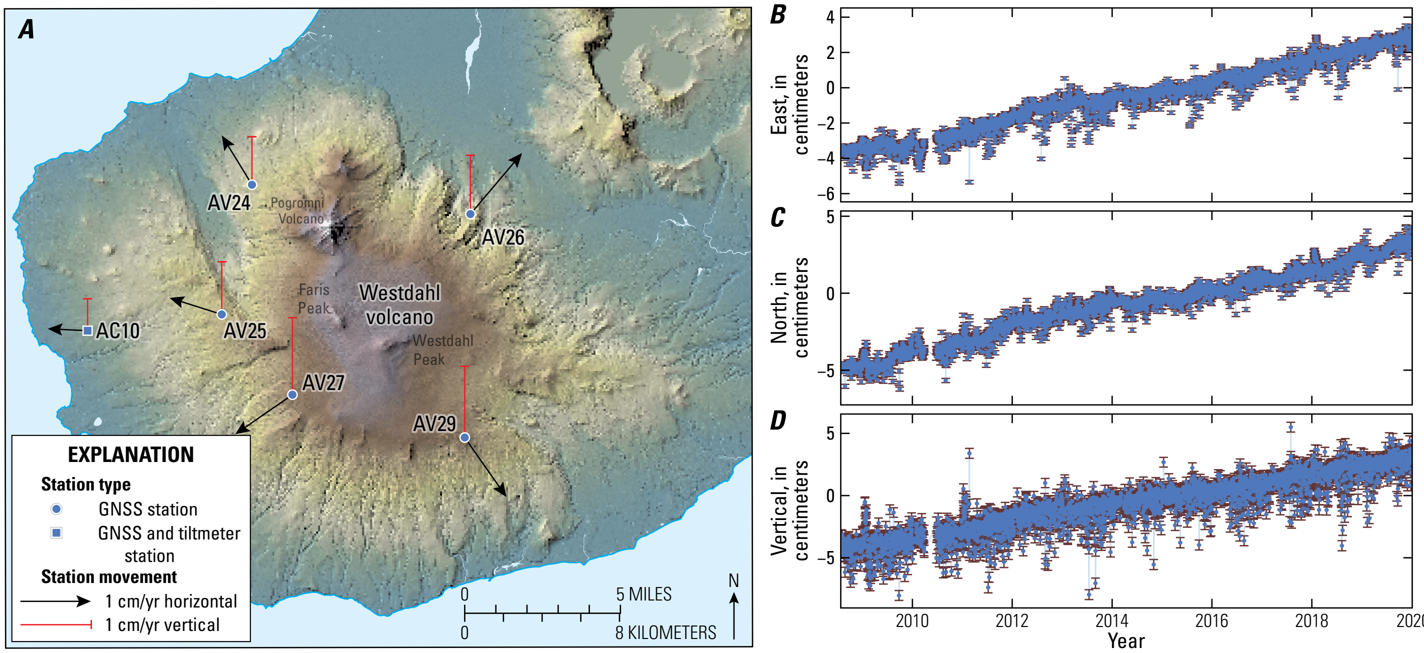

Base from National Map,
WGS 1984 Web Mercator

Figure 33. Global Navigation Satellite System (GNSS) station velocity map (*A*) and displacement time series graphs for station AV26 (*B*–*D*) showing deformation from July 30, 2008, through 2019 at Westdahl volcano, eastern Aleutian Islands, Alaska. Long-term displacement of AV26, plotted in the east, north, and vertical directions, indicates inflation as sites moved up and away from the volcano. Most GNSS stations at Westdahl volcano are co-located with tiltmeters. Velocities and displacement shown with respect to station AB06 near False Pass, Alaska. Error bars in *B*–*D* show 1-sigma error. cm/yr, centimeter per year.

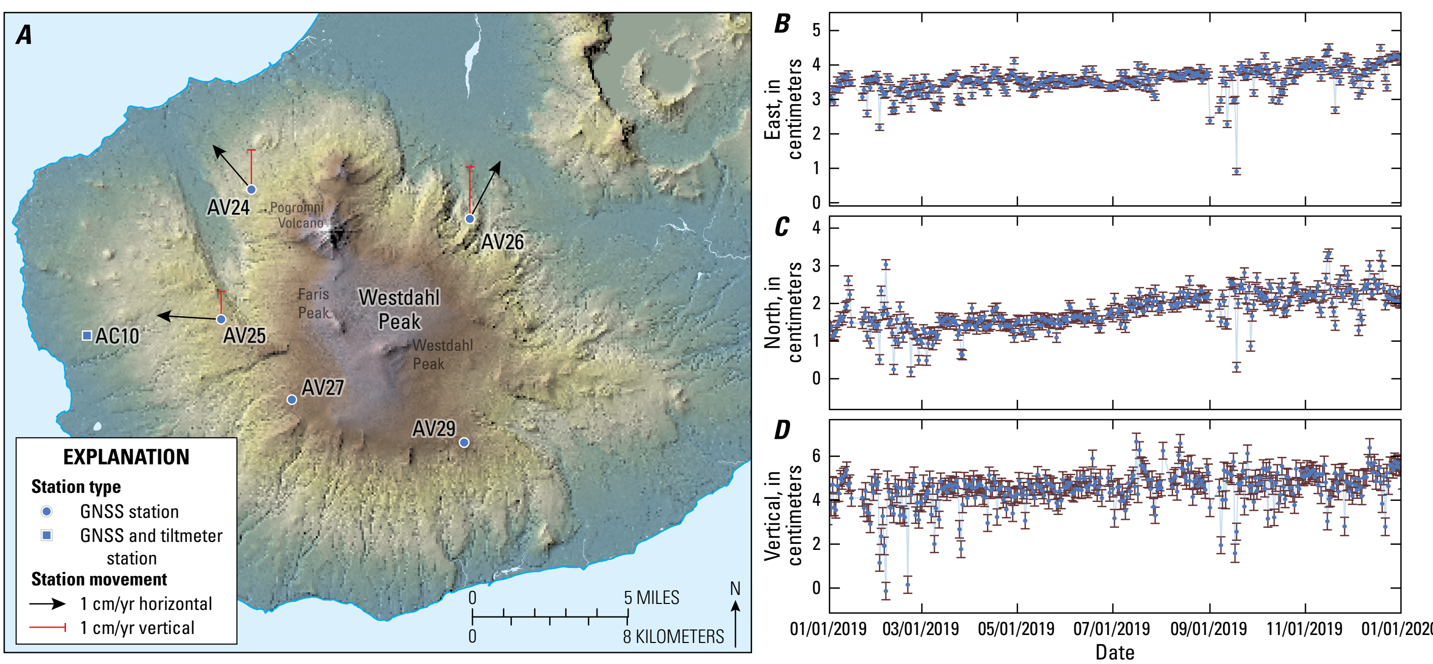

Base from National Map,
WGS 1984 Web Mercator

Figure 34. Global Navigation Satellite System (GNSS) station velocity map (*A*) and displacement time series graphs for station AV26 (*B*–*D*) showing deformation from January 1 to December 31, 2019, at Westdahl volcano, eastern Aleutian Islands, Alaska. Velocities and displacement shown with respect to AB06 near False Pass, Alaska. Error bars in *B*–*D* show 1-sigma error. Only three stations at Westdahl volcano—AV24, AV25, and AV26—provided enough data in 2019 to determine reliable velocities. Dates in month/day/year. cm/yr, centimeter per year.

erupted more than 31 times since 1790, most recently in 1992 (McGimsey and others, 1995). Its 2-kilometer-wide circular caldera, which is breached to the northwest, is ringed by several satellite vents ranging from the Pleistocene to late Holocene (Coombs and Jicha, 2021), although all historical activity has taken place at an intracaldera cinder cone measuring about 200 m high (Richter and others, 1998b; Waythomas and others, 1998).

Akutan Volcano is 45 km northeast of the City of Unalaska and 1,235 km southwest of Anchorage, although one of the region's largest seafood processing plants is only 10 km east of the caldera rim. In March 1996, two strong earthquake swarms took place on the island, causing minor damage and prompting some residents and plant workers to leave (Lu and others, 2000). In response, a permanent seismic network was installed on the island in the summer of 1996.

In prior years, activity at Akutan Volcano was characterized by a pattern of long-term reinflation (fig. 35), first observed after AVO field crews installed a Global Positioning System (GPS) network on the volcano in 2005. In 2019, however, the volcano deviated from this long-term trend by showing no systematic deformation that could be confidently linked to a volcanic source (fig. 36). DeGrandpre and others (2017) have previously noted the episodic nature of deformation at Akutan Volcano and suggested the inflation might reflect the unsteady recharge of a magma reservoir located 6–10 km beneath the volcano. The Aviation Color Code and Volcano Alert Level for the volcano remained at **GREEN** and **NORMAL** throughout 2019.

Makushin Volcano

GVP #311310
53.887° N., 166.932° W.
1,800 m
Unalaska Island, Fox Islands, Aleutian Islands

EARTHQUAKE SWARMS

Makushin Volcano is on Unalaska Island in the eastern Aleutian Islands, 25 km west of the City of Unalaska and 1,295 km southwest of Anchorage (fig. 1). The volcano is a broad, truncated, and deeply glaciated stratovolcano with a summit caldera about 3 km in diameter. The summit is capped by an icefield with an area of about 40 square kilometers (km^2), but as the ice cover has retreated, a small intracaldera cinder cone hosting a turquoise-colored lake, abundant fumaroles, and an ice cauldron has become a conspicuous feature. Makushin Volcano is credited with 18 historical eruptions, the latest of which took place on January 30, 1995, and which consisted

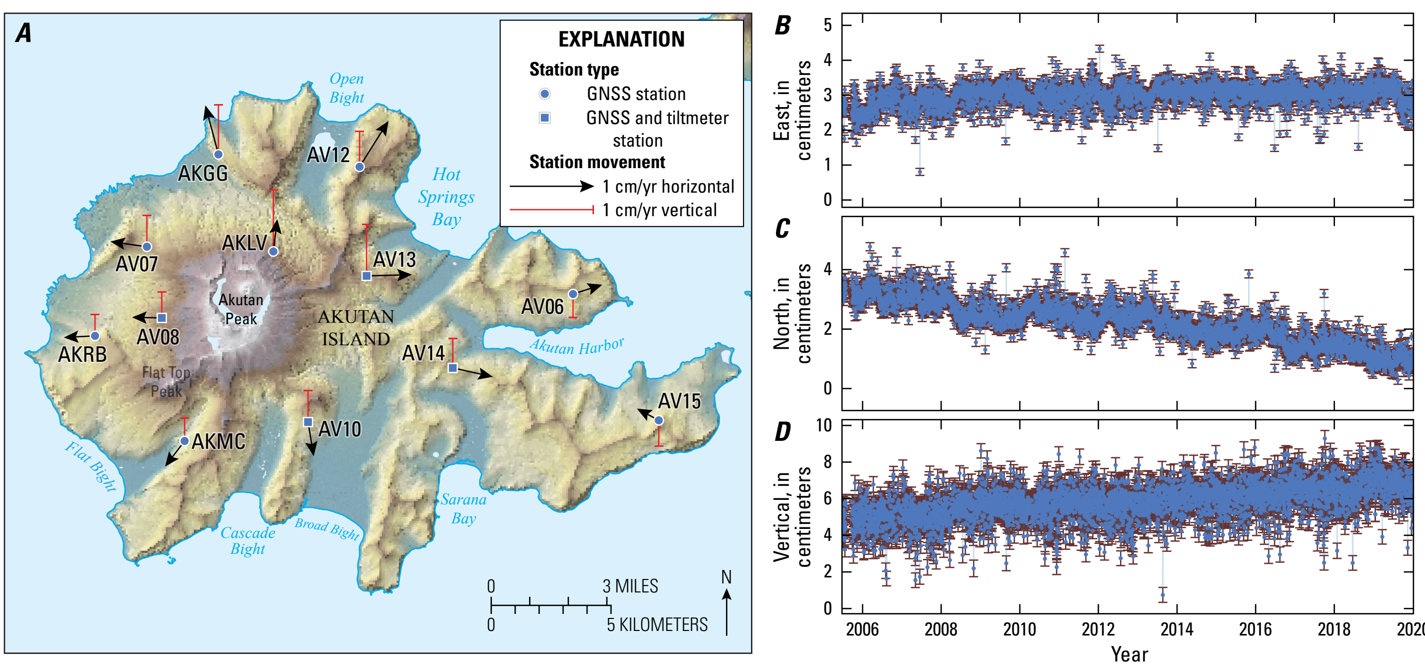

Base from National Map,
WGS 1984 Web Mercator

Figure 35. Global Navigation Satellite System (GNSS) station velocity map (*A*) and displacement time series graphs for station AV10 (*B*–*D*), showing deformation from 2005 through 2019 at Akutan Volcano, eastern Aleutian Islands, Alaska. The long-term displacement of AV10, plotted in the east, north, and vertical directions, indicates inflation at a subtle rate of less than 1 centimeter per year, with more rapid inflation steps modulating this background rate. Some GNSS stations at Akutan Volcano are co-located with tiltmeters. Velocities and displacement shown with respect to station AV09 near Dutch Harbor, Alaska. Error bars in *B*–*D* show 1-sigma error. Dates in month/day/year. cm/yr, centimeter per year.

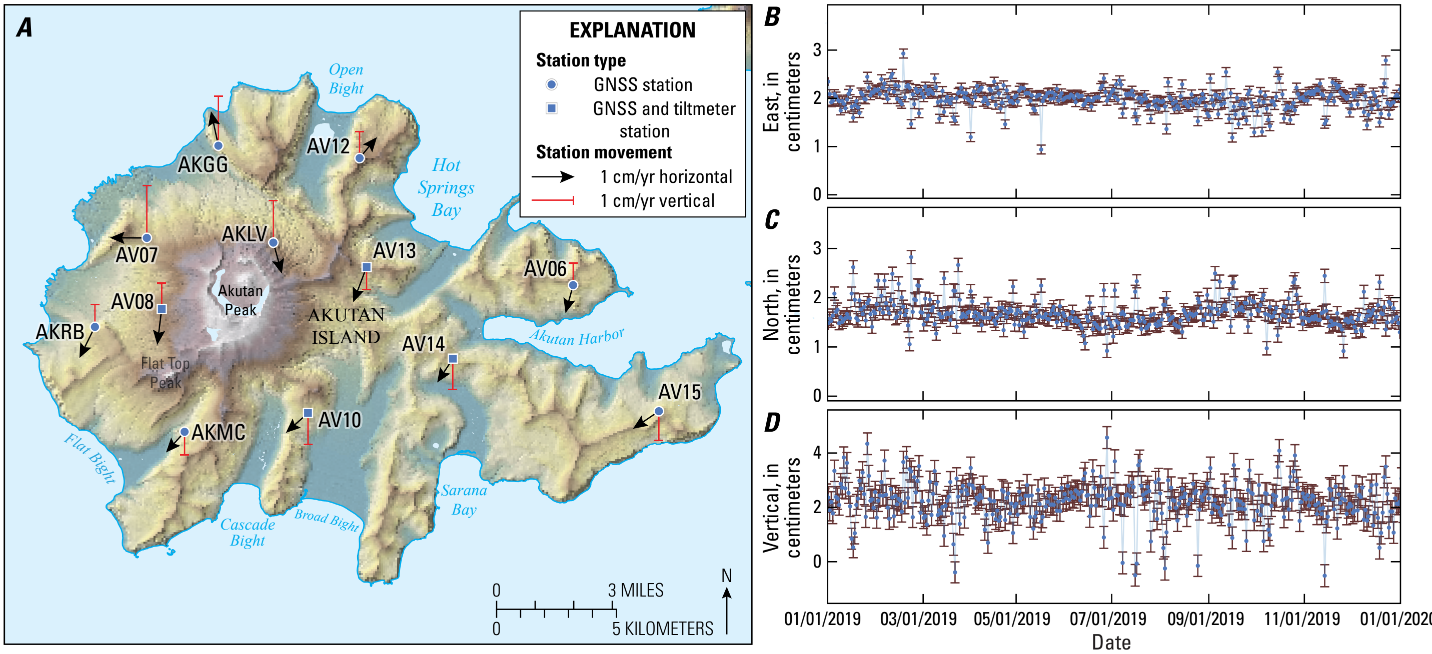

Base from National Map,
WGS 1984 Web Mercator

Figure 36. Global Navigation Satellite System (GNSS) station velocity map (*A*) and displacement time series graphs for station AV10 (*B*–*D*) showing deformation from January 1 to December 31, 2019, at Akutan Volcano, eastern Aleutian Islands, Alaska. The displacement of AV10, plotted in the east, north, and vertical directions, appears erratic, with no systematic deformation field. Some GNSS stations at Akutan Volcano are co-located with tiltmeters. Velocities and displacement shown with respect to station AV09 near Dutch Harbor, Alaska. Error bars in *B*–*D* show 1-sigma error. cm/yr, centimeter per year.

of a small summit explosion that ejected ash to an altitude of about 8,000 ft (2,400 m) ASL (McGimsey and Neal, 1996; Begét and others, 2000).

Earthquake swarms are common at Makushin Volcano and several took place in 2019. Most swarms consisted of fewer than 10 events each; however, two more prominent swarms (on May 15 and June 18) contained more than 40 events each. Earthquakes in both swarms were located at depths of 5–10 km. The May 15 swarm comprised 45 earthquakes, located 17 km east of the volcano's summit, and the June 18 swarm comprised 66 earthquakes, located 1–3 km southeast of the summit. A third, smaller swarm of 19 earthquakes took place on June 22, at similar depths to the earlier swarms and 11–12 km east-southeast of the summit. The Aviation Color Code and Volcanic Alert Level of Makushin Volcano remained at **GREEN** and **NORMAL** throughout the year.

Mount Okmok

GVP #311290
53.419° N., 168.132° W.
1,073 m
Umnak Island, Fox Islands, Aleutian Islands

INFLATION; SEISMIC TREMOR

Mount Okmok is a shield volcano comprising a 10-kilometer-wide caldera (Okmok Caldera), intracaldera cones, flank cones, and lava flows (fig. 37). Making up most of the east end of Umnak Island in the eastern Aleutian Islands, the volcano is about 115 km southwest of the City of Unalaska and 1,390 km southwest of Anchorage (fig. 1). Mount Okmok is built on a base of Tertiary volcanic rocks and consists of three rock series: (1) older flows and pyroclastic beds of a pre-caldera shield complex, (2) pyroclastic deposits of two major caldera-forming eruptions, and (3) a post-caldera field of small cones and lava flows (Byers, 1959; Larsen and others, 2007). Mount Okmok has erupted several times historically, typically producing small ash plumes, although some ash emissions reached higher altitudes. The caldera has a history of lava flows, with recent flows emplaced on its floor in 1945, 1958, and 1997 (Begét and others, 2005). The most recent eruption of Mount Okmok was a phreatomagmatic event in the summer of 2008 that produced an ash cloud that may have reached as high as 52,000 ft (15,800 m) ASL (Neal and others, 2011). Thermal springs and fumaroles occur within the caldera and at Hot Springs Cove, located between Mount Okmok and Mount Recheshnoi (20 km to the southwest).

In 2019, Mount Okmok continued the long-term reinflation that began after its last eruption in 2008. This deformation takes place in discrete pulses that appear modulated onto a lower-rate, steady background deformation

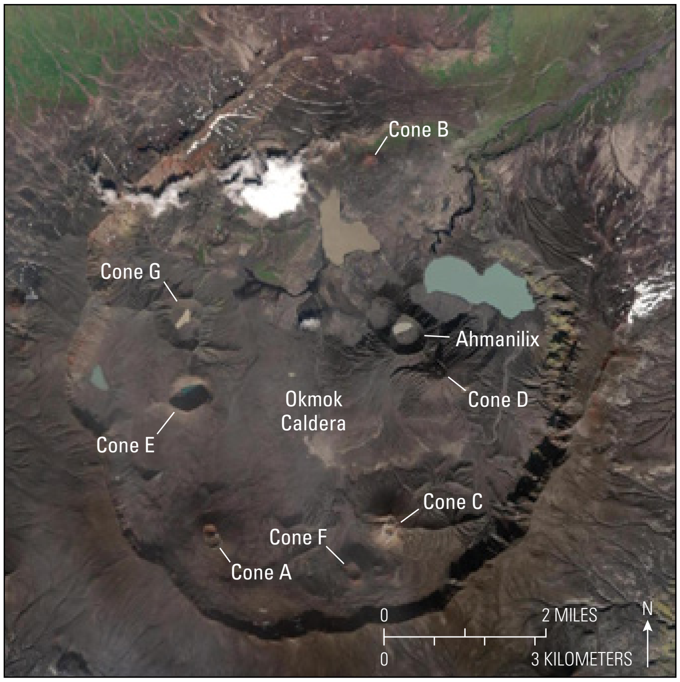

Figure 37. Satellite image of Mount Okmok in the eastern Aleutian Islands, Alaska, showing its caldera and intracaldera cones.

(for example, Xue and others, 2020). Like in 2018, a complete pulse took place in 2019 and was visible in the time series of monitoring station OKCE (fig. 38). The total displacement values were much less for the 2019 pulse, however, producing amplitudes of 4–5 centimeters (cm) in the horizontal and ~5 cm in the vertical components (fig. 39). These are roughly half the amplitudes of the horizontal and vertical components recorded in the 2018 pulse. Past analyses of geodetic data (GNSS and InSAR) suggested a magma reservoir lies 2–3 km below sea level beneath the caldera floor (for example, Freymueller and Kaufman, 2010; Lu and Dzurisin, 2014), but more recent work suggests the existence of a shallow sill at 0.9 km and a pressure point source at 3.2 km below sea level (Xue and others, 2020). Regardless, continued inflation of the volcano is consistent with ongoing accumulation of melt at shallow depths.

AVO scientists identified several seismic tremor episodes at Mount Okmok in September 2019. These began with a short tremor burst recorded on September 4 following observations of a few deep, low-frequency earthquakes on August 21 and 24. Several more tremor bursts were recorded on September 5. A series of longer (2–3 minute) tremor bursts took place on September 6, with bursts recurring every 10 minutes for about 90 minutes. AVO observed similar seismic activity again on September 9 (fig. 40). The tremor episodes were not formally locatable, but the difference in tremor amplitudes between

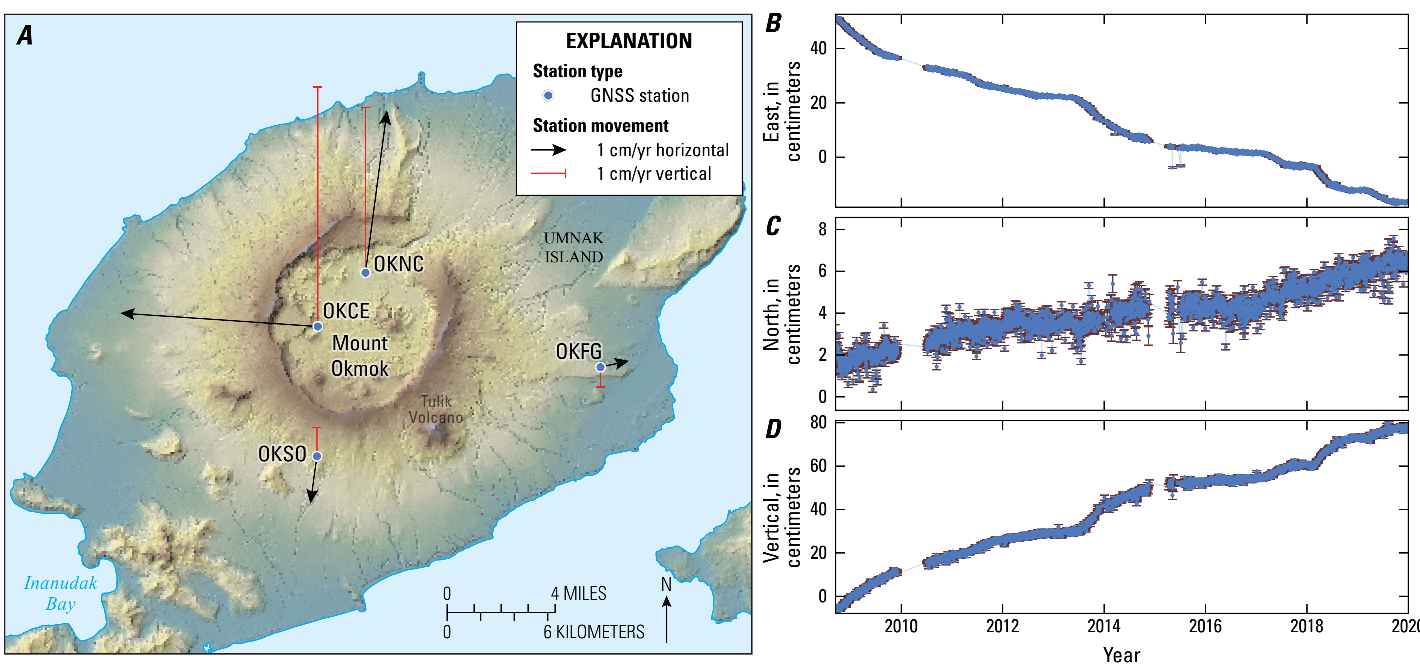

Base from National Map,
WGS 1984 Web Mercator

Figure 38. Global Navigation Satellite System station velocity map (*A*) and displacement time series graphs for station OKCE (*B*–*D*), showing deformation from September 15, 2008, through December 31, 2019, at Mount Okmok, eastern Aleutian Islands, Alaska. The displacement of OKCE, plotted in the east, north, and vertical directions, shows inflation that takes place in steps modulated onto a long-term inflation trend. Velocities and displacement shown with respect to station AV09 near Dutch Harbor, Alaska. Error bars in *B*–*D* show 1-sigma error. cm/yr, centimeter per year.

seismic stations suggests the tremor took place near cone A (fig. 37). Note that cone A and the other cones in Okmok Caldera have no formal names; the names used herein are informal.

In addition to monitoring this activity through daily seismic checks, AVO implemented internal seismic and infrasound alarms to detect any increases in unrest. Satellite data showed no signs of unrest at Mount Okmok during these events, and the local infrasound array recorded no acoustic emissions. A retrospective analysis, however, found that the tremor onset coincided with a stop in the long-term inflation signal typically seen in geodetic data (fig. 39). Intermittent tremor bursts continued after the early September activity before finally subsiding in late November. The tremor bursts of 2019 did not lead to greater unrest, so the Aviation Color Code and Volcano Alert Level of Mount Okmok remained at **GREEN** and **NORMAL** throughout the year.

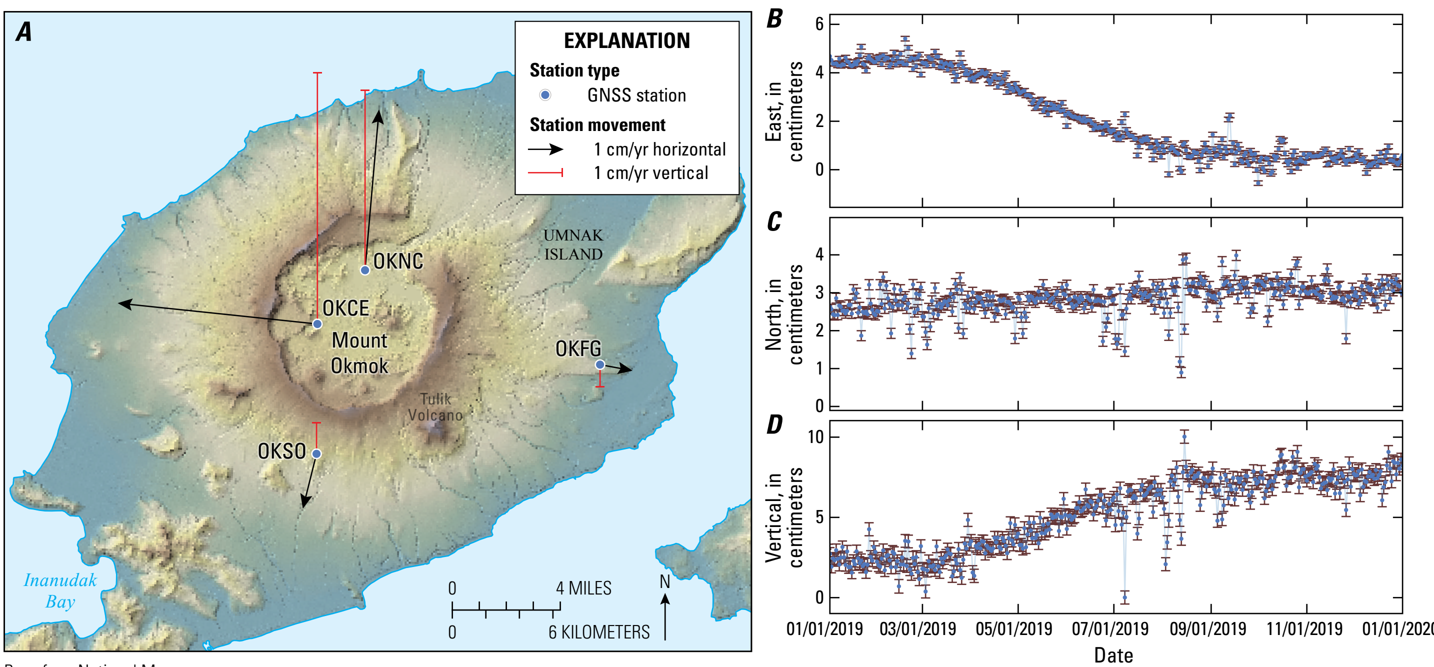

Base from National Map,
WGS 1984 Web Mercator

Figure 39. Global Navigation Satellite System (GNSS) station velocity map (*A*) showing deformation at Mount Okmok (eastern Aleutian Islands, Alaska) from January 1 to December 31, 2019, with contemporaneous displacement time series graphs for station OKCE (*B*–*D*). Velocities and displacement shown with respect to station AV09 near Dutch Harbor, Alaska. Error bars in *B*–*D* show 1-sigma error. Dates shown as month/day/year. cm/yr, centimeter per year.

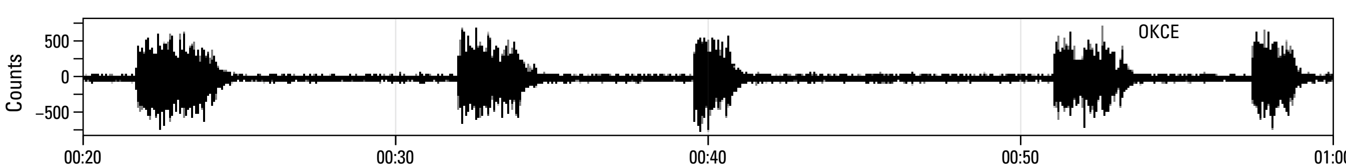

Figure 40. Seismic data from station OKCE, showing example tremor bursts at Mount Okmok (eastern Aleutian Islands, Alaska) from 00:20–01:00 coordinated universal time on September 9, 2019. Waveforms are band-pass filtered from 1 to 8 hertz.

Mount Cleveland

GVP #311240
52.822° N., 169.945° W.
1,730 m
Chuginadak Island, Islands of Four Mountains, Aleutian Islands

EXPLOSIVE ERUPTION AND DOME GROWTH

Mount Cleveland forms the west side of the uninhabited Chuginadak Island, part of the Islands of the Four Mountains group in the east-central Aleutian Islands (fig. 1). Mount Cleveland is about 75 km west of the community of Nikolski and 1,525 km southwest of Anchorage. Its historical eruptions have been characterized by short-lived ash explosions, lava fountaining, lava flows, and pyroclastic flows. In February 2001, after 6 years of quiescence, Mount Cleveland had three explosive events that sent ash to altitudes as high as 30,000 ft (9,100 m) ASL, produced a pyroclastic flow that reached the ocean, and erupted a rubbly lava flow (Dean and others, 2004; McGimsey and others, 2005). Intermittent explosive eruptions have taken place every year since 2001, most significantly during 2011–2012.

Mount Cleveland was relatively quiet during 2019, producing only one small explosive eruption in early January (figs. 41, 42). Despite the paucity of eruptions, its behavior otherwise was similar to that of previous years, with elevated surface temperatures (fig. 41) and nearly continuous degassing from the summit that produced weak steam emissions.

The volcano began 2019 at an Aviation Color Code and Volcano Alert Level of **ORANGE** and **WATCH**, having erupted a few days earlier on December 29, 2018. On January 7, 2019, after several days of quiescence, AVO downgraded the Aviation Color Code and Volcano Alert Level to **YELLOW** and **ADVISORY**. The volcano answered with a small explosion on January 9, recorded in local seismic (fig. 41) and infrasound data. No associated plume was observed above the meteorological clouds, which reached an altitude of about 10,000 ft (3,000 m) ASL at the time. Later satellite imagery showed a thin tephra deposit extending southeast from the summit (fig. 43). AVO did not change the Aviation Color Code and Volcano Alert Level in reaction to this event.

Satellite imagery taken on January 12 revealed the presence of a new dome 75 m in diameter, and by January 17, it had grown to 90 m. In response, AVO raised the Aviation Color Code and Volcano Alert Level to **ORANGE** and **WATCH**. The dome stopped growing soon after, and when no explosion took place, the Aviation Color Code and Volcano Alert Level were lowered back to **YELLOW** and **ADVISORY** on February 25.

Thermal anomalies and a small summit steam plume appeared occasionally in satellite imagery over the following several months. Clear satellite views in August 2019 showed that a pit, centered on the January dome (fig. 44), had formed since February. More satellite imagery acquired in

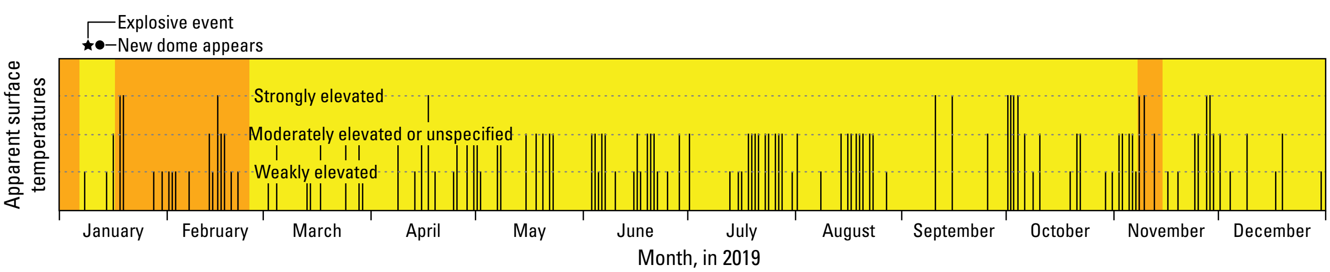

Figure 41. Chart of thermal anomalies in 2019 at Mount Cleveland (eastern Aleutian Islands, Alaska) showing the subjective strength (apparent surface temperatures) of anomalies as recorded in the Alaska Volcano Observatory's internal remote sensing database by analysts. Background colors indicate periods with Aviation Color Codes of YELLOW and ORANGE. The explosive event on January 9 and the appearance of a new dome on January 12 are also shown.

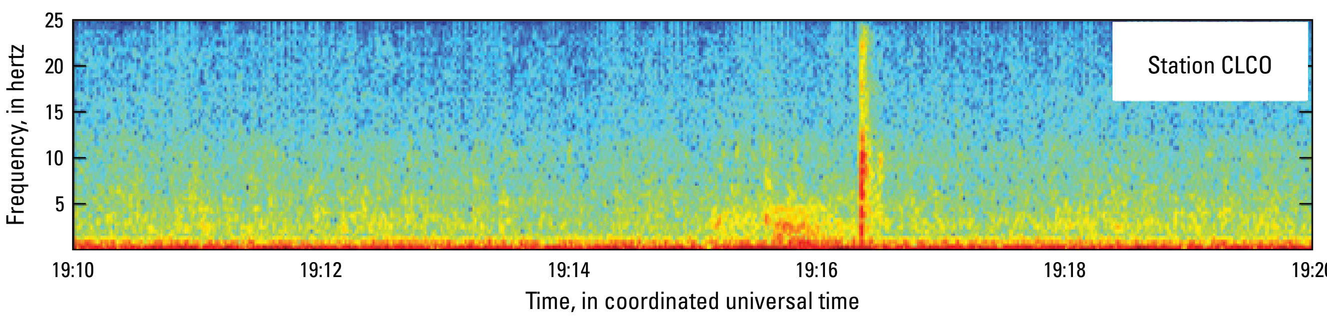

Figure 42. Spectrogram from station CLCO showing the explosion of January 9, 2019, at Mount Cleveland, located in the eastern Aleutian Islands, Alaska.

early November indicated uplift of the new summit dome. Because this uplift was coincident with an apparent increase in the brightness of the summit thermal anomaly and a more robust steam plume, AVO raised the Aviation Color Code and Volcano Alert Level to **ORANGE** and **WATCH**. Subsequent satellite imagery, however, showed that the uplift was an artifact from the satellite viewing angle and was not real. The Aviation Color Code and Volcano Alert Level for Mount Cleveland were returned to **YELLOW** and **ADVISORY** on November 15, where they remained for the rest of the year. The repose period of 2019 marked the longest at Mount Cleveland since its onset of eruptive activity in 2001.

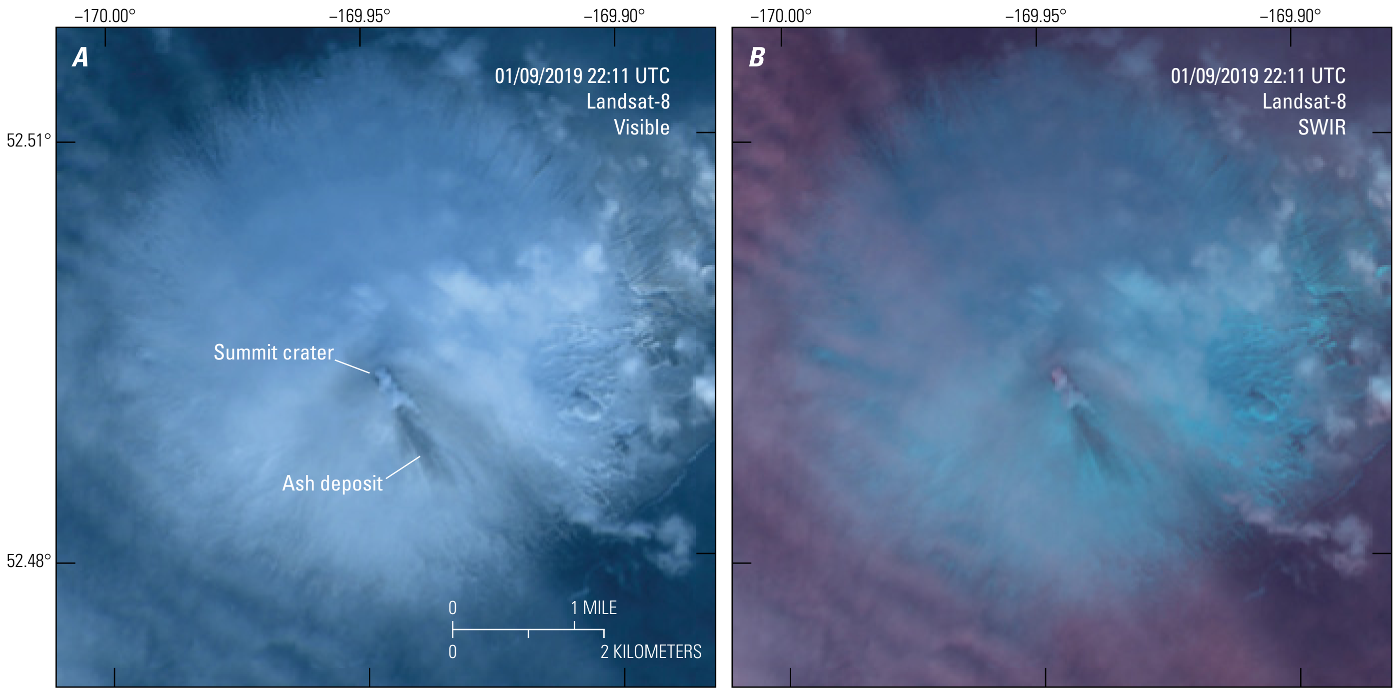

Figure 43. Landsat 8 satellite images of Mount Cleveland, located in the eastern Aleutian Islands, Alaska. *A*, Visible-spectrum image showing the typical steam plume from the summit crater and the ash deposited on the upper slopes of the edifice by the explosive eruption of January 9. *B*, Short-wave infrared (SWIR) image showing a short-wave infrared anomaly at the volcano’s summit.

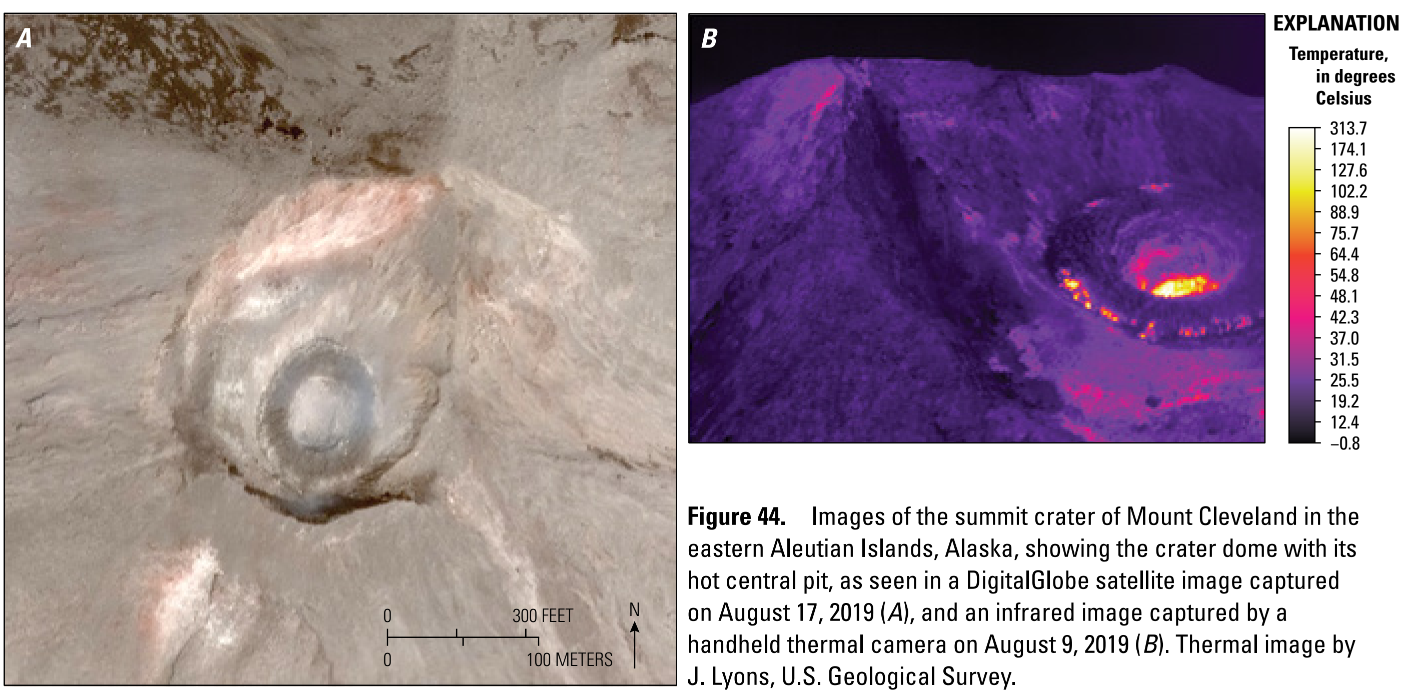

Figure 44. Images of the summit crater of Mount Cleveland in the eastern Aleutian Islands, Alaska, showing the crater dome with its hot central pit, as seen in a DigitalGlobe satellite image captured on August 17, 2019 (*A*), and an infrared image captured by a handheld thermal camera on August 9, 2019 (*B*). Thermal image by J. Lyons, U.S. Geological Survey.

Great Sitkin Volcano

GVP #311120
52.077° N., 176.111° W.
1,740 m
Great Sitkin Island, Andreanof Islands, Aleutian Islands

ELEVATED SEISMICITY; SMALL EXPLOSIVE ERUPTION

Great Sitkin Volcano is a basaltic andesite volcano located 40 km northeast of the City of Adak, Alaska, and 1,880 km southwest of Anchorage (fig. 1). It comprises most of the north half of Great Sitkin Island, part of the Andreanof Islands group of the central Aleutian Islands (Waythomas and others, 2003a, 2003b). The volcano consists of an older collapsed caldera and a younger parasitic cone, the latter of which contains a summit crater 2–3 km in diameter. A steep-sided dome occupies the center of this crater. Prior to a small phreatic eruption in 2019, Great Sitkin Volcano erupted at least twice in the 20th century. In 1974, a lava dome formed in its summit crater, accompanied by at least one ash cloud that reached an altitude as high as 10,000 ft (3,000 m) ASL (Associated Press, 1974). A poorly documented eruption in 1945 also produced a lava dome, which was then partially destroyed by the 1974 eruption. Additionally, at some point within the past 280 years, a large explosive eruption produced pyroclastic flows that partially filled a valley on the southwest flank of the volcano (Waythomas and others, 2003b).

In late July 2016, Great Sitkin Volcano entered a period of increased unrest characterized by an elevated frequency of earthquakes, anomalous steaming from its summit crater, and small explosive events (Dixon and others, 2020). This activity continued throughout 2019, with similar small earthquakes, steaming from the summit crater, and one small explosion.

During 2019, AVO located 629 earthquakes at Great Sitkin Volcano, principally clustered within the shallow crust extending from the summit to roughly 10 km deep. Additional shocks were also located between 10 and 35 km deep, with waveforms and frequency contents indicating both VT and deep LP events (fig. 45). Local magnitudes of located events ranged from −1.37 to 2.22 (fig. 46). The largest event was located roughly 20 km southwest of the summit of Great Sitkin Volcano at a depth of 8.6 km. This hypocenter was deeper than those for earthquakes typically associated with volcanic processes beneath the volcano.

The Great Sitkin Volcano seismic network experienced several station failures in 2019, impairing AVO's ability to locate earthquakes. The most notable failure period spanned January to mid-June. These failures are likely the cause of a reduction in the number of located earthquakes in early 2019 relative to 2018, and the cause of an absence of shallow hypocenters detected in the first half of 2019 (fig. 46). In response to the failures, AVO carried out a major upgrade to the seismic network in June 2019. The upgrades involved changing most of the older analog stations (installed in 1999) to broadband digital stations, although the analog stations GSSP and GSCK were left in operation for continuity. These network upgrades resulted in significantly improved station performance for the remainder of 2019.

AVO identified a single small explosion associated with Great Sitkin Volcano's seismic unrest. It took place at 05:40 UTC on June 2 (June 1 at 20:40 HADT) and produced an emergent waveform with most of its energy between 1 and 5 hertz, similar to other small explosions recorded at Great Sitkin Volcano since January 2017 (fig. 47). The event had a duration of 2 minutes and 17 seconds, determined using

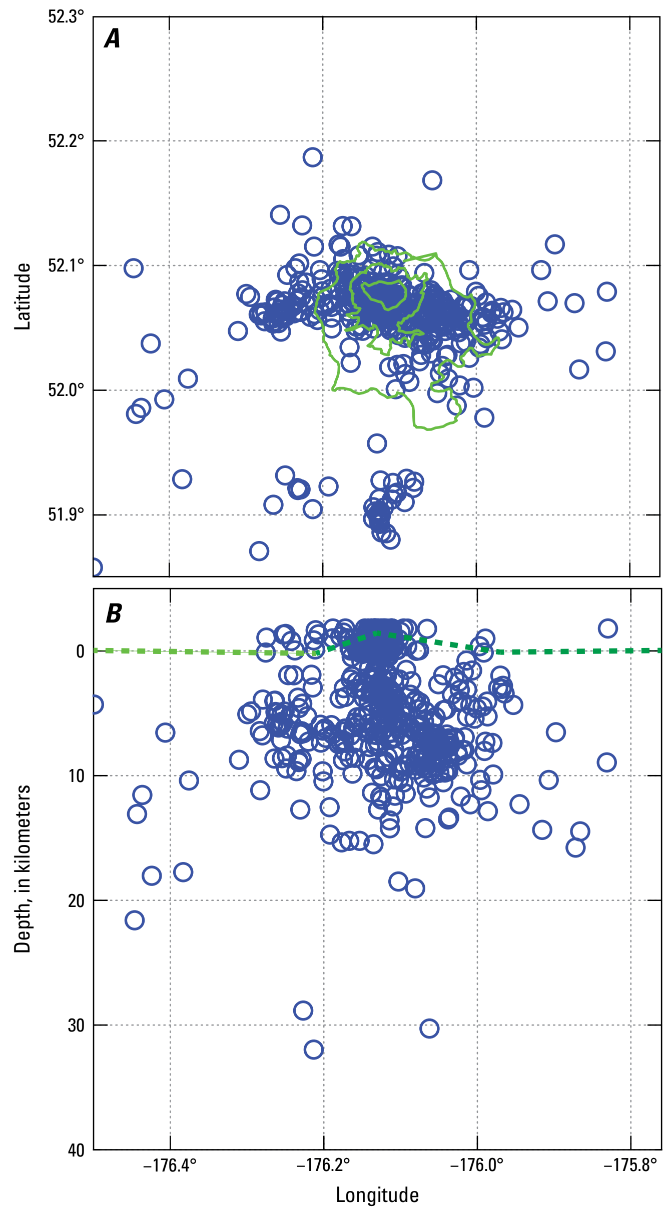

Figure 45. Map (*A*) and east–west cross section (*B*) showing earthquakes located at Great Sitkin Volcano (central Aleutian Islands, Alaska) by the Alaska Volcano Observatory in 2019. Solid lines represent 0-, 2,000-, and 4,000-foot topographic contours. The dashed line shows the approximate elevation profile of the island. Event depths were calculated relative to sea level; negative depths reflect elevation above sea level.

the methodology described in Searcy and Power (2020) for calculating the duration of explosions. No associated infrasound signal was observed on the instruments AVO operates in the City of Adak, indicating that the explosion was small. Figure 48 shows the sizes and progression of explosion events at Great Sitkin Volcano since 2016, when the current unrest period began. For many of these signals, some question remains about whether they reflect explosions, short volcanic tremor episodes, or minor steam bursts. Consequently, events with a duration of less than 2 minutes are excluded from figure 48, although any of these mechanisms might have produced the longer events as well. The exception is an explosion on June 10, 2018, for which ash deposits were identified (Cameron and others, 2023).

In response to shifting activity levels at Great Sitkin Volcano, AVO made three changes to the Aviation Color Code and Volcano Alert Level during 2019 (table 2). On February 2, because of declining earthquake activity, the Aviation Color Code and Volcano Alert Level were lowered from **YELLOW** and **ADVISORY**, where they had been since July 1, 2018, to **GREEN** and **NORMAL**. The Aviation Color Code and Volcano Alert Level were elevated back to **YELLOW** and **ADVISORY** on June 2, after the identification of the explosion signal recorded June 1. The Aviation Color Code and Volcano Alert Level were lowered again to **GREEN** and **NORMAL** on July 15, on the basis of declining seismicity. The Aviation Color Code and Volcano Alert Level remained there through the end of the year.

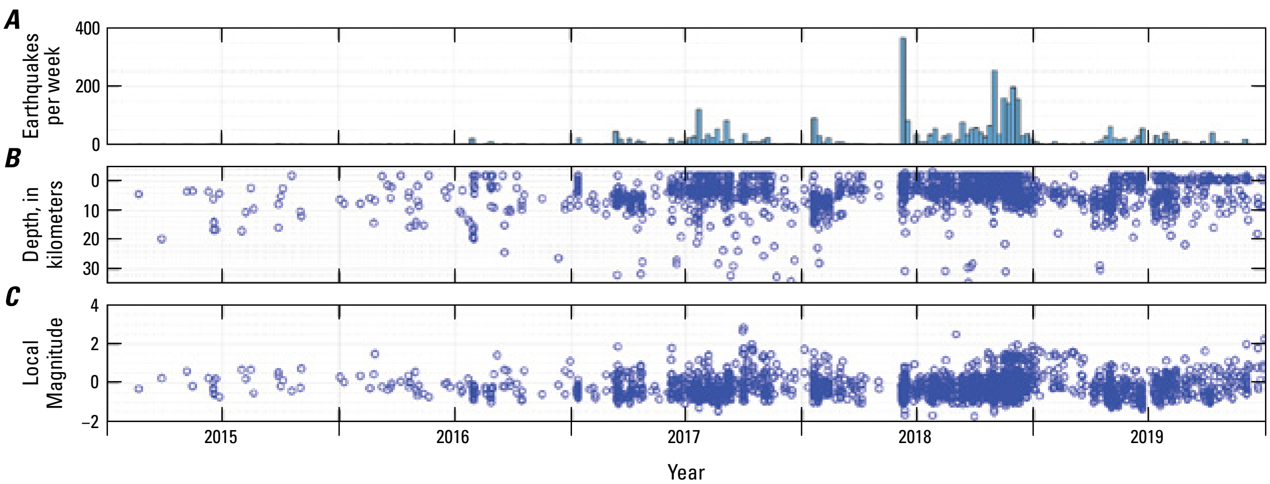

Figure 46. Plots showing the number of located earthquake hypocenters (*A*), earthquake hypocentral depths in kilometers (km) (*B*), and earthquake local magnitudes (*C*) from 2015 through 2019 at Great Sitkin Volcano (central Aleutian Islands, Alaska). The decline in the number of shallow earthquakes detected during the first six months of 2019 might reflect the loss of stations in the Great Sitkin Volcano seismic network. Event depths were calculated relative to sea level; negative depths reflect elevation above sea level.

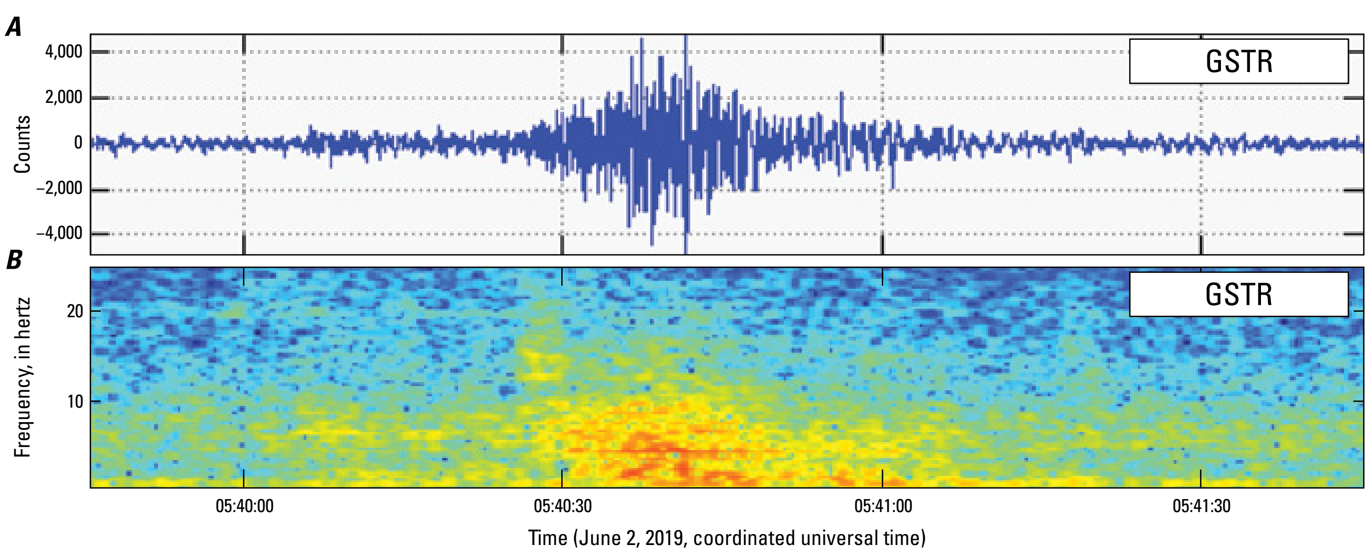

Figure 47. Waveform (*A*) and spectrogram (*B*) plots from station GSTR of the small explosion event at Great Sitkin Volcano (central Aleutian Islands, Alaska) recorded on June 2, 2019. No associated infrasound signal was detected by instruments in the nearby City of Adak, Alaska.

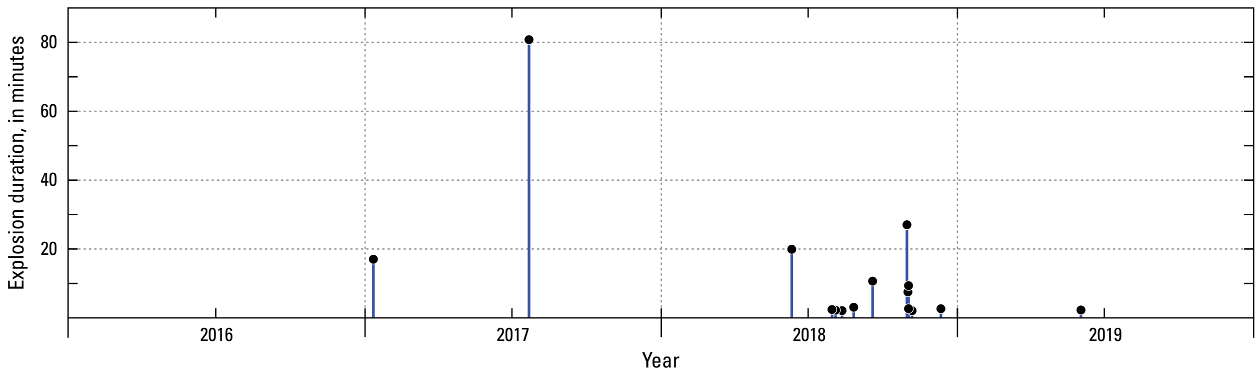

Figure 48. Graph of durations of seismic signals identified at Great Sitkin Volcano (central Aleutian Islands, Alaska), likely associated with explosions, between January 1, 2016, and January 1, 2020. Only signals with durations greater than 2 minutes are shown.

Semisopochnoi Island (Mount Young)

GVP #311060
51.929° N., 179.598° E.
800 m
Semisopochnoi Island, Rat Islands, Aleutian Islands

SPORADIC ERUPTIVE ACTIVITY

Semisopochnoi Island is a young, uninhabited volcanic island in the western Aleutian Islands, 260 km west of the City of Adak and 2,110 km southwest of Anchorage (fig. 1). Although its largest feature is a 7-kilometer-wide caldera that formed 6,900–5,000 years ago, it also has many post-caldera cones (Coombs and others, 2018). The last recorded eruption before its most recent activity (which started in 2018) took place in 1987 at Sugarloaf Peak, on the south end of the island. This event produced a 90-kilometer-long plume visible in satellite images, and pilots later reported ash deposited on the volcano's flanks (Reeder, 1990). Mount Young, a cluster of three cones within the caldera, has also erupted repeatedly in the Holocene, producing crystal-rich basaltic andesite lavas and tephra from all three cones. Most fall deposits associated with the cones are consistent with small- to moderate-sized ash clouds, but some lapilli-size units indicate eruption intensities with a volcanic explosivity index as high as 3 (Coombs and others, 2018). The most recent non-eruptive unrest at Semisopochnoi Island before the 2018 eruption was a period of increased seismicity and deformation in 2014–2015. Modeling by DeGrandpre and others (2019) explained this activity as the result of the rapid intrusion of 0.072 km^3 of magma (as two batches) into a spheroidal magma storage zone ~8 km beneath the caldera.

Activity at the north cone of Mount Young, which began in September 2018, continued in 2019 with sporadic eruptive activity (fig. 49). Seismic tremor and explosion signals captured most of this activity, along with infrequent infrasound detections and occasional satellite observations of steam and small ash deposits. Although the eruptive style and geophysical characteristics of the 2019 unrest were similar to those of 2018, AVO's ability to observe them in real time was limited for the first half of the year owing to a prolonged data outage. This outage, caused by a communication failure at the regional data network telemetry hub in Amchitka, lasted from November 2018 to June 2019, at which point communications were restored and the missing data were recovered.

Owing to the data outage, the first activity observed at the volcano in 2019 comprised satellite observations of steam in January and a small ash deposit on June 2 (table 3; fig. 50). Although the north crater of Mount Young has persistently steamed since 2018, the ash deposits observed on June 2

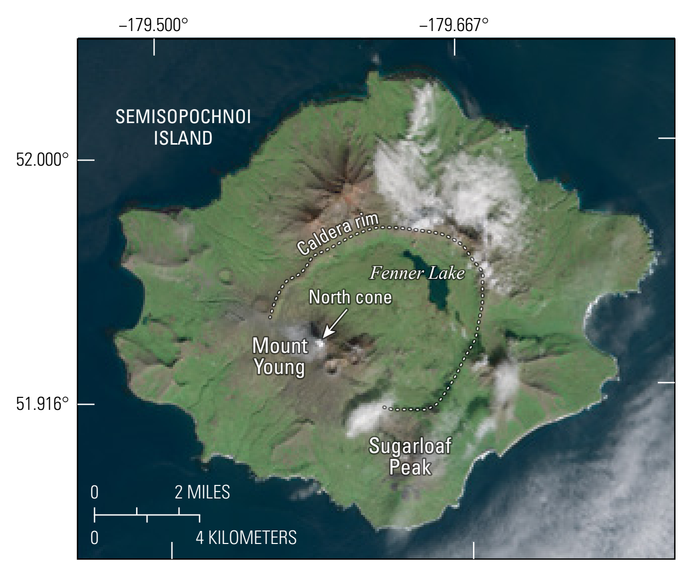

Figure 49. Satellite image showing active and recent volcanic features of Semisopochnoi Island, located in the Rat Islands, Alaska. The north cone of Mount Young is steaming in this image and a light dusting of gray ash is visible on the west flank of the cone. Image acquired by Sentinel-2 on September 10, 2018.

(fig. 51*A*) appear to be a more recent change, having followed tremor bursts in mid-May that probably correspond to when they erupted. AVO began receiving seismic data again on June 11 but kept the Aviation Color Code and Volcano Alert Level at **UNASSIGNED** until early July, when increased tremor prompted a change to **YELLOW** and **ADVISORY**. On July 18, the detection of SO_2 emissions in TROPOMI satellite data and the recording of ground-coupled airwaves triggered AVO to raise the Aviation Color Code and Volcano Alert Level to **ORANGE** and **WATCH**. SO_2, steam plumes,

Table 3. Summary of activity and observations in 2019 at Semisopochnoi Island, located in the Rat Islands, Alaska.

[Dates shown as month/day/year. SO_2, silicon dioxide]

Date	Aviation Color Code/Volcano Alert Level	Observation description
01/15/2019	**UNASSIGNED**	Steam plume
06/02/2019	**UNASSIGNED**	Ash deposit observed
06/11/2019	**UNASSIGNED**	Seismic data connection restored and prior data retrieved
07/05/2019	**YELLOW/ADVISORY**	Tremor increased; Aviation Color Code and Volcano Alert Level changed
07/17/2019	**YELLOW/ADVISORY**	Steam plume
07/18/2019	**YELLOW/ADVISORY**	Steam and SO_2 plumes; seismic tremor; ground-coupled airwaves detected
07/18/2019	**ORANGE/WATCH**	Aviation Color Code and Volcano Alert Level changed
07/19/2019	**ORANGE/WATCH**	SO_2 detected
07/25/2019	**ORANGE/WATCH**	SO_2 detected
07/26/2019	**ORANGE/WATCH**	Steam and SO_2 plumes
08/03/2019	**ORANGE/WATCH**	SO_2 detected
08/04/2019	**ORANGE/WATCH**	SO_2 detected
08/06/2019	**ORANGE/WATCH**	Steam plume
08/12/2019	**ORANGE/WATCH**	Ground-coupled airwave detected; increased tremor
08/21/2019	**ORANGE/WATCH**	Infrasound detected
08/23/2019	**ORANGE/WATCH**	Ground-coupled airwave detected
08/24/2019	**ORANGE/WATCH**	Infrasound and ground-coupled airwave detected
09/06/2019	**ORANGE/WATCH**	SO_2 detected
09/08/2019	**ORANGE/WATCH**	Steam plume
09/09/2019	**ORANGE/WATCH**	SO_2 detected
09/18/2019	**YELLOW/ADVISORY**	Aviation Color Code and Volcano Alert Level changed
12/07/2019	**YELLOW/ADVISORY**	Infrasound detected
12/07/2019	**ORANGE/WATCH**	Aviation Color Code and Volcano Alert Level changed
12/08/2019	**ORANGE/WATCH**	Infrasound detected
12/09/2019	**ORANGE/WATCH**	Infrasound detected; steam plume
12/11/2019	**ORANGE/WATCH**	Infrasound detected; ash plume
12/12/2019	**ORANGE/WATCH**	Infrasound and SO_2 detected
12/13/2019	**ORANGE/WATCH**	Ground-coupled airwave detected
12/14/2019	**ORANGE/WATCH**	Infrasound detected; ash plume
12/15/2019	**ORANGE/WATCH**	Infrasound detected
12/16/2019	**ORANGE/WATCH**	Infrasound detected
12/18/2019	**ORANGE/WATCH**	Ash plume; ground-coupled airwave detected
12/19/2019	**ORANGE/WATCH**	Infrasound detected
01/09/2020	**YELLOW/ADVISORY**	Aviation Color Code and Volcano Alert Level changed

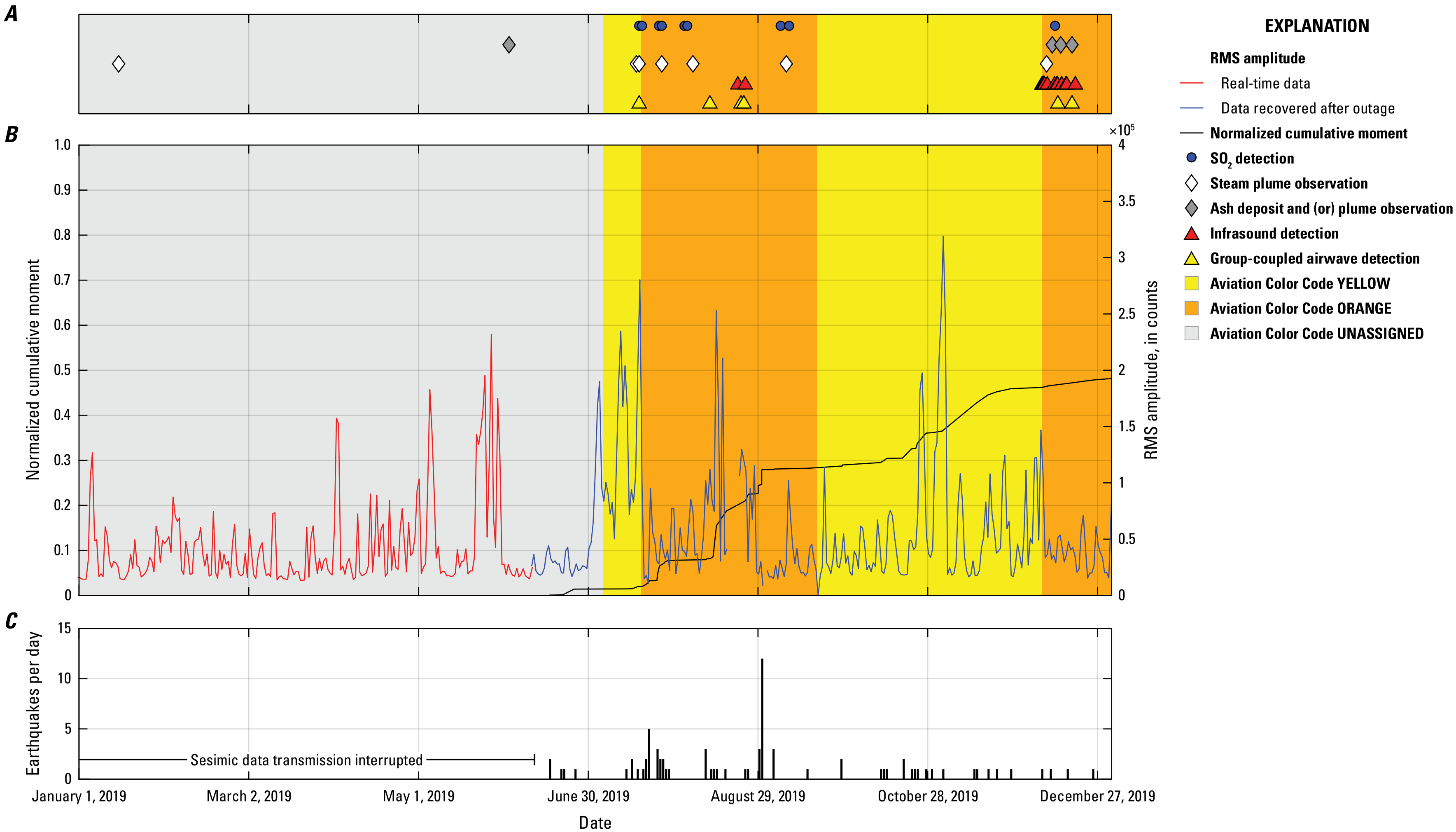

Figure 50. Charts of eruptive activity during 2019 at Semisopochnoi Island, located in the Rat Islands, Alaska. *A*, Timeline of observations and instrumental detections relating to volcanic activity. *B*, Graph showing the normalized cumulative moment of earthquakes from seismic station CERB and the root-mean-square (RMS) amplitude for the 1–5-hertz frequency band. *C*, Histogram of daily earthquake counts. Note that seismic data transmission was not operating between November 2018 and June 2019. No earthquakes were located for this period, but seismic amplitudes were later calculated on the retrieved data.

ground-coupled airwaves, and infrasound were detected throughout the summer, but no ash deposits were observed. After a period of quiescence, AVO lowered the Aviation Color Code and Volcano Alert Level to **YELLOW** and **ADVISORY** on September 18.

Beginning on December 7, the detection of many explosions by regional infrasound sensors indicated a renewal of activity at Semisopochnoi Island, triggering AVO to raise the Aviation Color Code and Volcano Alert Level to **ORANGE** and **WATCH**. In addition to producing infrasound, the explosions were accompanied by ash emissions visible in satellite imagery (fig. 51*B*), ground-coupled airwaves, and one SO_2 detection (on December 12) (fig. 50). No ash plumes reaching altitudes greater than 10,000 ft (3,000 m) ASL and no large ash deposits were observed during this eruptive period. The last activity recorded at the volcano in 2019 was an infrasound detection on December 18. On January 9, 2020, AVO lowered the Aviation Color Code and Volcano Alert Level back to **YELLOW** and **ADVISORY**.

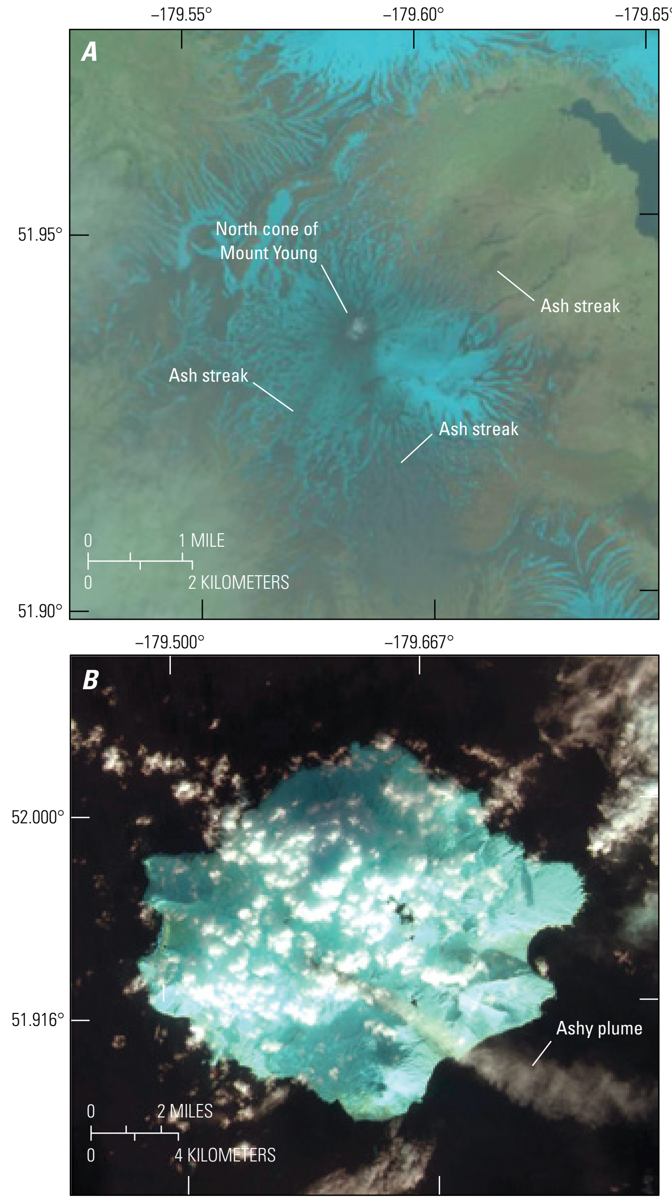

Figure 51. Satellite images from 2019 of Semisopochnoi Island, located in the Rat Islands, Alaska. *A*, Sentinel-2 multispectral image from June 2 at 23:16 coordinated universal time (UTC), showing a steam plume within the crater of the north cone of Mount Young. Small ash streaks radiate as far as 4 kilometers (km) from the crater. *B*, Sentinel-2 multispectral image from December 11 at 23:10 UTC, showing a tan-colored, ashy plume extending about 15 km from the crater to the southeast.

References Cited

Anchorage Daily News, 1955, Eruption of Shishaldin continuing: Anchorage Daily News, v. 8, no. 61, July 14, 1955, p. 1.

Andersen, P., 1956, Experts Eye Ash-Spitting Island: Anchorage Daily Times, January 25, 1976, p. 1.

Associated Press, 1974, Sitkin Island volcano puts on bright show: Fairbanks Daily News-Miner, February 21, 1974, p. 1.

Bacon, C.R., Sisson, T.W., Calvert, A.T., and Nye, C.J., 2009, Geologic map of the 350 km3 basalt-to-dacite Veniaminof Volcano, Aleutian Arc [abs.]: Geological Society of America Abstracts with Programs, v. 41, no. 7, p. 660–661.

Begét, J.E., Nye, C.J., and Bean, K.W., 2000, Preliminary volcano-hazard assessment for Makushin Volcano, Alaska: Alaska Division of Geological & Geophysical Surveys Report of Investigations 2000–4, 22 p, 1 sheet, scale 1:100,000, https://doi.org/10.14509/2679.

Begét, J.E., Larsen, J.F., Neal, C.A., Nye, C.J., and Schaefer, J.R., 2005, Preliminary volcano-hazard assessment for Okmok Volcano, Umnak Island, Alaska: Alaska Division of Geological & Geophysical Surveys Report of Investigations, 2004–3, 32 p., 1 sheet, scale 1:150,000, https://doi.org/10.14509/7042.

Byers, F.M., Jr., 1959, Geology of Umnak and Bogoslof Islands, Aleutian Islands, Alaska: U.S. Geological Survey Bulletin 1028–L, p. 267–369, 5 sheets, https://doi.org/10.3133/b1028L.

Calvert, A.T., Moore, R.B., and McGimsey, R.G., 2005, Argon geochronology of Late Pleistocene to Holocene Westdahl volcano, Unimak Island, Alaska, *in* Haeussler, P.J., and Galloway, J.P., eds., Studies by the U.S. Geological Survey in Alaska, 2004: U.S. Geological Survey Professional Paper 1709–D, 16 p., https://doi.org/10.3133/pp1709D.

Cameron, C.E., Crass, S.W., and AVO Staff, eds., 2022, Geologic Database of Information on Volcanoes in Alaska (GeoDIVA): Alaska Division of Geological & Geophysical Surveys Digital Data Series 20, https://doi.org/10.14509/30901.

Cameron, C.E., Dixon, J.P., Waythomas, C.F., Iezzi, A.M., Wallace, K.L., McGimsey, R.G., and Bull, K.F., 2020, 2016 Volcanic activity in Alaska—Summary of events and response of the Alaska Volcano Observatory: U.S. Geological Survey Scientific Investigations Report 2020–5125, 63 p., https://doi.org/10.3133/sir20205125.

Cameron, C.E., Orr, T.R., Dixon, J.P., Dietterich, H.R., Waythomas, C.F., Iezzi, A.M., Power, J.A., Searcy, C., Grapenthin, R., Tepp, G., Wallace, K.L., Lopez, T.M., DeGrandpre, K., and Perreault, J.M., 2023, 2018 Volcanic activity in Alaska—Summary of events and response of the Alaska Volcano Observatory: U.S. Geological Survey Scientific Investigations Report 2023–5029, 68 p., https://doi.org/10.3133/sir20235029.

Cameron, C.E., Schaefer, J.R., and Mulliken, K.M., 2018, Historically active volcanoes of Alaska: Alaska Division of Geological & Geophysical Surveys Miscellaneous Publication 133, v. 3, 2 sheets, https://doi.org/10.14509/30142.

Caplan-Auerbach, J., and Huggel, C., 2007, Precursory seismicity associated with frequent, large ice avalanches on Iliamna volcano, Alaska, USA: Journal of Glaciology, v. 53, no. 180, p. 128–140, https://doi.org/10.3189/172756507781833866.

Coombs, M.L., Larsen, J.F., and Neal, C.A., 2018, Postglacial eruptive history and geochemistry of Semisopochnoi volcano, western Aleutian Islands, Alaska: U.S. Geological Survey Scientific Investigations Report 2017–5150, 33 p., https://doi.org/10.3133/sir20175150.

Coombs, M.L., and Jicha, B.R., 2021, The eruptive history, magmatic evolution, and influence of glacial ice at long-lived Akutan volcano, eastern Aleutian Islands, Alaska, USA: Geological Society of America Bulletin, v. 133, no. 5–6, p. 963–991, https://doi.org/10.1130/B35667.1.

Dean, K.G., Dehn, J., Papp, K.R., Smith, S., Izbekov, P., Peterson, R., Kearney, C., and Steffke, A., 2004, Integrated satellite observations of the 2001 eruption of Mt. Cleveland, Alaska: Journal of Volcanology and Geothermal Research, v. 135, no. 1–2, p. 51–73, https://doi.org/10.1016/j.jvolgeores.2003.12.013.

Dean, K.G., Engle, K., Groves, J., Dehn, J., and Partington, K., 2002, Analysis of surface processes using SAR data—Westdahl Volcano, Alaska: International Journal of Remote Sensing, v. 23, no. 21, p. 4529–4550, https://doi.org/10.1080/01431160110113953.

DeGrandpre, K.G., Pesicek, J.D., Lu, Z., DeShon, H.R., and Roman, D.C., 2019, High rates of inflation during a noneruptive episode of seismic unrest at Semisopochnoi Volcano, Alaska in 2014–2015: Geochemistry, Geophysics, Geosystems, v. 20, no. 12, p. 6163–6186, https://doi.org/10.1029/2019GC008720.

DeGrandpre, K., Wang, T., Lu, Z., and Freymueller, J.T., 2017, Episodic inflation and complex surface deformation of Akutan volcano, Alaska revealed from GPS time-series: Journal of Volcanology and Geothermal Research, v. 347, p. 337–359, https://doi.org/10.1016/j.jvolgeores.2017.10.003.

Dixon, J.P., Cameron, C.E., Iezzi, A.M., Power, J.A., Wallace, K., and Waythomas, C.F., 2020, 2017 Volcanic activity in Alaska—Summary of events and response of the Alaska Volcano Observatory: U.S. Geological Survey Scientific Investigations Report 2020–5102, 61 p., https://doi.org/10.3133/sir20205102.

Endo, E.T., and Murray, T., 1991, Real-time Seismic Amplitude Measurement (RSAM)—A volcano monitoring and prediction tool: Bulletin of Volcanology, v. 53, no. 7, p. 533–545, https://doi.org/10.1007/BF00298154.

Fee, D., Haney, M.H., Matoza, R.S., Van Eaton, A.R., Cervelli, P., Schneider, D.J., and Iezzi, A.M., 2017, Volcanic tremor and plume height hysteresis from Pavlof Volcano, Alaska: Science, v. 355, no. 6320, p. 45–48, https://doi.org/10.1126/science.aah6108.

Fierstein, J., and Hildreth, W., 2000, Preliminary volcano-hazard assessment for the Katmai volcanic cluster, Alaska: U.S. Geological Survey Open-File Report 2000–489, 59 p., https://doi.org/10.3133/ofr00489.

Freymueller, J.T., and Kaufman, A.M., 2010, Changes in the magma system during the 2008 eruption of Okmok volcano, Alaska, based on GPS measurements: Journal of Geophysical Research, v. 115, no. B12, article B12415, 14 p., https://doi.org/10.1029/2010JB007716.

Gardner, C.A., and Guffanti, M.C., 2006, U.S. Geological Survey's alert notification system for volcanic activity: U.S. Geological Survey Fact Sheet 2006–3139, 4 p., https://doi.org/10.3133/fs20063139.

Hadley, D., Hufford, G.L., and Simpson, J.J., 2004, Resuspension of relic volcanic ash and dust from Katmai—Still an aviation hazard: Weather and Forecasting, v. 19, no. 5, p. 829–840, https://doi.org/10.1175/1520-0434(2004)019<0829:RORVAA>2.0.CO;2.

Hildreth, W., and Fierstein, J., 2012, The Novarupta-Katmai eruption of 1912—Largest eruption of the twentieth century; centennial perspectives: U.S. Geological Survey Professional Paper 1791, 259 p., https://doi.org/10.3133/pp1791.

Keith, T.E.C., ed., 1995, v. 2139. The 1992 eruptions of Crater Peak Vent, Mount Spurr volcano, Alaska, U.S. Geological Survey Bulletin, 220 p., https://doi.org/10.3133/b2139.

Larsen, J.F., Neal, C., Schaefer, J., Begét, J., and Nye, C., 2007, Late Pleistocene and Holocene caldera-forming eruptions of Okmok Caldera, Aleutian Islands, Alaska, *in* Eichelberger, J., Gordeev, E., Izbekov, P., Kasahara, M., and Lees, J., eds., Volcanism and Subduction—The Kamchatka Region: American Geophysical Union Geophysical Monograph Series, v. 172, p. 343–364, https://doi.org/10.1029/172GM24.

Lee, C.-W., Lu, Z., Jung, H.-S, Won, J.-S., and Dzurisin, D., 2010, Surface deformation of Augustine Volcano, 1992–2005, from multiple-interferogram processing using a refined small baseline subset (SBAS) interferometric synthetic aperture radar (InSAR) approach, chap. 18 *of* Power, J.A., Coombs, M.L., and Freymueller, J.T., eds., The 2006 eruption of Augustine Volcano, Alaska: U.S. Geological Survey Professional Paper 1769, p. 453–465, https://doi.org/10.3133/pp176918.

Loewen, M.L., Dietterich, H.R., Graham, N., and Izbekov, P., 2021, Evolution in eruptive style of the 2018 eruption of Veniaminof volcano, Alaska, reflected in groundmass textures and remote sensing: Bulletin of Volcanology, v. 83, no. 72, 19 p., https://doi.org/10.1007/s00445-021-01489-6.

Lu, Z., and Dzurisin, D., 2014, InSAR imaging of Aleutian volcanoes: Chichester, Springer: 390 p., https://doi.org/10.1007/978-3-642-00348-6.

Lu, Z., Masterlark, T., Dzurisin, D., Rykhus, R., and Wicks, C., Jr., 2003, Magma supply dynamics at Westdahl volcano, Alaska, modeled from satellite radar interferometry: Journal of Geophysical Research, v. 108, no. B7, article 2354, 22 p., https://doi.org/10.1029/2002JB002311.

Lu, Z., Wicks, C., Jr., Power, J.A., and Dzurisin, D., 2000, Ground deformation associated with the March 1996 earthquake swarm at Akutan volcano, Alaska, revealed by satellite radar interferometry: Journal of Geophysical Research, v. 105, no. B9, p. 21483–21496, https://doi.org/10.1029/2000JB900200.

March, R., Mayo, L.R., and Trabant, D., 1997, Snow and ice volume on Mount Spurr Volcano, Alaska, 1981: U.S. Geological Survey Water-Resources Investigations Report 97–4142, 36 p., https://doi.org/10.3133/wri974142.

McConnell, V.S., Begét, J.E., Roach, A.L., Bean, K.W., and Nye, C.J., 1998, Geologic map of the Makushin volcanic field, Unalaska Island, Alaska: Alaska Division of Geological & Geophysical Surveys Report of Investigations 97–20, unpaged, 2 sheets, scale 1:63,360, https://doi.org/10.14509/2576.

McGimsey, R.G., and Neal, C.A., 1996, 1995 Volcanic activity in Alaska and Kamchatka—Summary of events and response of the Alaska Volcano Observatory: U.S. Geological Survey Open-File Report 96–738, 23 p., https://doi.org/10.3133/ofr96738.

McGimsey, R.G., Neal, C.A., Dixon, J.P., and Ushakov, S., 2007, 2005 Volcanic activity in Alaska, Kamchatka, and the Kurile Islands—Summary of events and response of the Alaska Volcano Observatory: U.S. Geological Survey Scientific Investigations Report 2007–5269, 94 p., https://doi.org/10.3133/sir20075269.

McGimsey, R.G., Neal, C.A., and Doukas, M.P., 1995, Volcanic activity in Alaska—Summary of events and response of the Alaska Volcano Observatory, 1992: U.S. Geological Survey Open-File Report 95–83, 26 p., https://doi.org/10.3133/ofr9583.

McGimsey, R.G., Neal, C.A., and Girina, O., 2004, 1999 Volcanic activity in Alaska and Kamchatka—Summary of events and response of the Alaska Volcano Observatory: U.S. Geological Survey Open-File Report 2004–1033, 49 p., https://doi.org/10.3133/ofr20041033.

McGimsey, R.G., Neal, C.A., and Girina, O., 2005, 2001 Volcanic activity in Alaska and Kamchatka—Summary of events and response of the Alaska Volcano Observatory: U.S. Geological Survey Open-File Report 2004–1453, 57 p., https://doi.org/10.3133/ofr20041453.

McGimsey, R.G., Neal, C.A., Girina, O.A., Chibisova, M., and Rybin, A., 2014, 2009 Volcanic activity in Alaska, Kamchatka, and the Kurile Islands—Summary of events and response of the Alaska Volcano Observatory: U.S. Geological Survey Scientific Investigations Report 2013–5213, 125 p., https://doi.org/10.3133/sir20135213.

Miller, T.P., and Chouet, B.A., 1994, The 1989–1990 eruptions of Redoubt Volcano—An introduction: Journal of Volcanology and Geothermal research, v. 62, no. 1, p. 1–10, https://doi.org/10.1016/0377-0273(94)90025-6.

Miller, T.P., McGimsey, R.G., Richter, D.H., Riehle, J.R., Nye, C.J., Yount, M.E., and Dumoulin, J.A., 1998, Catalog of the historically active volcanoes of Alaska: U.S. Geological Survey Open-File Report 98–582, 104 p., https://doi.org/10.3133/ofr98582.

Miller, T.P., and Smith, R.L., 1987, Late Quaternary caldera-forming eruptions in the eastern Aleutian arc, Alaska: Geology, v. 15, no. 5, p. 434–438, https://doi.org/10.1130/0091-7613(1987)15<434:LQCEIT>2.0.CO;2.

Molnia, B.F., 2008, Glaciers of North America—Glaciers of Alaska, *in* Williams, R.S., Jr., and Ferrigno, J.G., eds., Satellite image atlas of glaciers of the world: U.S. Geological Survey Professional Paper 1386–K, 525 p., https://doi.org/10.3133/pp1386K.

Neal, C.A., Herrick, J., Girina, O.A., Chibisova, M., Rybin, A., McGimsey, R.G., and Dixon, J., 2014, 2010 Volcanic activity in Alaska, Kamchatka, and the Kurile Islands - Summary of events and response of the Alaska Volcano Observatory: U.S. Geological Survey Scientific Investigations Report 2014–5034, 76 p., https://doi.org/10.3133/sir20145034.

Neal, C.A., McGimsey, R.G., Dixon, J.P., Cameron, C.E., Nuzhaev, A.A., and Chibisova, Marina, 2011, 2008 Volcanic activity in Alaska, Kamchatka, and the Kurile Islands—Summary of events and response of the Alaska Volcano Observatory: U.S. Geological Survey Scientific Investigations Report 2010–5243, 94 p., https://doi.org/10.3133/sir20105243.

Neal, C.A., McGimsey, R.G., Dixon, J.P., Manevich, A., and Rybin, A., 2009, 2006 Volcanic activity in Alaska, Kamchatka, and the Kurile Islands—Summary of events and response of the Alaska Volcano Observatory: U.S. Geological Survey Scientific Investigations Report 2008–5214, 102 p., https://doi.org/10.3133/sir20085214.

Neal, C.A., McGimsey, R.G., Dixon, J., and Melnikov, D., 2005, 2004 Volcanic activity in Alaska and Kamchatka—Summary of events and response of the Alaska Volcano Observatory: U.S. Geological Survey Open-File Report 2005–1308, 71 p., https://doi.org/10.3133/ofr20051308.

Nichols, D.R., and Yehle, L.A., 1961, Mud volcanoes in the Copper River Basin, Alaska, *in* Raasch, G.O., ed., Geology of the Arctic—Proceedings of the First International Symposium on Arctic Geology: University of Toronto Press, v. 2, p. 1063–1087.

Nye, C.J., Keith, T.E.C., Eichelberger, J.C., Miller, T.P., McNutt, S.R., Moran, S., Schneider, D.J., Dehn, J., and Schaefer, J.R., 2002, The 1999 eruption of Shishaldin Volcano, Alaska—Monitoring a distant eruption: Bulletin of Volcanology, v. 64, no. 8, p. 507–519, https://doi.org/10.1007/s00445-002-0225-2.

Nye, C.J., and Turner, D.L., 1990, Petrology, geochemistry, and age of the Spurr volcanic complex, eastern Aleutian arc: Bulletin of Volcanology, v. 52, no. 3, p. 205–226, https://doi.org/10.1007/BF00334805.

O'Brien, J.F., Roman, D.C., Dixon, J.P., Power, J.A., and Arnold, R., 2012, Multiple causes for non-eruptive seismic swarms at Mt. Martin, Katmai Volcanic Cluster, Alaska (2004-2008): Journal of Volcanology and Geothermal Research, v. 229–230, p. 13–22, https://doi.org/10.1016/j.jvolgeores.2012.03.011.

Pesicek, J.D., Wellik, J.J. II, Prejean, S.G., and Ogburn, S.E., 2018, Prevalence of seismic rate anomalies preceding volcanic eruptions in Alaska: Frontiers of Earth Science, v. 6, article 100, 15 p., https://doi.org/10.3389/feart.2018.00100.

Planet Team, 2019, Planet Application Program Interface—In Space for Life on Earth [database]: Planet Labs PBC, accessed June 25, 2019, at https://www.planet.com/.

Power, J.A., 2004, Renewed unrest at Mount Spurr volcano, Alaska: Eos, Transactions, American Geophysical Union, v. 85, no. 43, p. 434, https://doi.org/10.1029/2004EO430004.

Power, J.A., Stihler, S.D., Dixon, J.P., Moran, S.C., Caplan-Auerbach, J., Prejean, S.G., McGee, K., Doukas, M.P., and Roman, D.C., 2004a, Renewed seismic unrest at Mount Spurr volcano, Alaska in 2004—Evidence for a magmatic intrusion [abs.]: Eos, Transactions, American Geophysical Union, v. 85, no. 47, Fall Meeting Supplement, no. S51A–0143, accessed October 28, 2022, at https://ui.adsabs.harvard.edu/abs/2004AGUFM.S51A0143P.

Power, J.A., Stihler, S.D., White, R.A., and Moran, S.C., 2004b, Observations of deep long-period (DLP) seismic events beneath Aleutian Arc volcanoes—1989–2002: Journal of Volcanology and Geothermal Research, v. 138, no. 3–4, p. 243–266, https://doi.org/10.1016/j.jvolgeores.2004.07.005.

Prejean, S.G., Werner, C.A., Buurman, H., Doukas, M.P., Kelly, P.J., Kern, C., Ketner, D.M., Stihler, S.D., Thurber, C.H., and West, M.E., 2012, Seismic and gas analyses imply magmatic intrusion at Iliamna Volcano, Alaska in 2012 [abs.]: Eos, Transactions, American Geophysical Union, Fall Meeting Supplement, no. V53B-2826, accessed October 28, 2022, at https://ui.adsabs.harvard.edu/abs/2012AGUFM.V53B2826P.

Reeder, J.W., 1990, Sugarloaf, *in* Annual report of the world volcanic eruptions in 1987: Bulletin of Volcanic Eruptions [Bulletin of Volcanology], Supplement, v. 52, no. 1, article 87-34, p. 36.

Richter, D.H., Symonds, R.B., Rosenkrans, D.S., McGimsey, R.G., Evans, W.C., and Poreda, R.J., 1998a, Report on the 1997 activity of Shrub mud volcano, Wrangell-St. Elias National Park and Preserve, southcentral [sic] Alaska: U.S. Geological Survey Open-File Report 98–128, 13 p., https://doi.org/10.3133/ofr98128.

Richter, D.H., Waythomas, C.F., McGimsey, R.G., and Stelling, P.L., 1998b, Geology of Akutan Island: U.S. Geological Survey Open-File Report 98–135, 1 sheet, scale 1:48,000, 22-p. pamphlet, https://doi.org/10.3133/ofr98135.

Riehle, J.R., 1985, A reconnaissance of the major Holocene tephra deposits in the upper Cook Inlet region, Alaska: Journal of Volcanology and Geothermal Research, v. 26, no. 1–2, p. 37–74, https://doi.org/10.1016/0377-0273(85)90046-0.

Roman, D.C., Power, J.A., Moran, S.C., Cashman, K.V., Doukas, M.P., Neal, C.A., and Gerlach, T.M., 2004, Evidence for dike emplacement beneath Iliamna Volcano, Alaska in 1996: Journal of Volcanology and Geothermal Research, v. 130, no. 3–4, p. 265–284, https://doi.org/10.1016/S0377-0273(03)00302-0.

Schaefer, J.R., ed., 2011, The 2009 eruption of Redoubt Volcano, Alaska: Alaska Division of Geological & Geophysical Surveys Report of Investigations 2011–5, 45 p., https://doi.org/10.14509/23123.

Schneider, D., Bartelt, P., Caplan-Auerbach, J., Christen, M., Huggel, C., and McArdell, B.W., 2010, Insights into rock-ice avalanche dynamics by combined analysis of seismic recordings and a numerical avalanche model: Journal of Geophysical Research, v. 115, no. F4, article F04026, 20 p., https://doi.org/10.1029/2010JF001734.

Searcy, C.K., and Power, J.A., 2020, Seismic character and progression of explosive activity during the 2016–2017 eruption of Bogoslof volcano, Alaska: Bulletin of Volcanology, v. 82, no. 1, 15 p., https://doi.org/10.1007/s00445-019-1343-4.

Siebert, L., Simkin, T., and Kimberly, P., 2010, Volcanoes of the World (3d ed.): Smithsonian Institution, Washington DC, University of California, Berkley, 568 p.

Stelling, P., Beget, J., Nye, C., Gardner, J., Devine, J.D., and George, R.M.M., 2002, Geology and petrology of ejecta from the 1999 eruption of Shishaldin Volcano, Alaska: Bulletin of Volcanology, v. 64, no. 8, p. 548–561, https://doi.org/10.1007/s00445-002-0229-y.

Toney, L., Fee, D., Allstadt, K.E., Haney, M.M., and Matoza, R.S., 2021, Reconstructing the dynamics of the highly similar May 2016 and June 2019 Iliamna Volcano (Alaska) ice–rock avalanches from seismoacoustic data: Earth Surface Dynamics, v. 9, no. 2, p. 271–293, https://doi.org/10.5194/esurf-9-271-2021.

U.S. Geological Survey, 2017, 5 Meter Alaska Digital Elevation Models (DEMs)—USGS National Map 3DEP Downloadable Data Collection: U.S. Geological Survey data release, accessed December 12, 2021, at https://elevation.alaska.gov/. [Also available at https://www.sciencebase.gov/catalog/item/530f4226e4b0e7e46bd2c315.]

Wallace, K.L., and Schwaiger, H.F., 2019, Volcanic ash resuspension from the Katmai region: Alaska Park Science, v. 18, no. 1, p. 63–70.

Waythomas, C.F., Dorava, J.M., Miller, T.P., Neal, C.A., and McGimsey, R.G., 1997, preliminary volcano-hazard assessment for Redoubt Volcano, Alaska: U.S. Geological Survey Open-File Report 97–857, 40 p., https://doi.org/10.3133/ofr97857.

Waythomas, C.F., and Miller, T.P., 1999, Preliminary volcano-hazard assessment for Iliamna Volcano, Alaska: U.S. Geological Survey Open-File Report 99–373, 31 p, https://doi.org/10.3133/ofr99373.

Waythomas, C.F., Miller, T.P., and Begét, J.E., 2000, Record of Late Holocene debris avalanches and lahars at Iliamna Volcano, Alaska: Journal of Volcanology and Geothermal Research, v. 104, no. 1–4, p. 97–130, https://doi.org/10.1016/S0377-0273(00)00202-X.

Waythomas, C.F., Miller, T.P., and Mangan, M.T., 2006, Preliminary volcano hazard assessment for the Emmons Lake volcanic center, Alaska: U.S. Geological Survey Scientific Investigations Report 2006–5248, 41 p., https://doi.org/10.3133/sir20065248.

Waythomas, C.F., Miller, T.P., and Nye, C., 2003a, Preliminary geologic map of Great Sitkin Volcano, Alaska, U.S. Geological Survey Open-File Report 2003–36, 1 plate, scale 1:250,000, https://doi.org/10.3133/ofr0336.

Waythomas, C.F., Miller, T.P., and Nye, C.J., 2003b, Preliminary volcano-hazard assessment for Great Sitkin Volcano, Alaska: U.S. Geological Survey Open-File Report 2003–112, 32 p., https://doi.org/10.3133/ofr03112.

Waythomas, C.F., Power, J.A., Richter, D.H., and McGimsey, R.G., 1998, Preliminary volcano-hazard assessment for Akutan Volcano, east-central Aleutian Islands, Alaska: U.S. Geological Survey Open-File Report 98–0360, 36 p., 1 plate, https://doi.org/10.3133/ofr98360.

Werner, C.A., Doukas, M.P., and Kelly, P.J., 2011, Gas emission from failed and actual eruptions from Cook Inlet volcanoes, Alaska, 1989–2006: Bulletin of Volcanology, v. 73, no. 2, p. 155–173, https://doi.org/10.1007/s00445-011-0453-4.

Xue, X., Freymueller, J., and Lu, Z. (2020). Modeling the posteruptive deformation at Okmok based on the GPS and InSAR time series—Changes in the shallow magma storage system: Journal of Geophysical Research, v. 125, no. B2, article e2019JB017801, https://doi.org/10.1029/2019JB017801.

Glossary of Selected Terms and Acronyms

A

andesite Volcanic rock composed of about 57–63 weight percent silica (silicon dioxide [SiO_2]).

ash Fine fragments (less than 2 millimeters across) of lava or rock formed in an explosive volcanic eruption.

B

basalt Volcanic rock composed of about 45–52 weight percent silica (SiO_2).

basaltic andesite Volcanic rock composed of about 52–57 weight percent silica (SiO_2).

C

caldera A large, roughly circular depression commonly caused by a volcanic collapse or explosion.

D

dacite Volcanic rock composed of about 63–69 weight percent silica (SiO_2).

E

earthquake swarm A flurry of closely spaced earthquakes or other ground shaking activity; often precedes an eruption.

F

fumarole A small opening or vent from which hot gases are emitted.

H

Holocene A geologic epoch that extends from the present to about 11,700 years ago.

I

incandescence The high-temperature emission of light.

infrasound Low-frequency sound waves, below the threshold of human hearing.

intracaldera Refers to something within the caldera.

J

juvenile material Volcanic material created from magma reaching the surface.

L

lahar A volcanic mud or debris flow of saturated mixtures of volcaniclastic sediment and water.

lava Molten rock that has reached the Earth's surface.

long-period earthquake An earthquake with dominant frequency content between 1 and 5 hertz. Used interchangeably with the term low-frequency earthquake.

Local magnitude (M_L) An earthquake magnitude scale based on the amplitude of ground motion as measured by a standard seismograph.

M

magma Molten rock below the surface of the Earth.

P

phreatic activity An explosive eruption caused by the sudden heating of groundwater as it contacts hot volcanic rock or magma, leading to a steam-driven explosion.

Pleistocene A geologic epoch that extends from about 11,700 to 2.6 million years ago.

pyroclast An individual particle ejected during a volcanic eruption; commonly classified by size (for example, ash and lapilli).

R

real-time seismic-amplitude measurement Amplitude of ground shaking caused by earthquakes and volcanic tremor averaged over 10-minute intervals.

S

satellite vent A subsidiary volcanic vent located on the flank of a larger volcano.

spatter cone A low, steep-sided cone of spatter built up on a fissure or vent.

steam emissions A general term used herein to indicate visible (partially condensed) degassing of mixed, typically unquantified gas compositions from volcanoes and thermal areas.

stratovolcano Also called a stratocone or composite cone; a steep-sided volcano, commonly conical in shape, built of interbedded lava flows and fragmental deposits from explosive eruptions.

Strombolian A type of explosive volcanic eruption characterized by intermittent bursts of fluid lava, commonly basalt or basaltic andesite, from a vent or crater as gas bubbles rise through a conduit and burst at the surface.

subplinian A type of volcanic eruption characterized by an unsteady but sustained convective eruption column that results in atmospheric injection and wide wind dispersal of ash. Plume height is generally less than about 12 miles (20 kilometers).

T

Tertiary A geologic epoch that extends from about 2.6 million to 66 million years ago.

tremor Low-amplitude, continuous earthquake activity commonly associated with magma movement.

V

vent An opening in the Earth's surface through which magma erupts or volcanic gases are emitted.

volcanic explosivity index A scale that describes the size of explosive volcanic eruptions based on magnitude and intensity.

Volcano Activity Notice A formal announcement of alert-level changes or significant volcanic activity within an alert level; covers all volcanic hazards—lahars (volcanic mud or debris flows), lava flows, ashfall, airborne ash, and pyroclastic flows.

Volcano Observatory Notice for Aviation A formal announcement of alert-level changes or significant volcanic activity within an alert level, focusing on ash emissions and specific to the aviation sector (for pilots, dispatchers, air-traffic managers, and meteorologists).

volcano-tectonic earthquake An earthquake generated within or near a volcano by brittle rock failure resulting from strain induced by volcanic processes.

Vulcanian A type of volcanic eruption that ejects material to heights less than about 12 miles (20 kilometers) and lasts on the order of seconds to minutes. They are characterized by discrete, violent explosions, the ballistic ejection of blocks and bombs, atmospheric shock waves, and the emission of tephra.

Appendixes 1–3

Appendix 1. Citations for Alaska Volcano Observatory Annual Summaries, 1992–2018

Table 1.1. Citations for Alaska Volcano Observatory annual summaries, 1992–2018.

Year	Citation	URL
1992	McGimsey, R.G., Neal, C.A., and Doukas, M.P., 1995, Volcanic activity in Alaska—Summary of events and response of the Alaska Volcano Observatory, 1992: U.S. Geological Survey Open-File Report 95-83, 26 p.	https://doi.org/10.3133/ofr9583
1993	Neal, C.A., McGimsey, R.G., and Doukas, M.P., 1996, Volcanic activity in Alaska—Summary of events and response of the Alaska Volcano Observatory, 1993: U.S. Geological Survey Open-File Report 96-24, 21 p.	https://doi.org/10.3133/ofr9624
1994	Neal, C.A., Doukas, M.P., and McGimsey, R.G., 1995, 1994 Volcanic activity in Alaska—Summary of events and response of the Alaska Volcano Observatory: U.S. Geological Survey Open-File Report 95-271, 18 p.	https://doi.org/10.3133/ofr95271
1995	McGimsey, R.G., and Neal, C.A., 1996, 1995 Volcanic activity in Alaska and Kamchatka—Summary of events and response of the Alaska Volcano Observatory: U.S. Geological Survey Open-File Report 96-738, 22 p.	https://doi.org/10.3133/ofr96738
1996	Neal, C.A., and McGimsey, R.G., 1997, 1996 Volcanic activity in Alaska and Kamchatka—Summary of events and response of the Alaska Volcano Observatory: U.S. Geological Survey Open-File Report 97-433, 34 p.	https://doi.org/10.3133/ofr97433
1997	McGimsey, R.G., and Wallace, K.L., 1999, 1997 Volcanic activity in Alaska and Kamchatka—Summary of events and response of the Alaska Volcano Observatory: U.S. Geological Survey Open-File Report 99-448, 42 p.	https://doi.org/10.3133/ofr99448
1998	McGimsey, R.G., Neal, C.A., and Girina, O., 2003, 1998 Volcanic activity in Alaska and Kamchatka—Summary of events and response of the Alaska Volcano Observatory: U.S. Geological Survey Open-File Report 03-423, 35 p.	https://doi.org/10.3133/ofr03423
1999	McGimsey, R.G., Neal, C.A., and Girina, O., 2004a, 1999 Volcanic activity in Alaska and Kamchatka—Summary of events and response of the Alaska Volcano Observatory: U.S. Geological Survey Open-File Report 2004-1033, 49 p	https://doi.org/10.3133/ofr20041033
2000	Neal, C.A., McGimsey, R.G., and Chubarova, O., 2004, 2000 Volcanic activity in Alaska and Kamchatka—Summary of events and response of the Alaska Volcano Observatory: U.S. Geological Survey Open-File Report 2004-1034, 37 p.	https://doi.org/10.3133/ofr20041034
2001	McGimsey, R.G., Neal, C.A., and Girina, O., 2004b, 2001 Volcanic activity in Alaska and Kamchatka—Summary of events and response of the Alaska Volcano Observatory: U.S. Geological Survey Open-File Report 2004-1453, 53 p.	https://doi.org/10.3133/ofr20041453
2002	Neal, C.A., McGimsey, R.G., and Girina, O., 2005, 2002 Volcanic activity in Alaska and Kamchatka—Summary of events and response of the Alaska Volcano Observatory: U.S. Geological Survey Open-File Report 2004-1058, 51 p.	https://doi.org/10.3133/ofr20041058
2003	McGimsey, R.G., Neal, C.A., and Girina, O., 2005, 2003 Volcanic activity in Alaska and Kamchatka—Summary of events and response of the Alaska Volcano Observatory: U.S. Geological Survey Open-File Report 2005-1310, 58 p.	https://doi.org/10.3133/ofr20051310
2004	Neal, C.A., McGimsey, R.G., Dixon, J.P., and Melnikov, D., 2005, 2004 Volcanic activity in Alaska and Kamchatka—Summary of events and response of the Alaska Volcano Observatory: U.S. Geological Survey Open-File Report 2005-1308, 67 p.	https://doi.org/10.3133/ofr20051308
2005	McGimsey, R.G., Neal, C.A., Dixon, J.P., and Ushakov, S., 2007, 2005 Volcanic activity in Alaska, Kamchatka, and the Kurile Islands—Summary of events and response of the Alaska Volcano Observatory: U.S. Geological Survey Scientific Investigations Report 2007-5269, 94 p.	https://doi.org/10.3133/sir20075269
2006	Neal, C.A., McGimsey, R.G., Dixon, J.P., Manevich, A., and Rybin, A., 2009, 2006 Volcanic activity in Alaska, Kamchatka, and the Kurile Islands—Summary of events and response of the Alaska Volcano Observatory: U.S. Geological Survey Scientific Investigations Report 2008-5214, 102 p.	https://doi.org/10.3133/sir20085214

Table 1.1. Citations for Alaska Volcano Observatory annual summaries, 1992–2018.—Continued

Year	Citation	URL
2007	McGimsey, R.G., Neal, C.A., Dixon, J.P., Malik, N., and Chibisova, M., 2011, 2007 Volcanic activity in Alaska, Kamchatka, and the Kurile Islands—Summary of events and response of the Alaska Volcano Observatory: U.S. Geological Survey Scientific Investigations Report 2010-5242, 110 p.	https://doi.org/10.3133/sir20105242
2008	Neal, C.A., McGimsey, R.G., Dixon, J.P., Cameron, C.E., Nuzhaev, A.A., and Chibisova, M., 2011, 2008 Volcanic activity in Alaska, Kamchatka, and the Kurile Islands—Summary of events and response of the Alaska Volcano Observatory: U.S. Geological Survey Scientific Investigations Report 2010-5243, 94 p.	https://doi.org/10.3133/sir20105243
2009	McGimsey, R.G., Neal, C.A., Girina, O.A., Chibisova, M., and Rybin, A., 2014, 2009 Volcanic activity in Alaska, Kamchatka, and the Kurile Islands—summary of events and response of the Alaska Volcano Observatory: U.S. Geological Survey Scientific Investigations Report 2013-5213, 125 p.	https://doi.org/10.3133/sir20135213
2010	Neal, C.A., Herrick, J., Girina, O.,A., Chibisova, M., Rybin, A., McGimsey, R.G., and Dixon, J., 2014, 2010 Volcanic activity in Alaska, Kamchatka, and the Kurile Islands—Summary of events and response of the Alaska Volcano Observatory: U.S. Geological Survey Scientific Investigations Report 2014-5034, 76 p.	https://doi.org/10.3133/sir20145034
2011	McGimsey, R.G., Maharrey, J.Z., and Neal, C.A., 2014, 2011 Volcanic activity in Alaska—Summary of events and response of the Alaska Volcano Observatory: U.S. Geological Survey Scientific Investigations Report 2014-5159, 50 p.	https://doi.org/10.3133/sir20145159
2012	Herrick, J.A., Neal, C.A., Cameron, C., Dixon, J., and McGimsey, R.G., 2014, 2012 Volcanic activity in Alaska—Summary of events and response of the Alaska Volcano Observatory: U.S. Geological Survey Scientific Investigations Report 2014-5160, 80 p.	https://doi.org/10.3133/sir20145160
2013	Dixon, J.P., Cameron, C., McGimsey, R.G., Neal, C.A., and Waythomas, C., 2015, 2013 Volcanic activity in Alaska—Summary of events and response of the Alaska Volcano Observatory: U.S. Geological Survey Scientific Investigations Report 2015–5110, 92 p.	https://doi.org/10.3133/sir20155110
2014	Cameron, C.E., Dixon, J.P., Neal, C.A., Waythomas, C.F., Schaefer, J.R., and McGimsey, R.G., 2017, 2014 Volcanic activity in Alaska—Summary of events and response of the Alaska Volcano Observatory: U.S. Geological Survey Scientific Investigations Report 2017–5077, 81 p.	https://doi.org/10.3133/sir20175077
2015	Dixon, J.P., Cameron, C.E., Iezzi, A.M., and Wallace, K., 2017, 2015 Volcanic activity in Alaska—Summary of events and response of the Alaska Volcano Observatory:: U.S. Geological Survey Scientific Investigations Report 2017–5104, 81 p.	https://doi.org/10.3133/sir20175104
2016	Cameron, C.E., Dixon, J.P., Waythomas, C.F., Iezzi, A.M., Wallace, K.L., McGimsey, R.G., and Bull, K.F., 2020, 2016 Volcanic activity in Alaska—Summary of events and response of the Alaska Volcano Observatory: U.S. Geological Survey Scientific Investigations Report 2020-5125, 63 p.	https://doi.org/10.3133/sir20205125
2017	Dixon, J.P., Cameron, C.E., Iezzi, A.M., Power, J.A., Wallace, K., and Waythomas, C.F., 2020, 2017 Volcanic activity in Alaska—Summary of events and response of the Alaska Volcano Observatory: U.S. Geological Survey Scientific Investigations Report 2020-5102, 61 p.	https://doi.org/10.3133/sir20205102
2018	Cameron, C.E., Orr, T.R., Dixon, J.P., Dietterich, H.R., Waythomas, C.F., Iezzi, A.M., Power, J.A., Searcy, C, Grapenthin, R, Tepp, G, Wallace, K.L., Lopez, T.M., DeGrandpre, K, and Perreault, J.M., 2023, 2018 Volcanic Activity in Alaska—Summary of Events and Response of the Alaska Volcano Observatory: U.S. Geological Survey Scientific Investigations Report 2023–5029, 68 p.	https://doi.org/10.3133/sir20235029

Appendix 2. Aviation Color Codes and Volcano Alert Levels Used by United States Volcano Observatories

The Aviation Color Code addresses the hazards to aviation posed by a volcano, whereas the Volcano Alert Level addresses the hazards on the ground. There could be situations where a volcano is producing lava flows that are dangerous on the ground and merit a **WATCH** or **WARNING**, but where the hazard to aviation is minimal, meriting an Aviation Color Code of **GREEN** or **YELLOW**. Where possible, Volcano Alert Level announcements contain additional explanations of volcanic activity and expected hazards (Gardner and Guffanti, 2006).

Table 2.1. Definitions of the Aviation Color Codes used by United States volcano observatories.

Aviation Color Code	Definition
GREEN	Volcano is in typical background, noneruptive state. **Or, after a change from a higher level:** Volcanic activity has ceased, and volcano reverted to its noneruptive state.
YELLOW	Volcano is showing signs of elevated unrest above known background level. **Or, after a change from a higher level:** Volcanic activity has decreased considerably but continues to be closely monitored for possible renewed increase.
ORANGE	Volcano is showing heightened or escalating unrest with increased potential of eruption, timeframe uncertain. **Or:** Eruption is underway but poses limited hazards.
RED	Eruption is imminent with considerable emission of volcanic ash into the atmosphere likely. **Or:** Eruption is underway or suspected with considerable emission of volcanic ash into the atmosphere (ash-plume height specified, if possible).
UNASSIGNED	Ground-based instrumentation is insufficient to establish that a volcano is in a typical background level (GREEN/NORMAL). When activity at such a volcano increases to the point of being detected by remote sensing, distant seismic networks, or eyewitness reports, an alert level and color code are then assigned accordingly. When activity decreases, the volcano goes back to UNASSIGNED without going through GREEN / NORMAL.

Table 2.2. Definitions of the Volcano Alert Levels used by United States volcano observatories.

Volcano Alert Level	Definition
NORMAL	Volcano is in typical background, noneruptive state. **Or, after a change from a higher level:** Volcanic activity has ceased, and volcano reverted to its noneruptive state.
ADVISORY	Volcano is showing signs of elevated unrest above known background level. **Or, after a change from a higher level:** Volcanic activity has decreased considerably but continues to be closely monitored for possible renewed increase.
WATCH	Volcano is showing heightened or escalating unrest with increased potential of eruption, timeframe uncertain. **Or:** Eruption is underway but poses limited hazards.
WARNING	Highly hazardous eruption is imminent, underway, or suspected.
UNASSIGNED	Ground-based instrumentation is insufficient to establish that a volcano is in a typical background level (GREEN/NORMAL). When activity at such a volcano increases to the point of being detected by remote sensing, distant seismic networks, or eyewitness reports, an alert level and color code are then assigned accordingly. When activity decreases, the volcano goes back to UNASSIGNED without going through GREEN/NORMAL.

Appendix 3. Volcanoes Included in Alaska Volcano Observatory Annual Summaries

Table 3.1. Compilation by year of volcanoes included in Alaska Volcano Observatory annual summaries from 1992 to 2019.

[Volcanoes of each year listed in geographic order, from east to west along the Wrangell-Aleutian volcanic arc]

Volcanoes mentioned
1992
Mount Spurr (Crater Peak)
Redoubt Volcano
Iliamna Volcano
Mount Mageik
Westdahl volcano
Akutan Volcano
Bogoslof volcano
Pyre Peak
1993
Mount Churchill
Mount Sanford
Mount Spurr (Crater Peak)
Mount Veniaminof
Shishaldin Volcano
Makushin Volcano
Pyre Peak
Atka volcanic complex (Mount Kliuchef)
Kanaga Volcano
1994
Mount Sanford
Iliamna Volcano
Trident Volcano
Mount Martin
Mount Mageik
Mount Veniaminof
Mount Kupreanof
Shishaldin Volcano
Makushin Volcano
Mount Cleveland
Kanaga Volcano
1995
Mount Martin
Mount Veniaminof
Shishaldin Volcano
Makushin Volcano
Atka volcanic complex (Mount Kliuchef)
Kanaga Volcano
1996
Mount Wrangell
Iliamna Volcano
Mount Martin
Mount Mageik
Pavlof Volcano
Shishaldin Volcano
Westdahl volcano
Akutan Volcano
Amukta Island
Atka volcanic complex (Korovin Volcano)
Kanaga Volcano
1997
Mount Wrangell
Mount Sanford
Shrub mud volcano
Iliamna Volcano
Kukak Volcano
Snowy Mountain
Mount Martin
Mount Mageik
Mount Chiginagak
Pavlof Volcano
Shishaldin Volcano
Mount Okmok
Mount Cleveland
Amukta Island
1998
Shrub mud volcano
Augustine Volcano
Becharof Lake area
Mount Chiginagak
Shishaldin Volcano
Akutan Volcano
Atka volcanic complex (Korovin Volcano)
1999
Mount Wrangell
Shrub mud volcano

Table 3.1. Compilation by year of volcanoes included in Alaska Volcano Observatory annual summaries from 1992 to 2019.—Continued

Volcanoes mentioned
Iliamna Volcano
Mount Veniaminof
Pavlof Volcano
Shishaldin Volcano
Mount Vsevidof
2000
Mount Wrangell
Snowy Mountain
Mount Chiginagak
Shishaldin Volcano
2001
Kukak Volcano
Snowy Mountain
Pavlof Volcano
Frosty Peak
Shishaldin Volcano
Makushin Volcano
Mount Okmok
Mount Cleveland
Great Sitkin Volcano
2002
Mount Wrangell
Mount Martin
Mount Mageik
Mount Veniaminof
Mount Hague
Shishaldin Volcano
Great Sitkin Volcano
2003
Mount Wrangell
Redoubt Volcano
Iliamna Volcano
Augustine Volcano
Mount Mageik
Mount Veniaminof
Pavlof Volcano
Mount Hague
Shishaldin Volcano
Akutan Volcano
2004
Mount Crillon (nonvolcanic peak)
Mount Spurr
Mount Martin

Volcanoes mentioned
Mount Veniaminof
Shishaldin Volcano
Westdahl volcano
2005
Mount Spurr
Iliamna Volcano
Augustine Volcano
Mount Katmai (Novarupta)
Trident Volcano
Mount Martin
Mount Mageik
Mount Chiginagak
Aniakchak Crater
Mount Veniaminof
Mount Hague
Shishaldin Volcano
Mount Cleveland
Atka volcanic complex (Korovin Volcano)
Kasatochi Island
Tanaga Volcano
2006
Klawasi group mud volcanoes (unnamed vent)
Mount Spurr
Augustine Volcano
Fourpeaked Mountain
Mount Martin
Mount Veniaminof
Mount Cleveland
Atka volcanic complex (Korovin Volcano)
Kasatochi Island
2007
Redoubt Volcano
Augustine Volcano
Fourpeaked Mountain
Mount Veniaminof
Pavlof Volcano
Akutan Volcano
Mount Cleveland
Atka volcanic complex (Korovin Volcano)
2008
Redoubt Volcano
Aniakchak Crater
Mount Veniaminof

Table 3.1. Compilation by year of volcanoes included in Alaska Volcano Observatory annual summaries from 1992 to 2019.—Continued

Volcanoes mentioned
Shishaldin Volcano
Mount Okmok
Mount Cleveland
Kasatochi Island
2009
Mount Sanford
Redoubt Volcano
Fourpeaked Mountain
Aniakchak Crater
Mount Veniaminof
Shishaldin Volcano
Mount Okmok
Mount Cleveland
2010
Mount Wrangell
Mount Sanford
Redoubt Volcano
Fourpeaked Mountain
Mount Katmai (Novarupta)
Becharof Lake area
Aniakchak Crater
Mount Veniaminof
Westdahl volcano
Makushin Volcano
Mount Cleveland
Kasatochi Island
2011
Aniakchak Crater
Mount Okmok
Mount Cleveland
2012
Mount Wrangell
Mount Spurr
Redoubt Volcano
Iliamna Volcano
Augustine Volcano
Fourpeaked Mountain
Mount Martin
Aniakchak Crater
Mount Cleveland
Kanaga Volcano
Little Sitkin Island

Volcanoes mentioned
2013
Redoubt Volcano
Iliamna Volcano
Fourpeaked Mountain
Mount Peulik
Aniakchak Crater
Mount Veniaminof
Pavlof Volcano
Shishaldin Volcano
Akutan Volcano
Makushin Volcano
Mount Okmok
Mount Cleveland
Atka volcanic complex (Korovin Volcano)
Great Sitkin Volcano
Mount Gareloi
2014
Mount Spurr
Redoubt Volcano
Iliamna Volcano
Fourpeaked Mountain
Mount Katmai (Novarupta)
Mount Martin
Mount Chiginagak
Aniakchak Crater
Mount Veniaminof
Pavlof Volcano
Shishaldin Volcano
Akutan Volcano
Mount Okmok
Mount Recheshnoi
Mount Cleveland
Kanaga Volcano
Tanaga Volcano
Semisopochnoi Island
2015
Mount Spurr
Redoubt Volcano
Iliamna Volcano
Augustine Volcano
Mount Katmai (Novarupta)
Becharof Lake area

Table 3.1. Compilation by year of volcanoes included in Alaska Volcano Observatory annual summaries from 1992 to 2019.—Continued

Volcanoes mentioned
Ugashik caldera
Aniakchak Crater
Mount Veniaminof
Mount Kupreanof
Pavlof Volcano
Shishaldin Volcano
Mount Recheshnoi
Mount Cleveland
Semisopochnoi Island
2016
Mount Wrangell
Mount Spurr
Iliamna Volcano
Augustine Volcano
Mount Douglas
Mount Katmai (Novarupta)
Aniakchak Crater
Pavlof Volcano
Frosty Peak
Shishaldin Volcano
Makushin Volcano
Bogoslof volcano
Mount Okmok
Mount Cleveland
Atka volcanic complex (Korovin Volcano)
2017
Mount Spurr
Redoubt Volcano
Iliamna Volcano
Augustine Volcano
Mount Katmai (Novarupta)
Pavlof Volcano
Shishaldin Volcano
Akutan Volcano
Makushin Volcano
Bogoslof volcano
Mount Okmok
Mount Cleveland
Great Sitkin Volcano

Volcanoes mentioned
Takawangha volcano
Mount Gareloi
Kiska Volcano
2018
Shrub mud volcano
Mount Spurr
Iliamna Volcano
Mount Katmai (Novarupta)
Mount Veniaminof
Pavlof Volcano
Shishaldin Volcano
Westdahl volcano
Akutan Volcano
Makushin Volcano
Mount Okmok
Mount Cleveland
Great Sitkin Volcano
Mount Gareloi
Semisopochnoi Island (Mount Young)
2019
Shrub mud volcano
Mount Spurr
Redoubt Volcano
Iliamna Volcano
Mount Katmai (Novarupta)
Mount Martin
Mount Veniaminof
Pavlof Volcano
Isanotski Volcano
Shishaldin Volcano
Westdahl volcano
Akutan Volcano
Makushin Volcano
Mount Okmok
Mount Cleveland
Great Sitkin Volcano
Semisopochnoi Island (Mount Young)

Table 3.2. Compilation of volcanic activity described in Alaska Volcano Observatory annual summaries from 1992 to 2019.

[Volcanic centers listed in geographic order from east to west along the Wrangell-Aleutian volcanic arc. Official volcano names may not reflect the geographic or geologic extent of the volcanic features. CO_2, carbon dioxide; PIREP, pilot weather report]

Volcano	Year mentioned	Type of activity
Mount Crillon (nonvolcanic)	2004	Anomalous clouds from rock avalanches
Mount Churchill	1993	Anomalous tectonic seismicity
Mount Wrangell	1996	Robust steam emissions
	1997	Steam emissions
	1999	Steam and possible ash emissions
	2000	Steam emissions
	2002	Anomalous clouds possibly associated with resuspended ash
	2003	Anomalous clouds
	2007	Triggered seismicity; steam emissions; resuspended ash
	2010	Anomalous weather clouds
	2012	Steam emissions
	2013	Resuspended ash; steam emissions
	2016	Snow melt prompts false report of new summit ash deposit
Mount Sanford	1993	Anomalous clouds, likely from rock, ice, and (or) snow avalanches
	1994	Anomalous cloud, likely from rock, ice, and (or) snow avalanche
	1997	Anomalous cloud, likely from rock, ice, and (or) snow avalanche
	2009	Anomalous weather cloud
	2010	Anomalous cloud related to weather or rock, ice, and (or) snow avalanche
Klawasi group mud volcanoes	1997	Eruption at Shrub mud volcano with energetic ejection of saline mud and CO_2
Shrub mud volcano	1998	Eruption of saline mud and CO_2 at Shrub mud volcano continues
	1999	Eruption of saline mud and CO_2 at Shrub mud volcano continues
	2018	Eruption at Shrub mud volcano continues; new mud eruption on southeast flank
	2019	Eruption at Shrub mud volcano continues; new mud eruption on north flank
Unnamed vent	2006	Possible new mud vent between Upper Klawasi and Lower Klawasi mud volcanoes
Mount Spurr	1992	Subplinian eruption with ash fall, pyroclastic flows, and lahars
	1993	Seismicity associated with glacial outburst
	2004	Elevated seismicity and heat flux; lahars; ice cauldron forms; steam emissions; increased CO_2 emissions
	2005	Elevated seismicity and heat flux; debris flows; cauldron evolves; steam emissions
	2006	Declining seismicity and heat flux; cauldron evolves; steam emissions
	2012	Glacial outburst flood; elevated seismicity
	2014	Earthquake swarm; glacial outburst flood
	2015	Earthquake swarm
	2016	Earthquake swarms
	2017	Earthquake swarm
	2018	Elevated seismicity, likely related to glacial movement
	2019	Ice and rock avalanche
Redoubt Volcano	1992	Eruption false alarm
	2003	Anomalous weather cloud

Table 3.2. Compilation of volcanic activity described in Alaska Volcano Observatory annual summaries from 1992 to 2019.—Continued

Volcano	Year mentioned	Type of activity
	2007	Steam emissions; increased heat flux
	2008	Increased gas and thermal flux; debris flows
Redoubt Volcano—Continued	2009	Major magmatic eruption; dome extrusion; lahars; ash and tephra fall; pyroclastic flows
	2010	Gas and steam emissions; seismicity briefly elevated; thermal anomalies
	2012	Robust steam emissions
	2013	Steam emissions
	2014	Steam emissions
	2015	Outburst flood caused by melting from avalanche of snow, ice, rock, and volcanic debris
	2017	Steam emissions
	2019	Resuspended ash
Iliamna Volcano	1992	Robust steam emissions; eruption false alarm
	1994	Vigorous steam emissions; ice and rock avalanche
	1996	Earthquake swarms related to magmatic intrusion; increased SO_2 and CO_2 flux
	1997	Earthquake swarm; ice and rock avalanche
	1999	Ice and rock avalanche
	2003	Ice and rock avalanche
	2005	Rock avalanche
	2012	Steam emissions; seismic swarms; ice and rock avalanches
	2013	Ice and rock avalanches
	2014	Ice and rock avalanches
	2015	Large tectonic earthquake
	2016	Steam emissions; ice and rock avalanche
	2017	Ice and rock avalanche
	2018	Ice and rock avalanche
	2019	Ice and rock avalanches; seismic network improvements
Augustine Volcano	1998	Spine of 1986 dome partially collapses and generates mudflow
	2003	Steam emissions
	2005	Elevated seismicity; weak phreatic eruptive activity; steam and ash emissions; deformation
	2006	Explosive and effusive eruption; steam and ash emissions; pyroclastic flows; ash fall; lahars, dome extrusion
	2007	Elevated seismicity; steam emissions
	2012	Steam emissions; sulfur odor; elevated seismicity
	2015	Steam emissions; rockfalls
	2016	Earthquake swarm
	2017	Elevated seismicity
Mount Douglas	2013	Steam emissions
	2016	Earthquake swarm
Fourpeaked Mountain	2006	Phreatic eruption; steam and ash emissions; debris flows; glacial outburst flood
	2007	Steam emissions; declining seismicity
	2009	Declining steam and gas emissions
	2010	Declining steam and gas emissions; sporadic earthquake swarms
	2012	Elevated seismicity
	2013	Elevated seismicity

Table 3.2. Compilation of volcanic activity described in Alaska Volcano Observatory annual summaries from 1992 to 2019.—Continued

Volcano	Year mentioned	Type of activity
	2014	Long-lasting seismic network outage
	2016	Earthquake swarm
Kukak Volcano	1997	Steam emissions
	2001	Steam emissions
Snowy Mountain	1997	Steam emissions
	2000	Steaming hole in glacier; sulfur odor
	2001	Steaming hole in glacier
Mount Katmai		
Novarupta	2003	Resuspension of 1912 ash
	2005	Resuspension of 1912 ash
	2010	Resuspension of 1912 ash
	2014	Resuspension of 1912 ash
	2015	Resuspension of 1912 ash
	2016	Resuspension of 1912 ash; deployment of particulate monitors
	2017	Resuspension of 1912 ash
	2018	Resuspension of 1912 ash
	2019	Resuspension of 1912 ash
Trident Volcano	1994	Anomalous weather cloud
	2005	New crater
Mount Mageik	1992	Anomalous weather cloud
	1994	Anomalous weather cloud
	1996	Seismicity related to glacial activity; earthquake swarm
	1997	Steam emissions
	2002	Steam emissions
	2003	Steam emissions
	2005	Steam emissions
Mount Martin	1994	Anomalous weather cloud
	1995	Robust steam emissions
	1996	Seismicity related to glacial activity; earthquake swarm
	1997	Steam emissions
	2002	Steam emissions
	2003	Steam emissions
	2004	Robust steam emissions
	2005	Steam emissions
	2006	Earthquake swarm
	2010	Resuspended ash
	2012	Elevated seismicity; steam emissions
	2014	Earthquake swarm; steam emissions
	2019	Steam emissions; earthquake swarm
Becharof Lake area	1998	Earthquake swarm
	2010	Earthquake swarm
	2015	Large earthquake with aftershocks

Table 3.2. Compilation of volcanic activity described in Alaska Volcano Observatory annual summaries from 1992 to 2019.—Continued

Volcano	Year mentioned	Type of activity
Mount Peulik	2013	Steam emissions; sulfur odor
Ugashik caldera	2015	Discolored water
Mount Chiginagak	1997	Steam emissions and sulfur odor from new fumarole field
	1998	Steam emissions and sulfur odor
	2000	Steam emissions
	2005	Increased summit heat flux; crater lake forms; acidic outburst flood
	2014	Increased fumarolic activity; thermal anomalies
Aniakchak Crater	2005	Elevated seismicity; thermal anomaly
	2008	Weather-related seismicity
	2009	Anomalous seismicity
	2010	Low-frequency earthquake swarms
	2011	Drainage of maar lake; destructive downstream flooding
	2012	Elevated seismicity
	2013	Earthquake swarms
	2014	Long-lasting seismic network outage
	2015	Seismic network reestablished
	2016	Notable nonvolcanic earthquake with aftershocks
Mount Veniaminof	1993	Strombolian eruptive activity; lava flows; steam and ash emissions
	1994	Strombolian eruptive activity; lava flows; steam and ash emissions
	1995	Strombolian eruptive activity; lava flows; steam and ash emissions
	1999	Increased glacial discharge; turbid river
	2002	Increased seismicity; weak phreatic activity; steam and ash emissions
	2003	Increased seismicity; weak phreatic activity; steam and ash emissions
	2004	Intermittent phreatic and Strombolian eruptive activity; steam and ash emissions
	2005	Intermittent phreatic and Strombolian eruptive activity; steam and ash emissions
	2006	Intermittent phreatic and Strombolian eruptive activity; steam and ash emissions
	2007	Decline in steam emissions
	2008	Weak phreatic eruptive activity; steam and ash emissions
	2009	Weak phreatic eruptive activity; steam emissions
	2010	Sporadic elevated seismicity; steam emissions
	2013	Strombolian eruptive activity; elevated seismicity; ash emissions; lava flows
	2014	Declining seismicity; thermal anomalies; steam emissions
	2015	Elevated seismicity
	2018	Intermittent minor eruption
	2019	Waning unrest following 2018 eruption
Mount Kupreanof	1994	Steam emissions
	2015	Steam emissions
Pavlof Volcano	1996	Strombolian eruptive activity; fountaining; lava flows; lahars, ash emissions
	1997	Strombolian eruptive activity
	1999	Summit snow melt; steam emissions; possible resuspended ash
	2001	Steam and possible ash emissions; steam emissions and sulfur odor from Mount Hague misattributed to Pavlof Volcano
	2003	Steam emissions from Mount Hague misattributed to Pavlof Volcano

Table 3.2. Compilation of volcanic activity described in Alaska Volcano Observatory annual summaries from 1992 to 2019.—Continued

Volcano	Year mentioned	Type of activity
	2005	Steam emissions from Mount Hague misattributed to Pavlof Volcano
	2007	Strombolian eruptive activity; ash emissions; lava flows; lahars
Pavlof Volcano—Continued	2013	Strombolian eruptive activity; elevated seismicity; ash emissions; lava flows; lahars
	2014	Strombolian eruptive activity; lava fountaining; steam and ash emissions; lava flows; lahars
	2015	End of 2014 eruptive unrest
	2016	Substantial eruption; ash emissions; pyroclastic flows; lahars
	2017	End of intermittent eruptive activity; elevated seismicity; steam emissions; thermal anomalies
	2018	Elevated seismicity
	2019	Elevated seismicity
Mount Hague	2001	Steam emissions from Mount Hague misattributed to Pavlof Volcano
	2002	Elevated seismicity; steam emissions
	2003	Crater lake drains and refills; steam emissions from Mount Hague misattributed to Pavlof Volcano
	2005	Steam emissions from Mount Hague misattributed to Pavlof Volcano
Frosty Peak	2001	Rockfall avalanches mistaken for eruptive activity
	2016	Ice and rock avalanche
Isanotski Volcano	2019	Earthquake swarm related to glacial activity
Shishaldin Volcano	1993	Weak eruptive activity; steam and ash emissions
	1994	Anomalous cloud
	1995	Weak eruptive activity; steam and ash emissions
	1996	Weak eruptive activity; steam and ash emissions
	1997	Weak eruptive activity; steam and ash emissions
	1998	Weak eruptive activity; steam and ash emissions
	1999	Subplinian eruption; ash emissions and ash fall; Strombolian eruptive activity; steam emissions
	2000	Weak eruptive activity; steam emissions
	2001	Increased seismicity; steam emissions
	2002	Increased seismicity; Steam emissions
	2003	Steam emissions
	2004	Elevated seismicity; steam and ash emissions
	2005	Elevated seismicity; steam emissions
	2008	Possible ash emission; steam emissions
	2009	Elevated seismicity; steam emissions; thermal anomalies
	2013	Elevated seismicity; steam emissions
	2014	Intermittent low-level eruptive activity; steam and ash emissions
	2015	Intermittent low-level eruptive activity; steam and ash emissions
	2016	Weak eruptive activity; thermal anomalies; steam emissions
	2017	Elevated seismicity; steam emissions; thermal anomalies
	2018	Declining volcanic unrest
	2019	Strombolian eruption; lava flows; lahars; ash clouds
Westdahl volcano	1992	Fissure eruption; lava fountaining; ash emissions; lava flows
	1996	Anomalous weather cloud

Table 3.2. Compilation of volcanic activity described in Alaska Volcano Observatory annual summaries from 1992 to 2019.—Continued

Volcano	Year mentioned	Type of activity
	2004	Earthquake swarm
	2010	Elevated lower crustal seismicity
Westdahl volcano—	2018	Long-term inflation
Continued	2019	Long-term inflation
Akutan Volcano	1992	Steam and ash emissions
	1996	Intense earthquake swarms; ground cracking
	1998	Tremor-like seismicity related to weather
	2003	Anomalous steam emissions
	2007	Triggered seismicity; inflation; anomalous steam emissions
	2013	Triggered seismicity; intermittent tectonic tremor
	2014	Earthquake swarm; uplift; probable magmatic inflation
	2017	Earthquake swarm
	2018	Long-term inflation
	2019	No systematic deformation
Makushin Volcano	1993	Minor phreatic activity; steam and ash emissions
	1994	Minor phreatic activity; steam and ash emissions
	1995	Steam and ash emissions
	2001	Elevated seismicity; steam emissions; sulfur odor
	2008	Discolored seawater and bubbles in Unalaska Bay (nonvolcanic)
	2010	Elevated seismicity; robust steam emissions
	2013	Intermittent tremor; steam emissions
	2016	Earthquake swarms
	2017	Earthquake swarm; steam emissions
	2018	Earthquake swarms; steam emissions
	2019	Earthquake swarms
Bogoslof volcano	1992	Dome extrusion; ash and steam emissions
	2016	Substantial explosive eruptive activity; steam and ash emissions; pyroclastic flows
	2017	Substantial explosive eruptive activity; steam and ash emissions; pyroclastic flows
Mount Okmok	1997	Strombolian eruptive activity; fountaining; steam and ash emissions; lava flows
	2001	Earthquake swarm
	2008	Major phreatomagmatic eruption; ash emissions and ash fall; pyroclastic flows; lahars
	2009	Tremor bursts; inflation
	2011	Inflation
	2013	Inflation; earthquake swarm; sporadic tremor
	2014	Inflation
	2016	Seismic tremor
	2017	Inflation
	2018	Inflation
	2019	Inflation; seismic tremor
Mount Recheshnoi	2014	Earthquake swarm

Table 3.2. Compilation of volcanic activity described in Alaska Volcano Observatory annual summaries from 1992 to 2019.—Continued

Volcano	Year mentioned	Type of activity
	2015	Elevated seismicity
Mount Vsevidof	1999	Steam emissions after regional earthquake
Mount Cleveland	1994	Small explosion; steam and ash emissions
	1997	Small explosion; steam and ash emissions
	2001	Explosive eruption; steam and ash emissions; lava flows; debris flows
	2005	Intermittent explosive eruptions; steam and ash emissions
	2006	Intermittent explosive eruptions; ash emissions
	2007	Intermittent explosive eruptions; steam, ash, and SO_2 emissions; ballistics; lahars
	2008	Intermittent explosive eruptions; ash emissions and ash fall; debris flows; ballistics; lava effusion
	2009	Intermittent explosive eruptions; ash emissions; debris flows; thermal anomalies
	2010	Intermittent explosive eruptions; steam and ash emissions; debris flows; thermal anomalies
	2011	Thermal anomalies; lava dome extrusion; minor ash emissions
	2012	Intermittent explosive activity; ash emissions; lava dome extrusion; thermal anomalies
	2013	Intermittent explosive activity; ash emissions; debris flows; pyroclastic flows; thermal anomalies
	2014	Intermittent explosive activity; steam and ash emissions; lava dome extrusion; pyroclastic flows
	2015	Intermittent explosive activity; steam and ash emissions; dome extrusion; thermal anomalies
	2016	Intermittent explosive activity; steam and ash emissions; dome extrusion; thermal anomalies
	2017	Intermittent explosive activity; steam and ash emissions; dome extrusion; thermal anomalies
	2018	Intermittent explosive activity; steam and ash emissions; dome extrusion; thermal anomalies
	2019	Explosive eruption
Amukta Island	1996	Small eruption; ash emissions
	1997	Small eruption; ash emissions
Pyre Peak	1992	Weak eruptive activity; steam and ash emissions
	1993	Fissure eruption; lava flow; ash emissions
Atka volcanic complex Mount Kliuchef	1993	Audible rumbling, strong sulfur odor, and increased steam emissions following earthquake
	1995	Anomalous cloud; strong sulfur odor
Korovin Volcano	1995	Thermal anomaly
	1996	Anomalous weather cloud
	1998	Eruption; ash emissions and ashfall
	2005	Minor eruption; steam and ash emissions; elevated seismicity
	2006	Earthquake swarms; tremor; uplift; steam emissions
	2007	Triggered seismicity; tremor bursts; steam and ash emissions
	2013	Earthquake swarm; tremor
	2016	Seismic tremor; steam emissions

Table 3.2. Compilation of volcanic activity described in Alaska Volcano Observatory annual summaries from 1992 to 2019.—Continued

Volcano	Year mentioned	Type of activity
Kasatochi Island	2005	Unusual bubbling and floating scum on crater lake
	2006	Continued bubbling in intracaldera lake
Kasatochi Island—Continued	2008	Major explosive eruption; ash emissions and ash fall; pyroclastic flows; crater widening; local tsunami
	2010	Waning seismicity; diffuse soil degassing; coastal erosion; lake refilling
Great Sitkin Volcano	2001	Elevated seismicity
	2002	Earthquake swarm; tremor
	2013	Earthquake swarms; thermal anomaly
	2017	Earthquake swarm; explosion
	2018	Earthquake swarm; explosions
	2019	Elevated seismicity; small explosive eruption
Kanaga Volcano	1993	Steam emissions; sulfur odor
	1994	Eruption; steam and ash emissions; lava flows; debris flows
	1995	Weak eruptive activity; steam and ash emissions
	1996	Steam and possible ash emissions; sulfur odor
	2012	Phreatic eruption; ash emissions; new summit fissure
	2014	Earthquake swarm
Tanaga Volcano	2005	Elevated seismicity
	2014	Earthquake swarm
Takawangha volcano	2005	Tremor
	2017	Earthquake swarm
Mount Gareloi	2013	Felt earthquakes; steam emissions
	2017	Steam emissions
	2018	Increased seismicity
Semisopochnoi Island	2014	Earthquake swarm; likely magmatic intrusion
	2015	Earthquake swarm
Mount Young	2018	Minor eruption
	2019	Sporadic eruptive activity
Little Sitkin Island	2012	Earthquake swarms; likely magmatic intrusion
Kiska Volcano	2017	Steam emissions

Moffett Field Publishing Service Center, California
Manuscript approved for publication March 24, 2023
Edited by Claire E. Ashcraft
Cartography and illustration support by Katie Sullivan
Layout and design by Kimber Petersen

USGS

Orr and others—**2019 Volcanic Activity in Alaska—Summary of Events and Response of the Alaska Volcano Observatory**—Scientific Investigations Report 2023–5039

ISSN 2338-0328 (online)
https://doi.org/10.3133/sir20235039